ISSN 2531-2189

Volume 8, Issue 21 – e20240821 January – December – 2024

Journal of Mechanical Engineering

15th ANNIVERSARY
ECORFAN
Special Edition

Journal of Mechanical Engineering Volume 8, Issue 21: e20240821 January – December 2024, is a Continuous publication - Journal edited by ECORFAN-Spain. Matacerquillas Street 38, CP: 28411. Moralzarzal - Madrid. WEB: http://www.ecorfan.org/spain/rj_ingenieria_mec.php, revista@ecorfan.org. Editor in Chief: SERRUDO-GONZALES, Javier, BsC. ISSN 2531-2189. Responsible for the last update of this issue ECORFAN Computer Unit. Imelda Escamilla Bouchán, PhD. Vladimir Luna Soto, PhD. Updated as of December 31, 2024.

Journal of Mechanical Engineering

Definition of Research Journal

Scientific Objectives

Support the international scientific community in its written production Science, Technology and Innovation in the Field of Engineering and Technology, in Subdisciplines of pumps and equipment for handling liquids, bearings, air compressors, gears, cooling equipment, mechanical power transmission equipment, pneumatic equipment, equipment and industrial machinery, agricultural machinery, oil extraction machinery, printing and reproduction machinery, mining machinery, hydraulic machinery, specialized industrial machinery, nuclear machinery, paper making machinery, machinery for the food industry, machinery for material handling, textile machinery, steam machinery, vending machines and distributors, machines, tools and accessories , heating material, construction material, dies, templates and gauges, internal combustion engines (general), gas engines, mechanized operations.

ECORFAN-Mexico SC is a Scientific and Technological Company in contribution to the Human Resource training focused on the continuity in the critical analysis of International Research and is attached to CONACYT-RENIECYT number 1702902, its commitment is to disseminate research and contributions of the International Scientific Community, academic institutions, agencies and entities of the public and private sectors and contribute to the linking of researchers who carry out scientific activities, technological developments and training of specialized human resources with governments, companies and social organizations.

Encourage the interlocution of the International Scientific Community with other Study Centers in Mexico and abroad and promote a wide incorporation of academics, specialists and researchers to the publication in Science Structures of Autonomous Universities - State Public Universities - Federal IES - Polytechnic Universities - Technological Universities - Federal Technological Institutes - Normal Schools - Decentralized Technological Institutes - Intercultural Universities - S & T Councils - CONACYT Research Centers.

Scope, Coverage and Audience

Journal of Mechanical Engineering is a Research Journal edited by ECORFAN-Mexico S.C in its Holding with repository in Spain, is a scientific publication arbitrated and indexed with semester periods. It supports a wide range of contents that are evaluated by academic peers by the Double-Blind method, around subjects related to the theory and practice of pumps and equipment for handling liquids, bearings, air compressors, gears, cooling equipment, mechanical power transmission equipment, pneumatic equipment, equipment and industrial machinery, agricultural machinery, oil extraction machinery, printing and reproduction machinery, mining machinery, hydraulic machinery, specialized industrial machinery, nuclear machinery, paper making machinery, machinery for the food industry, machinery for material handling, textile machinery, steam machinery, vending machines and distributors, machines, tools and accessories , heating material, construction material, dies, templates and gauges, internal combustion engines (general), gas engines, mechanized operations with diverse approaches and perspectives, that contribute to the diffusion of the development of Science Technology and Innovation that allow the arguments related to the decision making and influence in the formulation of international policies in the Field of Engineering and Technology. The editorial horizon of ECORFAN-Mexico® extends beyond the academy and integrates other segments of research and analysis outside the scope, as long as they meet the requirements of rigorous argumentative and scientific, as well as addressing issues of general and current interest of the International Scientific Society.

Arbitration Committee

Assignment of Rights

The sending of an Article to Journal of Mechanical Engineering emanates the commitment of the author not to submit it simultaneously to the consideration of other series publications for it must complement the Originality Format for its Article.

The authors sign the Authorization Format for their Article to be disseminated by means that ECORFAN-Mexico, S.C. In its Holding Spain considers pertinent for disclosure and diffusion of its Article its Rights of Work.

Declaration of Authorship

Indicate the Name of Author and Coauthors at most in the participation of the Article and indicate in extensive the Institutional Affiliation indicating the Department.

Identify the Name of Author and Coauthors at most with the CVU Scholarship Number-PNPC or SNI-CONACYT- Indicating the Researcher Level and their Google Scholar Profile to verify their Citation Level and H index.

Identify the Name of Author and Coauthors at most in the Science and Technology Profiles widely accepted by the International Scientific Community ORC ID - Researcher ID Thomson - arXiv Author ID - PubMed Author ID - Open ID respectively.

Indicate the contact for correspondence to the Author (Mail and Telephone) and indicate the Researcher who contributes as the first Author of the Article.

Plagiarism Detection

All Articles will be tested by plagiarism software PLAGSCAN if a plagiarism level is detected Positive will not be sent to arbitration and will be rescinded of the reception of the Article notifying the Authors responsible, claiming that academic plagiarism is criminalized in the Penal Code.

Arbitration Process

All Articles will be evaluated by academic peers by the Double Blind method, the Arbitration Approval is a requirement for the Editorial Board to make a final decision that will be final in all cases. MARVID® is a derivative brand of ECORFAN® specialized in providing the expert evaluators all of them with Doctorate degree and distinction of International Researchers in the respective Councils of Science and Technology the counterpart of CONACYT for the chapters of America-Europe-Asia- Africa and Oceania. The identification of the authorship should only appear on a first removable page, in order to ensure that the Arbitration process is anonymous and covers the following stages: Identification of the Research Journal with its author occupation rate - Identification of Authors and Coauthors - Detection of plagiarism PLAGSCAN - Review of Formats of Authorization and Originality-Allocation to the Editorial Board- Allocation of the pair of Expert Arbitrators-Notification of Arbitration -Declaration of observations to the Author-Verification of Article Modified for Editing-Publication.

Instructions for Scientific, Technological and Innovation Publication

Knowledge Area

The works must be unpublished and refer to topics of pumps and equipment for handling liquids, bearings, air compressors, gears, cooling equipment, mechanical power transmission equipment, pneumatic equipment, equipment and industrial machinery, agricultural machinery, oil extraction machinery, printing and reproduction machinery, mining machinery, hydraulic machinery, specialized industrial machinery, nuclear machinery, paper making machinery, machinery for the food industry, machinery for material handling, textile machinery, steam machinery, vending machines and distributors, machines, tools and accessories , heating material, construction material, dies, templates and gauges, internal combustion engines (general), gas engines, mechanized operations and other topics related to Engineering and Technology.

Presentation of the Content

In the first chapter we present, *Design and mechanical analysis of bushings made from TPU using additive manufacturing and the finite element method* by Contreras-Chávez, Axel A., Villagómez-Moreno, José, Manríquez-Padilla, Carlos G. and Pérez-Cruz, Ángel, with adscription in the Universidad Autónoma de Querétaro, as next article we present, *Design of a three-speed automatic transmission system with reverse for all-terrain vehicles (ATV)* by Ramírez-Ceja, Axel Iván, Manríquez-Padilla, Carlos Gustavo, Pérez-Cruz, Ángel and Torrez-Rico, Luis Armando, with adscription in the Universidad Autónoma de Querétaro and Universidad Politécnica de Juventino Rosas, as next article we present, *Camera calibration procedure for extracting form deviation features in machined parts through computer vision algorithms* by Meraz-Méndez, Manuel, Muñoz-López, Luis Enrique, Reynoso-Jardón, Elva Lilia and Corral- Ramírez, Guadalupe, with adscription in the Universidad Tecnológica de Chihuahua and Universidad Autónoma de Ciudad Juárez, as next article we present, *Experimental proposal of a 'HALO'-type security device in a FORMULA SAE 2024 type vehicle* by Noguez-Jimenez, Víctor Manuel, Cordero-Guridi, José de Jesús, Peréz-Carrillo, Daniel and García-Tépox, José Domingo, with adscription in the Universidad Popular Autónoma del Estado de Puebla, as last article we present, *Design and implementation of an embedded data logger for MAP sensors in automotive systems* by Durán-Fonseca, Miguel Ángel, Charre-Ibarra, Saida, Murgan-Ibañez, Jorge and Gudiño-Lau, Jorge, with adscription in the Universidad de Colima.

Content

Journal of Mechanical Engineering 8[21]1-11: e10821111
Article

Design and mechanical analysis of bushings made from TPU using additive manufacturing and the finite element method

Diseño y análisis mecánico de bujes fabricados en TPU aplicando manufactura aditiva y empleando el método por elemento finito

Contreras-Chávez, Axel A.[a], Villagómez-Moreno, José*[b], Manríquez-Padilla, Carlos G.[c] and Pérez-Cruz, Ángel[d]

[a] Universidad Autónoma de Querétaro • LTF-7342-2024 • 0009-0000-7834-8873 • 1345044
[b] Universidad Autónoma de Querétaro • LTY-7778-2024 • 0000-0001-7044-9282 • 1035567
[c] Universidad Autónoma de Querétaro • JKH-7361-2023 • 0000-0003-1332-5173 • 347939
[d] Universidad Autónoma de Querétaro • AAQ-5139-2021• 0000-0001-5320-4064 • 230815

CONAHCYT classification:

Area: Engineering
Field: Engineering
Discipline: Mechanical engineering
Subdiscipline: Mechanical design

https://doi.org/10.35429/JME.2024.8.21.1.11
Article History:
Received: January 30, 2024
Accepted: December 31, 2024

* ✉ [jose.villagomez@uaq.edu.mx]

Abstract

The study focused on analyzing the mechanical behavior of a front suspension fork bushing for an all-terrain vehicle (ATV), manufactured using Thermoplastic Polyurethane (TPU) through additive manufacturing, specifically 3D printing. This technology enables the creation of customized designs, reduces production time, and minimizes material waste. TPU, an elastomer with remarkable physical and mechanical properties, was evaluated as a potential substitute for natural rubber, which is the primary material traditionally used for bushings in the automotive industry, especially in the production of tires, hoses, and seals. The analysis was conducted through CAD modeling and finite element simulations, subjecting the bushing to torsional and shear stresses typical of vehicular suspension systems. The results indicated that TPU could serve as a replacement material for the established requirements. Given that replacement parts are not always acquired in a timely manner, the study focuses on providing a viable alternative for the automotive industry.

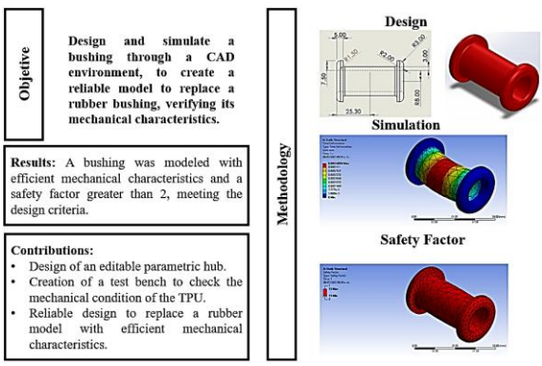

TPU, Additive manufacturing, FEM

Resumen

El estudio se centró en analizar el comportamiento mecánico de un buje de horquilla de la suspensión delantera de una cuatrimoto, fabricado en Poliuretano Termoplástico (TPU) utilizando manufactura aditiva, específicamente impresión 3D. Esta tecnología permite generar diseños personalizados, ahorrar tiempo de producción y reducir el desperdicio de material. El TPU, un elastómero con propiedades físicas y mecánicas destacadas, se evaluó como posible sustituto del caucho natural, el cual es el material que se usa principalmente en la fabricación de los bujes, tradicionalmente utilizado en la industria automotriz, particularmente en neumáticos, mangueras y sellos. El análisis se realizó mediante modelado CAD y simulaciones de elementos finitos, sometiendo el buje a esfuerzos torsionales y cortantes, típicos en sistemas de suspensión vehicular. Los resultados indicaron que el TPU podría ser un material sustituto para los requerimientos establecidos, ya que en ocasiones la refacciones no son adquiridas en tiempo, el estudio se centra en una opción viable en la industria automotriz.

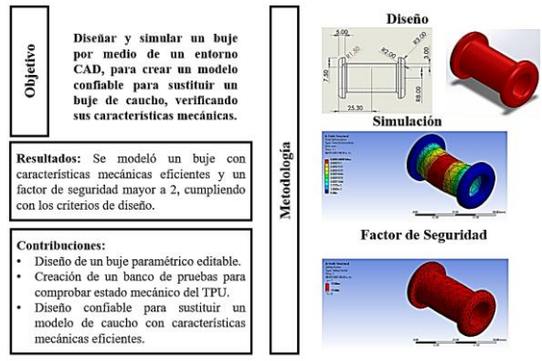

TPU, Manufactura aditiva, FEM

Citation: Contreras-Chávez, Axel A., Villagómez-Moreno, José, Manríquez-Padilla, Carlos G. and Pérez-Cruz, Ángel. [2024]. Design and mechanical analysis of bushings made from TPU using additive manufacturing and the finite element method. Journal of Mechanical Engineering. 8[21]-1-: e10821111.

Introduction

The relationship between man and machine has driven the development of technologies that have transformed society, with the automobile as a clear example of this evolution. Since the Industrial Revolution, advances in science and technology have enabled the creation of internal combustion engines (ICEs), an essential system in the history of the automobile, fuelled by the knowledge of oil as an energy source. Today, cars continue to evolve, integrating electric motors and continuously improving their systems to optimise performance, safety and efficiency.

One of the most relevant systems is the suspension system. This system absorbs road irregularities, controls inertias and is key to vehicle stability and comfort (Cortés et al., 2017). The bushings, vital elements within this system, allow flexibility in the joints, prevent component breakage and prevent impacts from directly affecting the chassis, thus guaranteeing the vehicle's safety and manoeuvrability.

In addition to advances in automotive engineering, manufacturing has also evolved. According to Cortés et al. (2017), companies are forced to reconfigure their processes due to global competition and technological development. Horst et al. (2018) point out that additive manufacturing, or 3D printing, has transformed production lines, allowing for reduced costs and development times. This technique offers greater flexibility, efficiency and the ability to produce complex and customised geometries, making it a key solution to current industry problems, such as the shortage of spare parts that can affect critical systems such as suspension, compromising driver safety.

In this way, additive manufacturing offers significant added value compared to traditional techniques, as it optimises processes and responds quickly to market demands, providing innovative solutions in sectors such as automotive. A new alternative to traditional manufacturing processes is presented, highlighting its development and associated issues.

The materials commonly used in the automotive industry and the type of tests carried out on the bushings are described, as well as the tools used to carry out these studies, for which the finite element method will be the fundamental task to calculate the stresses of the model. All this in order to develop a bushing for use on a quad bike capable of resisting the loads applied to it and with a safety factor greater than 2.

Background

The automotive industry has evolved significantly with the advent of Industry 4.0, with additive manufacturing (AM) standing out as one of the most important emerging technologies. Traditionally, the production of automotive components was carried out through subtractive processes, generating material waste. AM, on the other hand, makes it possible to generate objects in a precise and customised way, optimising resources and reducing manufacturing times (Dilberoglu et al., 2017; Haleem & Javaid, 2019). Despite its benefits, AM still faces challenges in terms of cost, material limitations and product strength. Nevertheless, its implementation offers significant advantages, particularly in the use of metals and, potentially, other innovative materials.

In relation to elastomeric polymers, these have gained ground in the automotive industry for their properties such as friction resistance and the ability to absorb impacts (Ramos, 2018). These materials, such as nitrile rubber and polyurethane, are mainly used for fuel seals and in suspension systems (Lewitzke & Lee, 2001). Despite their current applications, there is a field of opportunity in exploring novel elastomers in conjunction with MA to develop more advanced and functional components.

Recent studies have investigated the properties of elastomeric bushings through mechanical testing. Non-linear behaviours have been identified in these components due to material characteristics, which affect their response to torsional and deflectional stresses (Kadlowec et al., 2009). Simulations based on the finite element method (FEM) have allowed more accurate prediction of the behaviour of these components, although the computational results do not always completely match the experimental results (Elango et al., 2022).

ISSN: 2531-2189
RENIECYT-CONAHCYT: 1702902

Contreras-Chávez, Axel A., Villagómez-Moreno, José, Manríquez-Padilla, Carlos G. and Pérez-Cruz, Ángel. [2024]. Design and mechanical analysis of bushings made from TPU using additive manufacturing and the finite element method. Journal of Mechanical Engineering. 8[21]-1-: e10821111.
DOI: https://doi.org/10.35429/JME.2024.8.21.1.11

The use of FEM in combination with MA is positioned as a key tool to optimise the design and improve the durability of these components. The recent problem of automotive parts shortages has significantly affected the sector, with waiting times for spare parts increasing dramatically since 2020, reaching up to four months in some cases (Torres, 2022; Navarrete, 2022). In this situation, AM presents itself as a viable solution to mitigate this crisis, enabling the rapid and efficient manufacture of components, including those that are no longer in production. In summary, the combination of additive manufacturing and finite element simulation not only offers innovative solutions to address the shortage of automotive parts, but also allows optimising the design of components such as elastomeric bushings, improving their performance and reducing costs and production times.

Suspension system and bushings

The automotive suspension system, responsible for reducing road impacts, is composed of elements such as springs, shock absorbers and bushings (Arellano et al., 2016). Bushings, parts located at the junctions of the suspension system and the chassis, absorb much of the energy generated by road shocks and allow a slight movement of the suspension without compromising the rigidity of the system, avoiding the breakage of components and reducing noise and vibrations (Ortega, 2022). Bushings, generally made of rubber or synthetic materials, help prevent friction and improve the durability of the system (see Figure 1).

Box 1

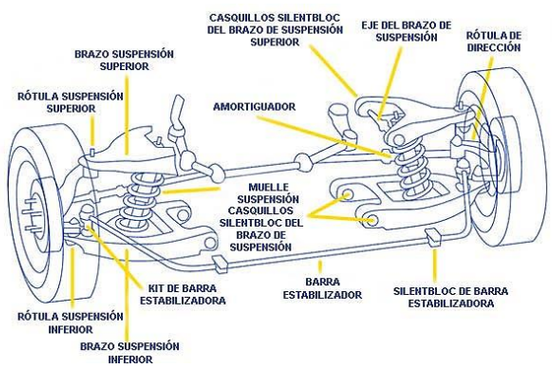

Figure 1

Main components of the suspension and steering system.

Source: MOOG®, 2023

Additive manufacturing

Additive manufacturing (AM), also known as 3D printing, is defined according to ISO/ASTM 52900-2015 as the set of technologies that create physical objects by successive addition of material (Costa, 2019). The material extrusion technique, also known as FFF (Fused Filament Fabrication) or FDM (Fused Deposition Modelling), consists of selectively depositing molten material through a nozzle. It is the most common method in 3D printing, as it is widely adopted in desktop printers. The process requires three axes of motion and a material capable of flowing through a nozzle, allowing layer-by-layer construction of a three-dimensional object. Layer height and control of material flow are key factors in print quality. In this case, the Dremel® DigiLab 3D45 printer was used (see Figure 2), which employs this material extrusion technology. It is a printer with advanced features such as an extruder that reaches temperatures of up to 280 °C, compatibility with materials such as PLA, nylon and eco-friendly ABS, and a layer resolution of between 50 and 100 microns. Its maximum printing volume is 25.5 x 15.5 x 17 cm, and it is operated via a 4.5" touch screen.

Polymaker is a brand of high quality filaments with high mechanical properties. To maintain this level of quality, Polymaker thoroughly controls every stage of production of its wide range of 3D printing materials. The filament that will be used to manufacture the bushings is PolyFlexTM TPU95 (see Figure 2).

Box 2

Figure 2

Dremel DigiLab 3D45 and PolyFlexTM TPU95.
Source: Dremel®, 2023.

ISSN: 2531-2189
RENIECYT-CONAHCYT: 1702902

Contreras-Chávez, Axel A., Villagómez-Moreno, José, Manríquez-Padilla, Carlos G. and Pérez-Cruz, Ángel. [2024]. Design and mechanical analysis of bushings made from TPU using additive manufacturing and the finite element method. Journal of Mechanical Engineering. 8[21]-1-: e10821111.
DOI: https://doi.org/10.35429/JME.2024.8.21.1.11

Thermoplastic polyurethane (TPU)

According to Xu et al. (2020) thermoplastic polyurethane (TPU) is a polymeric material that has high ductility, good biocompatibility and excellent abrasion resistance. It can be used in structures that require high ductility, such as energy absorbing structures and portable devices. These properties pave the way for the manufacture of functional TPU parts for applications in various fields, such as aerospace engineering, medical devices and sports equipment.

All test samples were printed under the following conditions:

- Nozzle temperature = 225 °C
- Print speed = 30 mm/s
- Nozzle diameter = 0.4 mm
- build plate temperature = 80 °C
- Filling = 100%
- Layer size = 0.1 mm

Bushing stresses

Typical stresses to which bushings are subjected are as follows:

Shear stress: According to Beer et al. (2017), it is generated when opposing transverse forces are applied on a body, producing a displacement parallel to the cross-section of the material. The average shear stress can be calculated by dividing the shear force by the cross-sectional area, as shown in Equation (1):

$$\tau_{prom} = \frac{P}{A} \quad [1]$$

EsfTorsional bending: Occurs when an object experiences a torsional moment that tends to rotate the object around its longitudinal axis. The maximum torsional shear stress is calculated by Eq. (2):

$$\tau_{max} = \frac{Tc}{J} \quad [2]$$

Where *T* is the torsional moment, c is the cross-sectional radius, and J is the polar moment of inertia. In the case of hollow shafts, the maximum shear stress is obtained from Eq. (3):

$$\tau_{max} = \frac{16TD}{\pi(D^4 - d^4)} \quad [3]$$

To ensure the structural integrity of the design, the factor of safety (FS), which relates the yield stress to the yield stress, is used.σ_y con the design effort $\sigma_{diseño}$ (Macías, 2019; Kumar, 2018). The formula is given by Equation (4):

$$F.S. = \frac{\sigma_y}{\sigma_{diseño}} \quad [4]$$

A **factor of safety** greater than 1 indicates that the component will resist the applied loads, while a value less than 1 suggests the need to redesign or change the material. In summary, shear and torsional stresses are fundamental to assessing the strength of components subjected to transverse forces or torsional moments. Through the corresponding equations, together with the calculation of the factor of safety, it is ensured that the designed components perform within the elastic limits of the material and do not fail under operational conditions.

Finite element method

The finite element method (FEM) is a key numerical technique in engineering for solving complex problems in structures, fluids and multi-physics phenomena. According to Bathe (2007), it allows modelling and predicting the behaviour of designs, improving their safety and efficiency. Dhatt et al. (2012) explain that FEM transforms partial differential equations into systems of algebraic equations, relying on engineering science, numerical methods and computational tools.

The FEM process consists of three stages:

1. **Pre-processing**: Geometry definition and meshing, assigning material properties and initial conditions.

2. **Solver**: Selection of the appropriate physical model and solving the equations until convergence is achieved.

3. **Post-processing**: Visualisation of results in 2D or 3D graphics to analyse stresses and deformations.

ISSN: 2531-2189
RENIECYT-CONAHCYT: 1702902

Contreras-Chávez, Axel A., Villagómez-Moreno, José, Manríquez-Padilla, Carlos G. and Pérez-Cruz, Ángel. [2024]. Design and mechanical analysis of bushings made from TPU using additive manufacturing and the finite element method. Journal of Mechanical Engineering. 8[21]-1-: e10821111.
DOI: https://doi.org/10.35429/JME.2024.8.21.1.11

This approach is essential for the implementation of a TPU bushing, where the FEM will be applied to develop a viable model to ensure its performance under various conditions, optimising its design to achieve a balance between flexibility and strength in automotive applications.

Methodology

The criteria and processes followed for the development of the TPU bushing model and the tools used to calculate the stresses in the model are presented below, in order to calculate the integrity of the design and to have a viable alternative linked to the stress concentration and the safety factor. We start by defining the geometric characteristics and material properties of the suspension system fork bushing. Subsequently, the model is designed using CAD software, in this case SolidWorks®. Subsequently, a structural analysis is performed using the finite element method (FEM) to evaluate the behaviour of the bushing under torsional and shear forces. Based on the FEM results, the design will be adjusted if necessary to later print the model and have a design which can be used in the fork of the ATV.

Bushing Modelling

The development of the TPU bushing for the suspension system of a quad bike donated to UAQ started with a literature review of elastomeric polymers in the automotive industry (see Figure 3).

Box 3

Figure 3
ATV fork with bushings of interest.

The geometric properties of the bushing were defined, using as a reference the front suspension bushing, which was decoupled using a hydraulic press, revealing deformations in the rubber parts. It was decided to redesign the bushing in a single piece of TPU to improve its flexibility and elasticity, providing greater security to the steel axle. Rounded edges with a radius of 3 mm were implemented to increase the contact surface and reduce the concentration of stresses in the areas of diameter change. The modelling was carried out in SolidWorks® (see Figure 4), creating a sketch with the dimensions of the reference bushing and its modifications.

Box 4

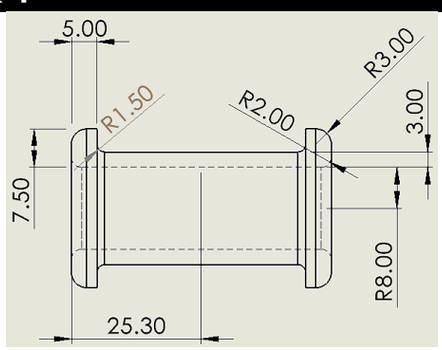

Figure 4
Dimensions corresponding to the hub

TPU material properties

As mentioned, in the pre-processing stage, once the geometry model is available, the material properties will be assigned, the ANSYS® software student version does not have the TPU material, in order to characterise the properties of the TPU filament that will be used, in this case, PolyFlexTM TPU95 (see Figure 5), as well as the reference of other filaments such as TPU 95A of the Ultimaker brand (see Figure 5), will be taken as the properties of the TPU filament that will be used, in this case, PolyFlexTM TPU95 (see Figure 5), as well as the reference of other filaments such as the case of TPU 95A of the Ultimaker brand.

ISSN: 2531-2189
RENIECYT-CONAHCYT: 1702902

Contreras-Chávez, Axel A., Villagómez-Moreno, José, Manríquez-Padilla, Carlos G. and Pérez-Cruz, Ángel. [2024]. Design and mechanical analysis of bushings made from TPU using additive manufacturing and the finite element method. Journal of Mechanical Engineering. 8[21]-1-: e10821111.
DOI: https://doi.org/10.35429/JME.2024.8.21.1.11

Box 5

	A	B	C
1	Property	Value	Unit
2	Density	7850	kg m^-3
3	Isotropic Secant Coefficient of Thermal Expansion		
5	Isotropic Elasticity		
6	Derive from	Young's Modu…	
7	Young's Modulus	2E+11	Pa
8	Poisson's Ratio	0.3	
9	Bulk Modulus	1.6667E+11	Pa
10	Shear Modulus	7.6923E+10	Pa
11	Strain-Life Parameters		
19	S-N Curve	Tabular	
23	Tensile Yield Strength	2.5E+08	Pa
24	Compressive Yield Strength	2.5E+08	Pa
25	Tensile Ultimate Strength	4.6E+08	Pa
26	Compressive Ultimate Strength	0	Pa

Figure 5
Characterisation of the TPU in ANSYS ®.

The meshing will be performed automatically with the tetrahedral elements that the software offers by default, in this case different numbers of elements and nodes were calculated, generating automatically 2422 elements and 4605 interaction nodes. The bushing will be subjected to torsional and shear forces, so it is necessary to perform a static analysis that recreates these forces, which is why the beam element was selected for the approximation (BEAM188).

Initial loading conditions

According to a variety of models of Italika ATVs such as the ATV200 or ATV150 the maximum load capacity is 150 kg. Ideally, the weight carried by a vehicle is distributed over the number of wheels. In the case of an ATV, a value of approximately 40 kg load will be assigned to each wheel under maximum load conditions, taking into account the occupant and the weight of the chassis.

Calculation of the stress and torsional moment

The first type of stress to be analysed will be torsional stresses, therefore, it will be necessary to calculate the torsional moment applied on the hub:

$$F_{carga} = 40\ kg * 9.81 \frac{m}{s^2} = 392.4\ N \quad [5]$$

The torsional moment is therefore:

$$M = 392.4\ N * 0.07343\ m = \mathbf{28.8139\ Nm} \quad [6]$$

Two fixed supports will be assigned to the ends, where ideally the bolt and nut assembly will be fixed to the fork, likewise in the central part of the bushing the calculated torsional moment is set, see Figure 6:

Box 6

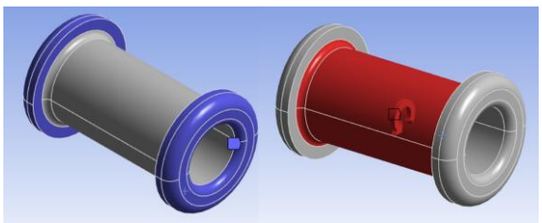

Figure 6
Bushing end supports and moment configuration

Shear stress

A longitudinal load shall be applied to simulate a shear force. The force value to be applied will be 394.4 N, calculated force and fixed support previously selected, the selected area of interest will be the same in red as in the moment configuration shown in figure 6.

Results

The results obtained by the simulation will be shown in which the stresses to which the bushing is subjected in the two stress representations are represented and at the end the factor of safety of the bushing will be denoted to validate the use of the model as a viable design.

Torsional stress in ANSYS®.

In the following, the results obtained for the behaviour of the bushing under torsional stress are presented, the selected diagrams of interest are: Equivalent Stress (Von-Mises), the Total Deformation and the corresponding safety factor. Figure 7 shows the Von-Mises equivalent stress with a maximum value of only 0.018998 MP and it is just in the stress concentration zone due to the variation of the bushing diameter.

ISSN: 2531-2189
RENIECYT-CONAHCYT: 1702902

Contreras-Chávez, Axel A., Villagómez-Moreno, José, Manríquez-Padilla, Carlos G. and Pérez-Cruz, Ángel. [2024]. Design and mechanical analysis of bushings made from TPU using additive manufacturing and the finite element method. Journal of Mechanical Engineering. 8[21]-1-: e10821111.
DOI: https://doi.org/10.35429/JME.2024.8.21.1.11

Box 7

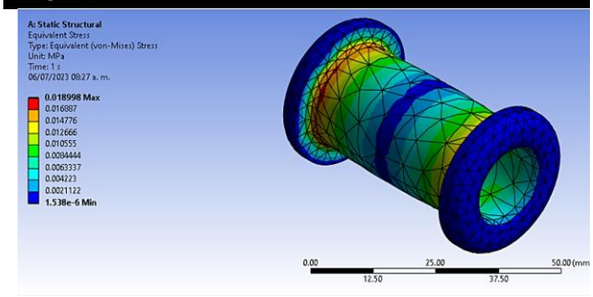

Figure 7
Von-Mises equivalent stress under torsional stress.

On the other hand, Figure 8 shows the total deformation obtained and it is approximately$1.3484x10^{-6}\,mm$, ua fairly small value which does not generally deform the TPU bushing.

Box 8

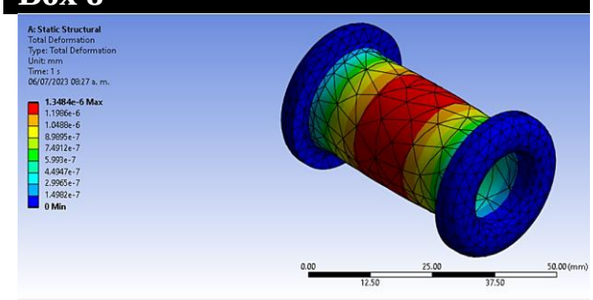

Figure 8
Total deformation under torsional stress

Finally, the safety factor value shown in Figure 9 indicates that it is 15, both the minimum and the maximum, since the ANSYS® software works with this maximum safety factor value. It can be said that the material is sufficiently safe for this type of stress.

Box 9

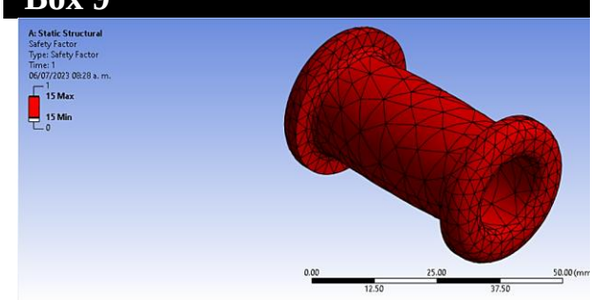

Figure 9
Corresponding factor of safety against torsional stress

Shear stress in ANSYS ®

Equally favourable shear behaviour was obtained, where the maximum equivalent stress is 3.6991 MPa present at the highest stress concentration (see Figure 10).).

Box 10

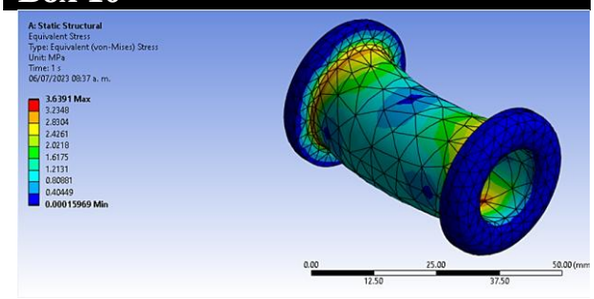

Figure 10
Von-Mises equivalent Von-Mises shear stress

The deformation obtained is barely is of$3.499x10^{-4}mm$, pr The steel is practically not deformed under this stress, with the greatest deformation occurring in the middle of the bushing (see Figure 11).

Box 11

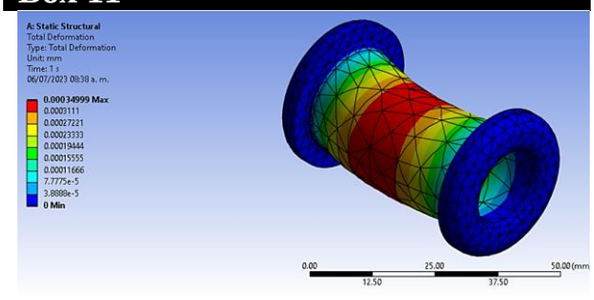

Figure 11
Total shear deformation

Similarly, the factor of safety obtained indicates that the material will be safe enough to be used for this type of stress as it is greater than 2 as shown in Figure 12.

ISSN: 2531-2189
RENIECYT-CONAHCYT: 1702902

Contreras-Chávez, Axel A., Villagómez-Moreno, José, Manríquez-Padilla, Carlos G. and Pérez-Cruz, Ángel. [2024]. Design and mechanical analysis of bushings made from TPU using additive manufacturing and the finite element method. Journal of Mechanical Engineering. 8[21]-1-: e10821111.
DOI: https://doi.org/10.35429/JME.2024.8.21.1.11

Box 12

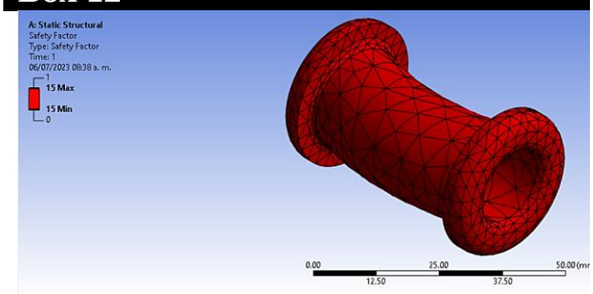

Figure 12

Corresponding factor of safety for shear stress.

Conclusions

Based on the above tests, it was concluded that a better print quality is obtained when the printing speed percentage is decreased, on the other hand, the component was too soft and flexible due to the 20% filler, so it was found to be too soft and flexible, for the last test with the printing speed parameters of 20% and a filling of 100%, a bushing was obtained that was rigid enough to be able to fulfil the corresponding function of cushioning and providing flexibility, similar to having a real bushing with the manufacturing process by means of injection moulds, as this way the quality of the filling is not lost nor does it present faults due to having hollow spaces in its interior (see Figure 13).

Box 13

Figure 13

Printed bushings for experimentation.

The present analysis of the Thermoplastic Polyurethane (TPU) bushing has demonstrated its potential as a viable solution to address the shortage of spare parts in the automotive industry, especially for parts that are difficult to obtain or discontinued in Mexico.

Throughout the development of the project, the mechanical behaviour of TPU has been evaluated in comparison to conventional rubber, suggesting the possibility of replacing rubber in its entirety, although a simultaneous analysis of both materials is needed to confirm this hypothesis.

It is essential to note that this study is based on mechanical testing only, and the thermal behaviour of TPU represents a valuable area of future research, given that the suspension system experiences temperature variations during operation. With the results obtained according to the deformations and stresses it can be observed that the desirable factor of safety is greater than 2 obtaining a feasible model within the desired design characteristics.

Experimental validation, which is still under development, will benefit from the stress calculations obtained in this analysis, which will allow more accurate testing under real conditions. Moving forward, it is suggested that the hub be mounted on a functional quad bike, as the current quad bike, which is disassembled, limits the scope of practical testing. All in all, the results obtained so far indicate that the TPU could be a promising alternative to solve the current problem of spare parts availability.

Disclosures

Conflict of interest

The authors declare that they have no conflict of interest. They have no known competing financial interests or personal relationships that might have appeared to influence the article reported in this paper.

Contribution of authors

The contribution of each researcher to each of the points developed in this research was defined on the basis of the following:

Contreras-Chávez Axel Aldahir: Contributed in the conceptualisation, methodology, software, writing and preparation of the main draft.

Villagómez-Moreno José: Contributed to the conceptualisation, writing, revision and editing, supervision and administration of the project.

Manríquez-Padilla Carlos Gustavo: Contributed to the conceptualisation, writing, review and editing, supervision and administration of the project.

Pérez-Cruz Ángel: Contributed to the conceptualisation, drafting, review and editing, supervision and administration of the project.

ISSN: 2531-2189
RENIECYT-CONAHCYT: 1702902

Contreras-Chávez, Axel A., Villagómez-Moreno, José, Manríquez-Padilla, Carlos G. and Pérez-Cruz, Ángel. [2024]. Design and mechanical analysis of bushings made from TPU using additive manufacturing and the finite element method. Journal of Mechanical Engineering. 8[21]-1-: e10821111.
DOI: https://doi.org/10.35429/JME.2024.8.21.1.11

Availability of information and materials

For any information related to the project please contact the reference author.

Funding

This project was not funded in any way.

Acknowledgements

The authors would like to thank the Consejo Nacional de Humanidades, Ciencias y Tecnologías (CONAHCYT CVU: 1345044 and 1035567) of Mexico for the support provided for the development of the project.

Abbreviations

ABS	Acrylonitrile Butadiene Styrene
ATV	All-Terrain Vehicle
CAD	Computer-Aided Design
FDM	Fused Deposition Modeling
FEM	Finite Element Method
FFF	Fused Filament Fabrication
FS	Factor of Safety
MA	Additive Manufacturing
MCI	Internal Combustion Engines
MEF	Finite Element Method
PLA	Polylactic Acid
TPU	Thermoplastic Polyurethane
UAQ	Autonomous University of Querétaro

References

Background

Arellano Villares, J. C., & Taday Yupanqui, E. F. (2016). Diseño y construcción de un sistema de suspensión para un vehículo tipo fórmula para la Escuela de Ingeniería Automotriz (Bachelor's thesis, Escuela Superior Politécnica de Chimborazo).

Cortés, C. B. Y., Landeta, J. M. I., Chacón, J. G. B., Pereyra, F. A., & Osorio, M. L. (2017). El entorno de la industria 4.0: implicaciones y perspectivas futuras. Conciencia tecnológica, (54).

Dilberoglu, U. M., Gharehpapagh, B., Yaman, U., & Dolen, M. (2017). The role of additive manufacturing in the era of industry 4.0. Procedia manufacturing, 11, 545-554.

Haleem, A., & Javaid, M. (2019). Additive manufacturing applications in industry 4.0: a review. Journal of Industrial Integration and Management, 4(04), 1930001.

Horst, D. J., Duvoisin, C. A., & de Almeida Vieira, R. (2018). Additive manufacturing at Industry 4.0: a review. International journal of engineering and technical research, 8(8).

Ortega, J. (2022). What are suspension bushings and what are they for? AutoMexico. Recuperado 18 de marzo de 2023, de https://automexico.com/mantenimiento/bujes-de-suspension-que-son-para-que-sirven-datos-aid12597

Basics

Elango, C., Pandi, S. K., Mahadule, R. N., & Zarrin-Ghalami, T. (2022). Fatigue Life Prediction and Correlation of Engine Mount Elastomeric Bushing using A Crack Growth Approach (No. 2022-01-0760). SAE Technical Paper.

Navarrete, F. (2022). Refacciones para automóviles tienen 'lento avance' en México. El Financiero. Recuperado 18 de marzo de 2023, de https://www.elfinanciero.com.mx/empresas/2022/09/28/tardan-hasta-4-meses-en-llegar-las-refacciones-para-automoviles/

Ramos Rivero, V. L. (2018). Evolución del uso de los materiales plásticos en la industria automotriz. Recuperado 18 de marzo de 2023, de https://revistas.uide.edu.ec/index.php/innova/article/view/928

Torres, O. (2022). Escasez de refacciones para autos puede durar hasta 2024. Expansión. Recuperado 26 de marzo de 2023, de https://expansion.mx/empresas/2022/09/20/escasez-refacciones-autos-durara-hasta-2024

Support

Costa, J. A. (2019). Procesos de manufactura con tecnología 3D. CTS Cafe, 40-49.

Kadlowec, J., Gerrard, D., & Pearlman, H. (2009). Coupled axial–torsional behavior of cylindrical elastomer bushings. Polymer Testing, 28(2), 139-144.

ISSN: 2531-2189
RENIECYT-CONAHCYT: 1702902

Contreras-Chávez, Axel A., Villagómez-Moreno, José, Manríquez-Padilla, Carlos G. and Pérez-Cruz, Ángel. [2024]. Design and mechanical analysis of bushings made from TPU using additive manufacturing and the finite element method. Journal of Mechanical Engineering. 8[21]-1-: e10821111. DOI: https://doi.org/10.35429/JME.2024.8.21.1.11

Kumar, A. (2018). Safety factor: definition, equation, examples, calculator (with PDF). What is Piping.

Lewitzke, C., & Lee, P. (2001). Application of elastomeric components for noise and vibration isolation in the automotive industry (No. 2001-01-1447). SAE Technical Paper.

Macías, A. (2019). Cálculo e Interpretación del Factor de Seguridad. Recuperado 21 de junio de 2023, de https://intelligy.com/blog/2019/05/07/calculo-e-interpretacion-del-factor-de-seguridad/

Xu, T., Shen, W., Lin, X., & Xie, Y. M. (2020). Mechanical properties of additively manufactured thermoplastic polyurethane (TPU) material affected by various processing parameters. Polymers, 12(12), 3010.

Discussions

Bathe, K. J. (2007). Finite element method. Wiley encyclopedia of computer science and engineering, 1-12.

Beer, F. P., Johnston, E. R., DeWolf, J. T., & Mazurek, D. F. (2017). Mecánica de materiales. Mc Graw Hill.

Dhatt, G., Lefrançois, E., & Touzot, G. (2012). Finite element method. John Wiley & Sons

ISSN: 2531-2189
RENIECYT-CONAHCYT: 1702902

Contreras-Chávez, Axel A., Villagómez-Moreno, José, Manríquez-Padilla, Carlos G. and Pérez-Cruz, Ángel. [2024]. Design and mechanical analysis of bushings made from TPU using additive manufacturing and the finite element method. Journal of Mechanical Engineering. 8[21]-1-: e10821111.
DOI: https://doi.org/10.35429/JME.2024.8.21.1.11

Journal of Mechanical Engineering 8[21]1-12: e20821112
Article

Design of a three-speed automatic transmission system with reverse for all-terrain vehicles (ATV)

Diseño de un sistema de transmisión automática de tres velocidades con reversa para vehículos todo terreno (ATV)

Ramírez-Ceja, Axel Iván*[a], Manríquez-Padilla, Carlos Gustavo[b], Pérez-Cruz, Ángel[c] and Torrez-Rico, Luis Armando[d]

[a] Universidad Autónoma de Querétaro • LTF-2732-2024 • 0009-0008-1340-3673
[b] Universidad Autónoma de Querétaro • JKH-7361-2023 • 0000-0003-1332-5173 • 337939
[c] Universidad Autónoma de Querétaro • 0000-0001-5320-4064 • 230815
[d] Universidad Politécnica de Juventino Rosas • LTF-1239-2024 • 0000-0002-6873-0363 • 373689

CONAHCYT classification:

Area: Engineering
Field: Engineering
Discipline: Mechanical engineering
Subdiscipline: Mechanical desing

https://doi.org/10.35429/JME.2024.8.21.2.12
Article History:
Received: January 30, 2024
Accepted: December 31, 2024

* ✉ [axlivanrc@gmail.com]

Abstract

This work proposes the design and simulation of a conventional three-speed automatic transmission, including reverse gear, for an all-terrain utility vehicle (ATV). The proposed design was generated considering the power requirements needed for the selected vehicle to operate on a specific driving cycle over uneven terrain with variable slopes ranging from -0.5° to 2.5°. A vehicle with well-defined mass, dimensions, and engine displacement was selected as the design criteria. Using the numerical software MATLAB, the power requirements were calculated, establishing that the transmission ratios range from 0.18 to 1. Using commercial Multibody Dynamics (MBD) software, ADAMS, the reliability of the proper functioning of the gear trains was determined based on boundary conditions. Similarly, to verify that the selected materials and components can withstand critical loads, structural static simulations were carried out using the finite element method with the commercial software ANSYS.

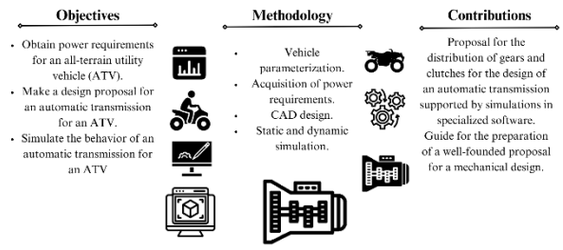

Finite element analysis, Simulation CAE, Automatic Transmission

Resumen

Este trabajo propone el diseño y la simulación de una transmisión automática convencional de tres velocidades, incluyendo reversa, para un vehículo utilitario todoterreno (ATV). El diseño propuesto se generó tomando en cuenta los requerimientos de potencia necesarios para que el vehículo seleccionado sea capaz de circular, siguiendo un ciclo de manejo específico, sobre un terreno irregular con pendientes variables oscilantes entre -0.5° y 2.5°. Utilizando el software numérico MATLAB©, se calcularon los requerimientos de potencia, que van desde 0.18 hasta 1. Empleando un software de Multibody Dynamics (MBD) comercial, ADAMS©, se corroboró el adecuado funcionamiento de los trenes de engranajes con base en las condiciones de frontera, de forma similar, para corroborar que los materiales y componentes seleccionados soporten las cargas críticas, se realizaron simulaciones estáticas estructurales mediante el software comercial ANSYS©, basado en la teoría de los elementos finitos.

Análisis por elemento finito, Simulación CAE, Transmisión automática

Citation: Ramírez-Ceja, Axel Iván, Manríquez-Padilla, Carlos Gustavo, Pérez-Cruz, Ángel and Torrez-Rico, Luis Armando. [2024]. Design of a three-speed automatic transmission system with reverse for all-terrain vehicles (ATV). Journal of Mechanical Engineering. 8[21]-1-12: e20821112.

Introduction

The design of vehicle transmissions is a fundamental process in automotive development and innovation, as it allows vehicles to operate effectively in various terrains and under different driving conditions. To achieve this, it is essential to carry out a thorough analysis of the power and torque requirements necessary for the vehicle to perform its functions properly. Several research studies on this subject have been documented in the literature. For example, CENIDET (Centro Nacional de Investigación y Desarrollo) mathematically modelled the mechanical part of an electric vehicle, determining the differential equation that describes the forces exerted by the road and the equations that govern its transmission (M. Durán, 2009). For its part, the University of Chile developed a power system for a single-seater vehicle, using simulations of the SolidWorks© 2015 Motion Analysis module to determine the power requirements based on the Theo Jansen mechanism (Andrade, M. A. L., 2016).

The power requirements are directly related to the exhaust emissions as a function of the driving dynamics, which in turn reflects the engine load. Thus, the driving dynamics calculation must consider the five main resistances that affect engine load: wheel force (Fw), drag resistance (Rd), rolling resistance (Rr), gradient resistance (Rg) and acceleration resistance (Ra) (Song, J., & Cha, J., 2021).

Once the power requirements are established, the design criteria for the drive system can be defined. For example, Zarate, W. E. H. (2020) evaluated the design criteria for an electronic continuously variable transmission (E-CVT), considering as initial criteria the maximum torques and the rated power of the three motors that make up the powertrain, and then defining the characteristics of the planetary gears, including dimensions, module, and number of teeth. Similarly, Pórtilla, L. V., et al. (2013) emphasised the importance of the type of material from which the components of the transmission system are manufactured, highlighting the relevance of strength and reliability analysis, as well as the appropriate selection of materials based on the normal tensile stresses and shear stresses to which the system is subjected.

The development of transmissions for vehicles is not only limited to internal combustion vehicles, as can be seen in the work carried out at the Escuela Tecnológica Instituto Técnico Central in Bogotá, where a transmission was adapted to improve the efficiency and performance of a human traction vehicle (VTH), Castro Escobar, W. A., & Ramírez Moreno, L. E. (2024). The University of the Armed Forces also developed a transmission that allows coupling an internal combustion engine with an electric motor in very extreme conditions, with slopes of 15° and an engine of 486 kg, which makes the development and selection of materials and components a complex and interesting work, the difference to what is proposed in this article is that this work opts for the analysis and selection of a manual transmission. Gavilanes, A., Arturo, C., et al. (2024).

Taking into consideration the above, this article focuses on the design of an automatic transmission for an all-terrain vehicle (ATV), starting from the power curve generated by the engine and the power requirements of the road. The main objective is to design the gear and clutch layout of a conventional three-speed automatic transmission with reverse, so that it meets the specific power requirements of the vehicle. In addition, the correct operation of the proposed design will be validated through a series of numerical experiments consisting of static structural and dynamic multi-physical simulations of the gears that make up the transmission ratios of the planetary systems using software based on finite element theory

.

Development of headings and subheadings of the article with subsequent numbers

Design criteria

We start with the parameterisation of the vehicle to be analysed, taking as a basis the chassis of an Italika© 150 ATV. Figure 1 shows the dimensions of the vehicle and the wheelbase.

ISSN: 2531-2189
RENIECYT-CONAHCYT: 1702902

Ramírez-Ceja, Axel Iván, Manríquez-Padilla, Carlos Gustavo, Pérez-Cruz, Ángel and Torrez-Rico, Luis Armando. [2024]. Design of a three-speed automatic transmission system with reverse for all-terrain vehicles (ATV). Journal of Mechanical Engineering. 8[21]-1-12: e20821112
DOI: https://doi.org/10.35429/JME.2024.8.21.2.12

Box 1

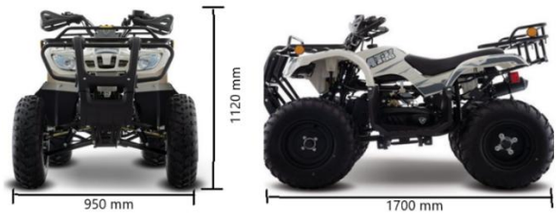

a) b)

Figure 1

a) Height and width of the vehicle b) Wheelbase of the vehicle

Source: Own elaboration

Subsequently, Table 1 details the system design criteria that underpin the transmission box proposal developed in this work.

Box 2

Table 1

Numerical vehicle design criteria.

Experiment conditions	Value
Road slope	Variable according to graph
Wind speed	1 km/h
Rolling resistance coefficient	0.092
Drag coefficient	0.62
Air density	1.18 kg/m^3
Dynamic radius	0.2667 m
Vehicle parameters	Valor
Rim diameter	0.254 m
Tyre size	21\7 - 10
ATV total mass (with rider and transmission)	245 kg
Total frontal area of ATV (with rider)	1.031 m^2
Centre of mass in X	1.34 m
Centre of mass in Y	1.21 m
Centre of mass in Z	0.60 m
Engine size	177.3 cc
Gear ratios	Value
M_{v1}	0.266
M_{v2}	0.53
M_{v3}	1
$M_{v\ reversa}$	0.2

Source: Own elaboration

Once the chassis model has been selected, a rider with an average height of 1900 mm is chosen. Using SolidWorks© software, a virtual model of the ATV including the rider is developed, as shown in Figure 2. In this process, the total frontal area of the vehicle is calculated together with the rider.

Box 3

Figure 2

CAD model of the rider with the ATV

Source: Own elaboration

In addition to the criteria presented in Table 1, specific objectives for the possible implementation of the design are set out below:

- **Light weight:** The design should be as light as possible to optimise vehicle performance.
- **Number of drivetrains:** The vehicle should have three forward gears and one reverse gear.
- **Drive cycle:** The vehicle shall be able to move according to the driving cycle on slopes, as illustrated in Figure 3.
- **Engine power and torque curve:** The engine selected to power the vehicle develops the power and torque curve shown in Figure 4.

Box 4

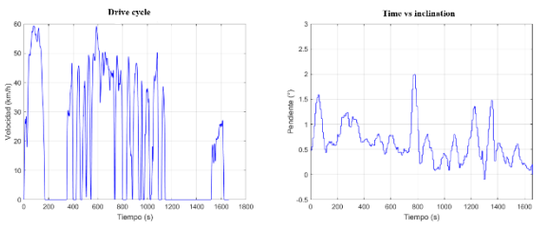

a) b)

Figure 3

a) Management cycle and b) Terrain slope.

Source: Own elaboration

ISSN: 2531-2189
RENIECYT-CONAHCYT: 1702902

Ramírez-Ceja, Axel Iván, Manríquez-Padilla, Carlos Gustavo, Pérez-Cruz, Ángel and Torrez-Rico, Luis Armando. [2024]. Design of a three-speed automatic transmission system with reverse for all-terrain vehicles (ATV). Journal of Mechanical Engineering. 8[21]-1-12: e20821112
DOI: https://doi.org/10.35429/JME.2024.8.21.2.12

Box 5

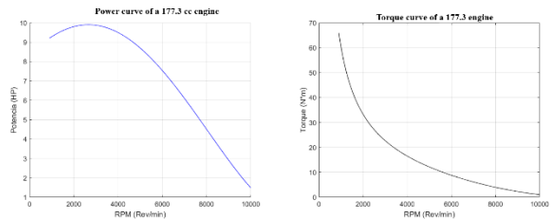

Figure 4

a) Management cycle and b) Slope of the terrain
Source: Own elaboration

By considering weight criteria, transmission functionality, hill performance and engine characteristics, it is sought to ensure that the vehicle not only meets the technical requirements, but also adapts to the actual operating conditions. This holistic approach ensures that the final design is efficient, effective and suitable for implementation in the intended context of use.

Power requirements

To meet the above-mentioned criteria and the specific parameters of the ATC, it is essential to consider the power requirements of the ATC. These requirements are directly related to the driving resistances faced by vehicles in general. As illustrated in Figure 5, there are several forces that affect vehicle dynamics, which must be overcome and taken into account when designing any type of automotive transmission.

Box 6

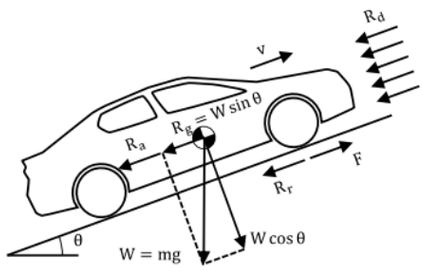

Figure 5

Forces affecting vehicle dynamics
Source: (Song, J., & Cha, J., 2021)

The total resistance to conduction can be calculated using the following expression.

$$F_w = R_r + R_d + R_g + R_a \quad (1)$$

where, R_r represents the rolling resistance force, R_d represents the drag resistance force of the air, R_g represents the resistance of the road slope, and R_a represents the acceleration resistance (Song, J., & Cha, J., 2021).

The air drag force models the opposing force that a wind volume presents when it is displaced in order for the vehicle to take its place. It is calculated by:

$$R_d = 0.5\, Cd\, A\rho v^2 \quad (2)$$

In equation (2), the coefficient Cd is the dimensional drag coefficient, while A contains the value of the frontal area of the vehicle in metres, ρ represents the value of the air density in kg/m^3, and v represents the ratio of vehicle speed to wind speed at m/s.

Rolling resistance force, R_r, contains the magnitude of the opposing force that the road exerts on the wheel, thus preventing its movement, and is determined by the following expression:

$$R_r = \left(Csr + Cdr\left(\frac{v}{100}\right)^{2.5}\right) * Wcos(\theta) \quad (3)$$

Where;

$$Csr = -514.7\left(\frac{Ptire}{100}\right)^3 + 53.72\left(\frac{Ptire}{100}\right)^2 - 1.877\left(\frac{Ptire}{100}\right) + 0.03051 \quad (4)$$

$$Cdr = -793.1\left(\frac{Ptire}{100}\right)^3 + 83.98\left(\frac{Ptire}{100}\right)^2 - 2.977\left(\frac{Ptire}{100}\right) + 0.0375 \quad (5)$$

while$v$, represents the speed of the vehicle in m/s, W is the weight of the vehicle in N, Θ son los grados de inclinación del camino y *Ptire* representa a la presión de la rueda en unidades bar.

On the other hand, the slope resistance, R_g, indicates the magnitude of the force required to keep the vehicle in a steady state when moving on a road with a gradient θ. The slope resistance is determined using:

$$R_g = Wsin(\theta) \quad (6)$$

Where, W, represents the proportional weight of the vehicle.

ISSN: 2531-2189
RENIECYT-CONAHCYT: 1702902

Ramírez-Ceja, Axel Iván, Manríquez-Padilla, Carlos Gustavo, Pérez-Cruz, Ángel and Torrez-Rico, Luis Armando. [2024]. Design of a three-speed automatic transmission system with reverse for all-terrain vehicles (ATV). Journal of Mechanical Engineering. 8[21]-1-12: e20821112
DOI: https://doi.org/10.35429/JME.2024.8.21.2.12

In addition to the acceleration resistance, R_a, determines the amount of force required to increase the vehicle speed from an initial speed to a final speed in a given time.

$$R_a = ma \qquad (7)$$

where, m represents the mass of the vehicle and a represents the acceleration of the vehicle. (m/s^2).

Based on the elements collected so far, MALAB© is used to analyse the behaviour of the engine power and torque distribution as a function of time during the driving cycle. This analysis allows to start the selection of commercial components for the final design of the transmission system.

Transmission design

For the design of this transmission, planetary gear systems have been used, which are composed of a sun gear (central gear), planetary gears (intermediate gears) and a ring gear (external gear with internal teeth), as shown in Figure 6.

Box 7

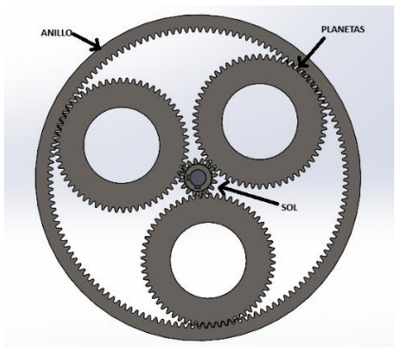

Figure 6
Planetary gear system
Source: Own elaboration

To establish the gear ratios presented in Table 1, it is necessary to select the module, pressure angle and number of teeth of the gears as shown in Table 2. In this case, two planetary systems with a single ring gear arrangement have been used, which are connected by an arm and a central shaft, as shown in Figure 7.

Box 8

Table 2
Gear selection

Gear design			
Position	No teeth	Module	Ang. Pressure °
Solar 1	16	2	20
Planets 1	60	2	20
Ring	136	2	20
Solar 2	16	2	20
Planets 2	68	2	20

Source: Own elaboration

Box 9

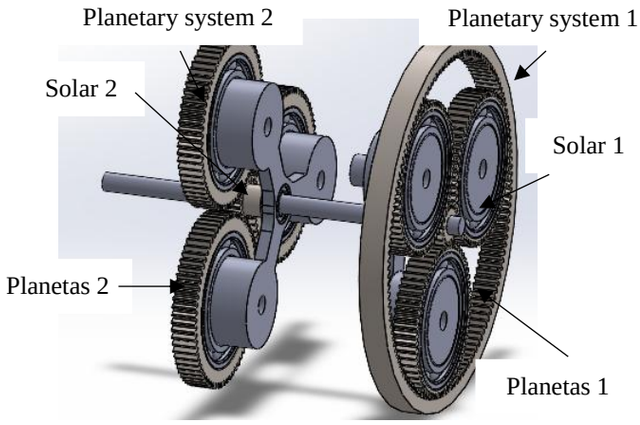

Figure 7
Planetary gear system
Source: Own elaboration

With this arrangement, it is intended that, with the help of clutches, the drive trains can be configured to transmit the engine power to the wheels. In first gear, the ring gear is required to remain completely static by actuating the clutches, thus allowing the sun gear of the first planetary system to rotate with the angular velocity of the engine. This motion is transmitted to the planets, of which the connected output shaft generates the first gear ratio.

For the second gear, the solar gear of the second system rotates with the power input of the engine, transmitting the power to the planets of that system. By disengaging the clutch system that holds the ring stationary, the planets can rotate it, thus transmitting motion to the planets of the first system, and again, the shaft connected to these planets allows the output of the second ratio.

ISSN: 2531-2189
RENIECYT-CONAHCYT: 1702902

Ramírez-Ceja, Axel Iván, Manríquez-Padilla, Carlos Gustavo, Pérez-Cruz, Ángel and Torrez-Rico, Luis Armando. [2024]. Design of a three-speed automatic transmission system with reverse for all-terrain vehicles (ATV). Journal of Mechanical Engineering. 8[21]-1-12: e20821112
DOI: https://doi.org/10.35429/JME.2024.8.21.2.12

For the third gear, the rotational motion of both the planets and the ring is prevented in both systems, so that the whole assembly rotates at the same speed as the solar gear, which coincides with the input speed of the motor, thus achieving a 1:1 ratio.

For reverse gearing, a third planetary system is commonly used. However, due to sizing limitations of the test vehicle, a configuration is proposed that allows the reverse motion to be performed using only two planetary systems. This configuration requires decoupling the output axis of the planets and coupling it to the ring, which will generate the motion of the output axis in the opposite direction. It is necessary to decouple the planetary systems, which are connected by means of two crown gears that are kept in contact through clutches as required.

Finally, rotational movement around the solar gear of the planets is prevented, allowing the planets to move on their own axis. In this way, the ring gear is made to rotate in the opposite direction, transmitting the speed ratio of the reverse gear. The final distribution can be seen in Figure 8.

Box 10

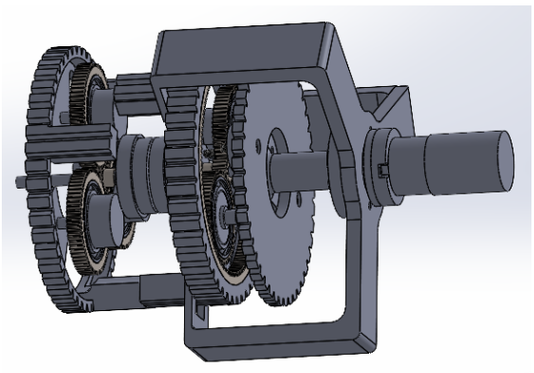

Figure 8
Main transmission distribution
Source: Own elaboration

As a final part of the transmission design, a proposal is made for the housing that will contain the whole mechanism as shown in figure 9 together with the clutch layout.

Box 11

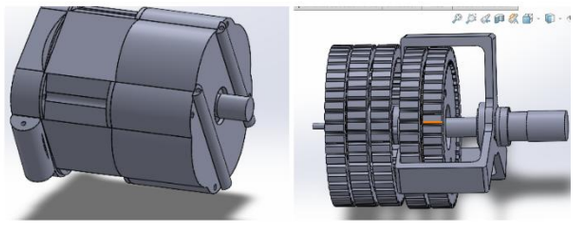

a) b)

Figure 9
a) Proposed housing b) Clutch distribution
Source: Own elaboration

Structural static analysis of critical components

With the design established, it is essential to verify that the selected components can withstand the critical loads that the transmission will demand. For this purpose, a structural static analysis based on the finite element theory is carried out using the commercial software ANSYS Workbench©. The maximum torque expected in the case is taken as a reference, and the analysis will be carried out on the critical elements of the assembly. In particular, a torque of 330 Nm is used for the analysis on the central shaft, as well as on the sun gears and the 60-tooth gear, which is the component with the smallest amount of material.

In addition, a structural analysis of the *housing* supports will be carried out, considering a total mass of 50 kg. In this case, the housing supports must be able to withstand at least 490.5 N, which means that they must resist 2,662 kPa. Next, figure 10 shows the analysis of the central axis where the maximum torque is applied to the solar gears, figure 11 shows the same torque, but in the 60-tooth gear, which is the one that contains the least material, and finally, figure 12 shows the analysis of the *housing*.

ISSN: 2531-2189
RENIECYT-CONAHCYT: 1702902

Ramírez-Ceja, Axel Iván, Manríquez-Padilla, Carlos Gustavo, Pérez-Cruz, Ángel and Torrez-Rico, Luis Armando. [2024]. Design of a three-speed automatic transmission system with reverse for all-terrain vehicles (ATV). Journal of Mechanical Engineering. 8[21]-1-12: e20821112
DOI: https://doi.org/10.35429/JME.2024.8.21.2.12

Box 12

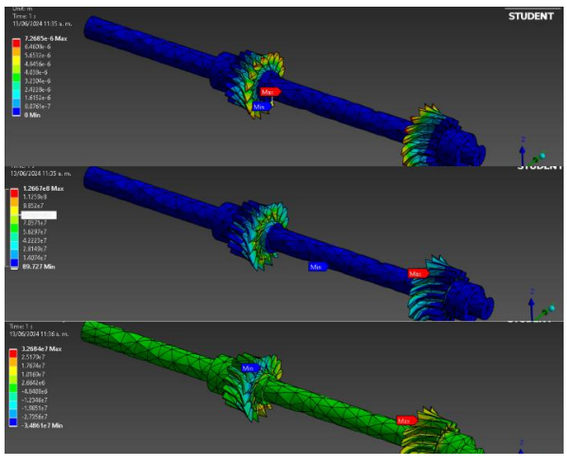

Figure 10
ANSYS© analysis of deformation, Von-Mises stress and shear stress on axis and suns
Source: Own elaboration

Box 13

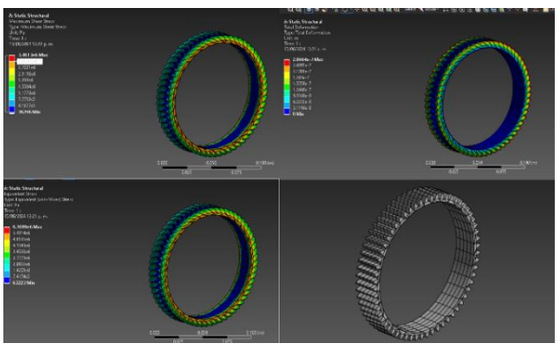

Figure 11
ANSYS© analysis of deformation, Von-Mises stress and shear forces on the 60-tooth planet
Source: Own elaboration

Box 14

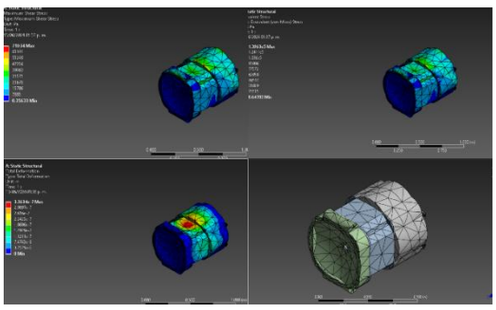

Figure 12
ANSYS© analysis of deformation, Von-Mises stress and shear forces on the *housing*
Source: Own elaboration

Dynamic gear simulation

With the structure analysis developed in ANSYS© it is possible to determine whether or not the material will support the loads to which the mechanism is subjected. However, these studies do not ensure the correct movement of the proposed design, so it is necessary to carry out a dynamic study of the mechanism to verify the proper functioning of the transmission system. For this purpose, the ADAMS© commercial software has been used, which allows the power curve of the motor to be introduced in order to verify the transformation of the power at the output of the system. In addition, the software allows the presence of possible interferences in the components, derived from a deficient design, to be determined. Within the software, only the distribution of the planetary systems has been used for simulation, as can be seen in Figure 13.

Box 15

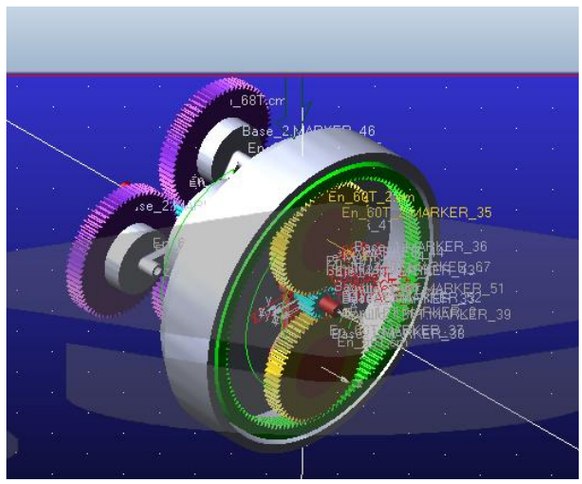

Figure 13
Dynamic simulation in ADAMS©
Source: Own elaboration

Results

Based on the elements collected so far, MATLAB© is used to analyse the behaviour of the engine power and torque distribution as a function of time during the driving cycle. Figure 14 can be consulted for a detailed visualisation, where the maximum and minimum torque and power that the vehicle delivers throughout the driving cycle to pass over the established terrain can be observed.

ISSN: 2531-2189
RENIECYT-CONAHCYT: 1702902

Ramírez-Ceja, Axel Iván, Manríquez-Padilla, Carlos Gustavo, Pérez-Cruz, Ángel and Torrez-Rico, Luis Armando. [2024]. Design of a three-speed automatic transmission system with reverse for all-terrain vehicles (ATV). Journal of Mechanical Engineering. 8[21]-1-12: e20821112
DOI: https://doi.org/10.35429/JME.2024.8.21.2.12

Box 16

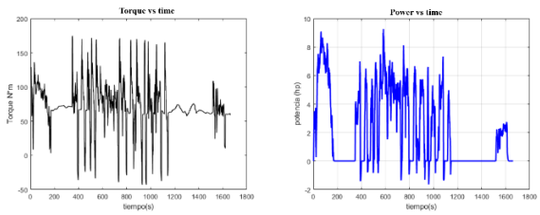

Figure 14

a) Torque vs. time and b) Power vs. time.

Source: Own elaboration

Figure 15 shows how the slope changes over the course of the driving cycle and the power required by the vehicle to pass through the terrain described by the slopes.

Box 17

a) b)

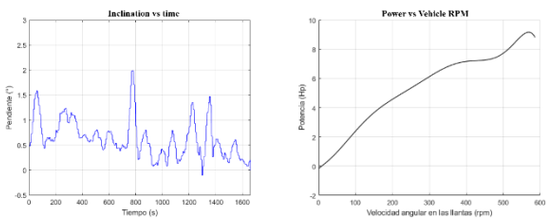

Figure 15

a) a) Slope vs. time and b) Power requirement.

Source: Own elaboration

On carrying out the test using simulink and obtaining the graph of torque vs. time, power vs. time and finally the graph of speed vs. time. It is observed that there is similarity in the graphs obtained. When testing with Simulink and obtaining the graphs of torque vs. time, power vs. time, and speed vs. time, there is a notable similarity in the graphs obtained, as shown in Figure 16.

Box 18

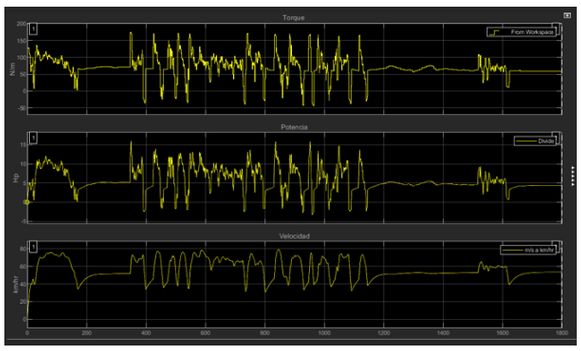

Figure 16

Testing graphs with Simulink.

Source: Own elaboration

Figure 17a shows the transmission response with the gear ratios, in red colour the Mv1, in blue colour the Mv2, in yellow colour the Mv3 and in green colour the Mvr, in the same order for the torque response, it can be seen in Figure 17b.

Box 19

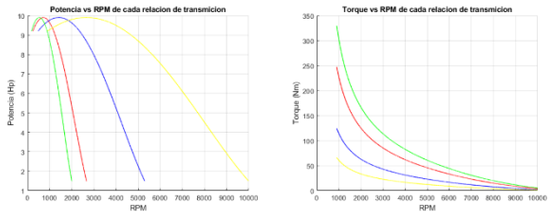

a) b)

Figure 17

a) Power vs transmission rpm and b) Torque vs transmission rpm.

Source: Own elaboration

Figure 18 shows the comparison between the power output and the power required to travel the set route, which includes both the road gradients and the speed variations captured in the driving cycle. The black graph represents the power required to complete this route. As can be seen, the graphs of the power supplied by the transmission confirm that the proposed transmission system adequately transforms the power coming from the engine in such a way that it allows the vehicle to drive along the selected road following the driving cycle described in Figure 3a.

ISSN: 2531-2189
RENIECYT-CONAHCYT: 1702902

Ramírez-Ceja, Axel Iván, Manríquez-Padilla, Carlos Gustavo, Pérez-Cruz, Ángel and Torrez-Rico, Luis Armando. [2024]. Design of a three-speed automatic transmission system with reverse for all-terrain vehicles (ATV). Journal of Mechanical Engineering. 8[21]-1-12: e20821112
DOI: https://doi.org/10.35429/JME.2024.8.21.2.12

Box 20

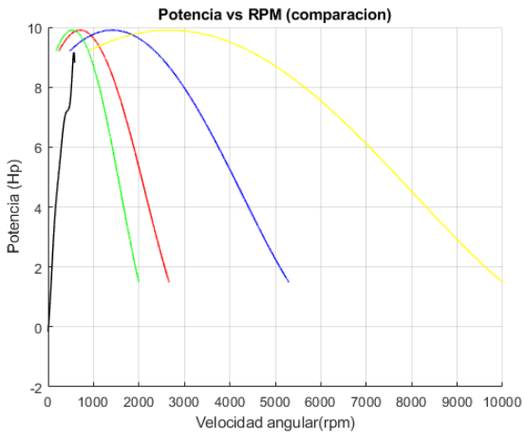

Figure 18

Comparison between the power required by the road and the power delivered by the transmission.

Source: Own elaboration

With these results the design can be concluded, leaving the configurations described above as follows and can be seen in figures 19 and 20, where the different configurations of the clutches can be seen, in figure 19a it can be seen how the crowns are fixed together with the ring to a clutch fixed to the housing, in 19b the clutch is released from the housing, allowing the crowns and ring to rotate; in figure 20b we can see how the arms are locked together, joining the movement of the suns to the planets and the ring and finally in figure 20b we can see how the crowns are separated and the movement of the planetary system 2 is locked and how the output shaft is moved to connect with the ring and the arms are locked together so that the planets only rotate on their own axis.

Box 21

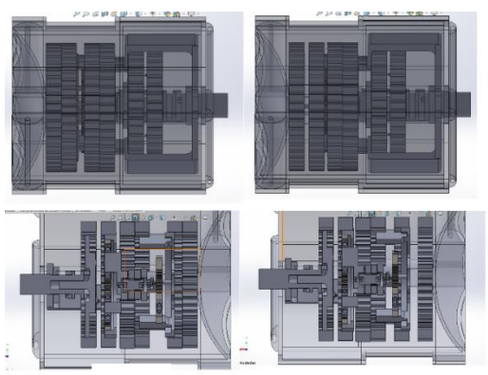

a) b)

Figure 19

a) march 1 and b) march 2.

Source: Own elaboration

Box 22

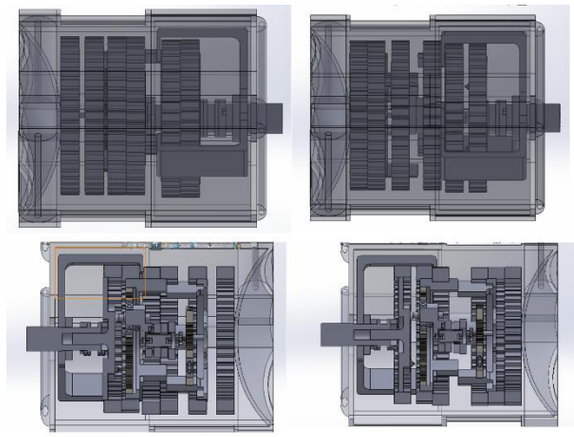

a) b)

Figure 20

b) March 3 and b) Reverse.

Source: Own elaboration

As mentioned above, it is necessary to verify that the elements support the expected loads. Structural steel has been selected as the main material for the internal components, its main characteristics can be seen in table 3, while for the housing aluminium Series 5000 has been selected, its properties are presented in table 4. The mechanical properties of steel and aluminium are presented in figures 11 and 12, respectively. It is important to mention that these data are standardised and are provided by ANSYS Workbench© as part of its material libraries.

Box 23

Table 3

Mechanical properties of structural steel obtained from ANSYS *Workbench* ©

Steel properties	
Mechanical property	**Value**
Young's modulus	2e11 Pa
Bulk modulus	1.667e11 Pa
Shear modulus	7.6923e10 Pa
Creep modulus	2.5e8 Pa

Source: Own elaboration

ISSN: 2531-2189
RENIECYT-CONAHCYT: 1702902

Ramírez-Ceja, Axel Iván, Manríquez-Padilla, Carlos Gustavo, Pérez-Cruz, Ángel and Torrez-Rico, Luis Armando. [2024]. Design of a three-speed automatic transmission system with reverse for all-terrain vehicles (ATV). Journal of Mechanical Engineering. 8[21]-1-12: e20821112
DOI: https://doi.org/10.35429/JME.2024.8.21.2.12

Box 24

Table 4

Mechanical properties of aluminium 5000 obtained from *ANSYS Workbench©*

Properties of aluminium	
Mechanical property	**Value**
Young's modulus	7.1e10 Pa
Bulk modulus	6.9608e10 Pa
Shear modulus	2.6692e10 Pa
Creep modulus	2.8e8 Pa

Source: Own elaboration

The results obtained in the structural static analysis carried out in ANSYS Workbench© are summarised in Table 5.

Box 25

Table 5

Results of ANSYS©

Análisis estructural				
Element	**Study**	**Minimo**	**Maximum**	**Average**
Shaft with suns	Deformation	0 m	7.2685e-6 m	7.9278 e-7 m
Shaft with suns	Von-Mises Stress	89.727 Pa	1.2667e8 Pa	1.3434e7 Pa
Shaft with suns	Shear Stress	3.4861e7 Pa	3.2684e7 Pa	25287 Pa
Planet 60 teeth	Deformation	0 m	2.8e-7 m	4.6558e-8 m
Planet 60 teeth	Von-Mises Stress	63223 Pa	6.1699e6 Pa	2.0598 e6Pa
Planet 60 teeth	Shear Stress	36206 Pa	3.4613e6 Pa	1.147e6 Pa
Housing	Deformation	0 m	3.3634e-7 m	2.3255e-8 m
Housing	Von-Mises Stress	0.64702 Pa	1.3963e5 Pa	13569 Pa
Housing	Shear Stress	0.35633 Pa	71034 Pa	7543.6 Pa

Source: Own elaboration

As can be seen in Table 5, the deformations are in the order of10^{-7} Pa and the greatest effort in the components is $1.3434 \cdot 10^{7}$ Pa. For the steel used, its yield stress is of the order of$2 \cdot 10^{11}$ Pa, so that the maximum stress in the transmission system is the $1.3434 \cdot 10^{7}$ de the creep resistance of the material. Therefore, it can be said that the transmission system supports the workloads adequately.

To finalise the validation of the proper functioning of the proposed transmission, a dynamic simulation is carried out with the help of the ADAMS© commercial software, as shown in the following figures.

Figure 21 shows the representation of the reverse, where the blue colour shows the input speed of the motor and the red one is the output which, with the change of sign, shows that it is turning towards the opposite side, achieving the reverse. Figure 22 shows the transition of the input and output between first and second speed with an increase in speed as time increases.

Box 26

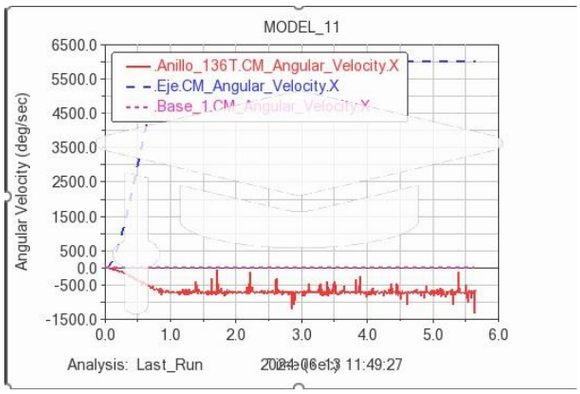

Figure 21

Angular exit speeds from first to third gear.

Source: Own elaboration

Box 27

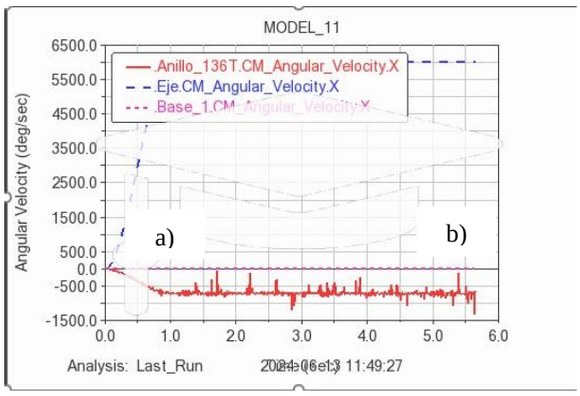

Figure 22

Reverse output angular speeds.

Source: Own elaboration

To appreciate the movement of the transmission, a link to videos of the transmission configurations and the dynamic behaviour of the transmission is included, https://drive.google.com/drive/folders/1aRXZoZLg_rRX8rjhOMRphyDVrRsDpLXf?usp=drive_link.

ISSN: 2531-2189
RENIECYT-CONAHCYT: 1702902

Ramírez-Ceja, Axel Iván, Manríquez-Padilla, Carlos Gustavo, Pérez-Cruz, Ángel and Torrez-Rico, Luis Armando. [2024]. Design of a three-speed automatic transmission system with reverse for all-terrain vehicles (ATV). Journal of Mechanical Engineering. 8[21]-1-12: e20821112
DOI: https://doi.org/10.35429/JME.2024.8.21.2.12

Conclusions

At the end of the previous work, the proposal for the distribution of gears and clutches for the design of a conventional automatic transmission for an ATV vehicle has been completed, where it can be observed that in order to carry out different transmission ratios it is not necessary to use an excessive amount of gears, since with the help of a single planetary system the Mv1, Mv3 and reverse ratios are carried out, which allows saving space and components at the time of making the box, which is essential due to the limited space for the transmission that these vehicles have.

Furthermore, this work can serve as a small guide for the validation of any mechanism, showing the key points necessary for its validation and reliability, which would be: obtaining design criteria, numerical analysis, design sketch, validation of the resistance of the materials, numerical validation and dynamic simulation for the validation of the movement. It also serves as a background for future research such as the control system for the movement of the clutches or for a possible implementation of a prototype with this design proposal.

Declarations

Conflict of interest

The authors declare no conflict of interest. They have no known competing financial interests or personal relationships that could have appeared to influence the article reported in this article.

Author contribution

Ramírez-Ceja, Axel Ivan: Contributed to obtaining power requirements, vehicle parameterisation, CAD proposal and realisation, static structure simulation, dynamic CAE simulation and development of the written article.

Manríquez-Padilla, Carlos Gustavo: Contributed to the assessment and development of a Matlab code to determine the power requirements that allowed the development of the vehicle.

Pérez-Cruz, Angel: Contributed to the advice on the proposal of the vehicle dynamics to obtain the forces affecting the vehicle.

Torrez-Rico, Luis Armando: Contributed to the advice on the use of ADAMS© software.

Availability of data and materials

Contact the author of reference for any information or clarification related to the materials or data seen in the article.

Funding

No funding.

Acknowledgements

Thanks to the Universidad Autónoma de Querétaro for the tools provided for the realisation of this article.

Abbreviations

List abbreviations in alphabetical order.

ATV	All-Terrain Vehicle
CAD	Computer-Aided Design
CAE	Computer-Aided Engineering
CENIDET	National Research and Development Centre
E-CVT	Electronic Continuously Variable Transmission
MBD	Multi Body Dynamics

References

Antecedents

Andrade, m. a. l. (2016). Diseño e implementación de sistema de potencia para un vehículo monoplaza con mecanismo de theo jansen. universidad de chile.

Durán, m., guerrero-ramírez, g., & claudio, a. (2009). determinación de los requerimientos de par, velocidad angular y potencia para el motor de un vehículo eléctrico. congreso anual de la asociación de méxico de control automático.

Castro Escobar, W. A., & Ramírez Moreno, L. E. (2024). Selección y adaptación de un sistema de transmisión para un vehículo de tracción humana VTH de competencia.

Gavilanes, A., Arturo, C., Vivanco Sopa, J. D., & Cruz Arcos, G. M. Dimensionamiento e implementación del sistema motor, transmisión y eléctrico del vehículo prototipo tipo tumbler.

ISSN: 2531-2189
RENIECYT-CONAHCYT: 1702902

Ramírez-Ceja, Axel Iván, Manríquez-Padilla, Carlos Gustavo, Pérez-Cruz, Ángel and Torrez-Rico, Luis Armando. [2024]. Design of a three-speed automatic transmission system with reverse for all-terrain vehicles (ATV). Journal of Mechanical Engineering. 8[21]-1-12: e20821112
DOI: https://doi.org/10.35429/JME.2024.8.21.2.12

Basics

Song, j., & cha, j. (2021). analysis of driving dynamics considering driving resistances in on-road driving. energies, 14(12), 3408. https://doi.org/10.3390/en14123408

Zarate, w. e. h. (2020). evaluación de los criterios de diseño de los engranajes magnéticos para una transmisión e-cvt en los vehiculos híbridos. universidad de ingeniería y tecnología (utec).

ISSN: 2531-2189
RENIECYT-CONAHCYT: 1702902

Ramírez-Ceja, Axel Iván, Manríquez-Padilla, Carlos Gustavo, Pérez-Cruz, Ángel and Torrez-Rico, Luis Armando. [2024]. Design of a three-speed automatic transmission system with reverse for all-terrain vehicles (ATV). Journal of Mechanical Engineering. 8[21]-1-12: e20821112
DOI: https://doi.org/10.35429/JME.2024.8.21.2.12

Journal of Mechanical Engineering 8[21]1-11: e30821111
Article

Camera calibration procedure for extracting form deviation features in machined parts through computer vision algorithms

Procedimiento de calibración de cámaras para la extracción de características de desviación de forma en piezas mecanizadas mediante algoritmos de visión por ordenador

Meraz-Méndez, Manuel*[a], Muñoz-López, Luis Enrique[b], Reynoso-Jardón, Elva Lilia[c] and Corral-Ramírez, Guadalupe[d]

[a] Universidad Tecnológica de Chihuahua • S-4565-2018 • 0000-0001-8254-957 • 250582
[b] Universidad Tecnológica de Chihuahua • X-9772-2019 • 0000-0003-3184-7602 • 456614
[c] Universidad Autónoma de Ciudad Juárez • AFZ-2483-2022 • 0000-0002-0729-2822 • 264446
[d] Universidad Tecnológica de Chihuahua • IDX-9786-2019 • 0000-0003-4874-4036 • 520946

CONAHCYT classification:

Area: Engineering
Field: Industrial engineer
Discipline: Programming and manufacturing
Sub-discipline: Technological innovation

https://doi.org/10.35429/JME.2024.8.21.3.11
Article History:
Received: January 30, 2024
Accepted: December 31, 2024

* ✉ [mmeraz@utch.edu.mx]

Abstract

Camera calibration and computer vision algorithms have revolutionized form deviation analysis in machined parts. This study focuses on the camera calibration procedure for extracting form deviation features using 45 image captures of curves, lines, and slope geometries. The calibration process involves capturing high-quality images of a calibration pattern with known dimensions from various angles and orientations. The acquired images are then processed using computer vision algorithms to estimate the camera parameters. Once calibrated, the camera captures images of machined parts with curve, line, and slope geometries. Computer vision algorithms are applied to analyze these images and extract relevant form deviation features. The results demonstrate the effectiveness of the camera calibration procedure in accurately measuring form deviations in machined parts with curve, line, and slope geometries.

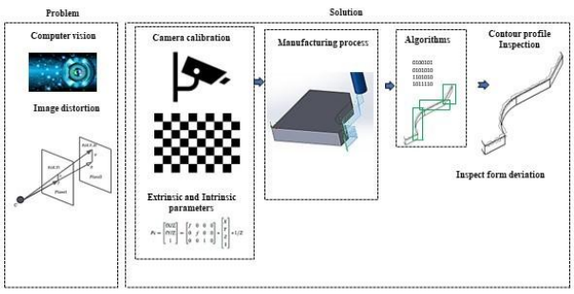

Computer vision, Calibration, Image processing

Resumen

La calibración de cámaras y los algoritmos de visión por computadora han revolucionado el análisis de desviaciones de forma en piezas mecanizadas. Este estudio se centra en el procedimiento de calibración de cámaras para la extracción de características de desviación de forma mediante 45 capturas de imágenes de curvas, líneas y geometrías de pendiente. El proceso de calibración implica capturar imágenes de alta calidad de un patrón de calibración con dimensiones conocidas desde varios ángulos y orientaciones. Las imágenes adquiridas se procesan luego utilizando algoritmos de visión por computadora para estimar los parámetros de la cámara. Una vez calibrada, la cámara se utiliza para capturar imágenes de piezas mecanizadas con geometrías de curvas, líneas y pendientes.

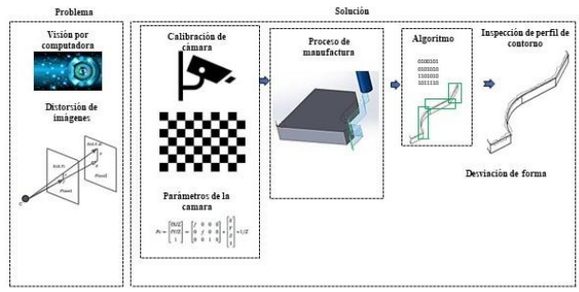

Visión por computadora, Calibración, Procesamiento de imágenes

Citation: Meraz-Méndez, Manuel, Muñoz-López, Luis Enrique, Reynoso-Jardón, Elva Lilia and Corral- Ramírez, Guadalupe. [2024]. Camera calibration procedure for extracting form deviation features in machined parts through computer vision algorithms. Journal of Mechanical Engineering. 8[21]-1-: e30821111.

Introduction

Computer vision technology has revolutionized various industries, including manufacturing, by enabling precise analysis of part geometry and detecting shape deviation features (Wang et al., 2009). This technology plays a crucial role in CNC machining, where even minor deviations can significantly impact the performance and functionality of machined parts (Feng et al., 2019). By utilizing advanced image processing techniques, such as spatial filtering and Gaussian smoothing, computer vision enhances the quality and interpretability of captured images, providing a solid foundation for shape contour extraction and Fourier descriptor calculations.

Furthermore, computer vision technology allows for the identification of complex patterns and non-linear features in data from different sources, making it highly effective in transforming raw data into feature spaces and generating models for prediction, classification, detection, regression, and forecasting (Ngiam et al., 2011).

Such an integrated real and virtual presentation and interaction technology, which incorporates computer vision, has been highly recommended by researchers as a potential approach to developing more powerful and supportive learning environments (Feng et al., 2019).

Additionally, thanks to deep learning techniques, computer vision algorithms have made significant progress in tasks such as image classification, object detection, and image segmentation. These advancements have not only replaced traditional machine learning algorithms but also improved the accuracy and efficiency of computer vision applications in various research fields, including computer vision for medical imaging, autonomous vehicles, surveillance systems, and robotics (Yang, 2020).

Machine learning techniques, particularly deep learning, have played a crucial role in the advancement of computer vision algorithms. They have helped extract meaningful features from images and videos, enabling computers to identify and process objects like humans.

In manufacturing, machine learning techniques have emerged as viable solutions to overcome the challenges faced by complex manufacturing systems. These techniques can effectively analyze data from different sources, find complex patterns, and transform raw data into models for prediction, detection, classification, regression, or forecasting. These innovative approaches have the potential to revolutionize manufacturing processes by optimizing efficiency, minimizing errors, and improving overall product quality (Voulodimos et al., 2018).

In summary, computer vision technology, with its advanced image processing techniques and machine learning algorithms, plays a crucial role in various fields including manufacturing (Feng et al., 2019). It enables accurate analysis, prediction, and classification of data, leading to improved efficiency and quality in manufacturing processes (Voulodimos et al., 2018). In today's rapidly changing world, the significance of accurate forecasting and analysis in various fields, including manufacturing, cannot be overstated (Feng et al., 2019).

Background

Burger et al. (2022) state for image processing it is necessary to address perspective distortion, as the positioning of a lens distorts the geometry of objects observed in image processing.

An uncalibrated camera will capture distorted images. Sun et al (2014) defines calibration as the process of identifying the internal and optical properties of a camera (intrinsic parameters) and/or establishing the three-dimensional position and orientation of the camera concerning a global coordinate system (extrinsic parameters).

Figure 1 defines the relationship of the distortion of an image, which is given by the distance between the projection center C and the plane where the point P is located. This distance is determined by the Z coordinate of the point, and the distance separating the image plane from the projection center is called the focal length f. Based on this, the extrinsic calibration parameters are defined as the focal length, the rotation matrix, and the translation matrix.

ISSN: 2531-2189
RENIECYT-CONAHCYT: 1702902

Meraz-Méndez, Manuel, Muñoz-López, Luis Enrique, Reynoso-Jardón, Elva Lilia and Corral- Ramírez, Guadalupe. [2024]. Camera calibration procedure for extracting form deviation features in machined parts through computer vision algorithms. Journal of Mechanical Engineering. 8[21]-1-: e30821111.
DOI: https://doi.org/10.35429/JME.2024.8.21.3.11

Box 1

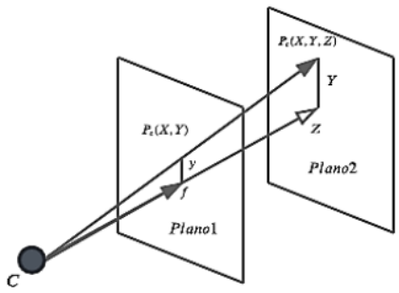

Figure 1
Image perspective distortion

To determine these parameters, similar triangles are applied in the following equation 1:

$$\frac{Y}{z} = \frac{y}{f} \qquad [1]$$

The focal length f depends on the lens and is associated with the power or magnification. In perspective projection, we start from a point with coordinates X, Y, Z, 1 and end at a point Pc with coordinates fX/Z, fY/Z, 1. Thus, this projection is expressed in Equation 2 as a scaling through a matrix product with the scaling factor f.

$$P_c = \begin{bmatrix} \frac{fX}{z} \\ \frac{fY}{z} \\ 1 \end{bmatrix} = \begin{bmatrix} f & 0 & 0 & 0 \\ 0 & f & 0 & 0 \\ 0 & 0 & 1 & 0 \end{bmatrix} * \begin{bmatrix} X \\ Y \\ z \\ 1 \end{bmatrix} * \frac{1}{z} \qquad [2]$$

Where Pc is the three-dimensional point P in metric units (real units) such as meters or centimeters. However, the units of the images are pixels. To convert from metric units to pixels, we use the constants in Equations 3 and 4, such as the pixel density per meter of the sensor, through a scaling transformation as shown in Equation 5.

$$k\_u[píxel/metro] \qquad [3]$$

$$k\_v[píxel/metro] \qquad [4]$$

$$P_C = \begin{bmatrix} k_v & 0 & v_0 \\ 0 & k_u & v_0 \\ 0 & 0 & 1 \end{bmatrix} * Pc \qquad [5]$$

The projection of a point, in this case, Pc, is a fundamental process in the representation of objects in an imaging system, based on the background theory a methodology is proposed to calibrate a camera mounted in a CNC machine.

Methodology

The methodology for applying computer vision technology in a CNC machine is presented in Figure 2.

Box 2

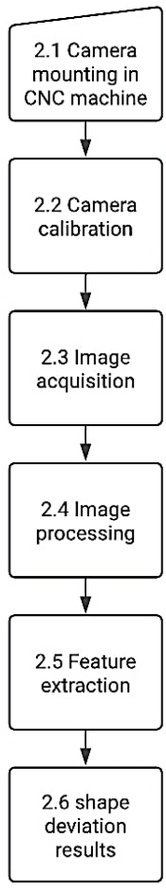

Figure 2
Methodology

The methodology involves several steps (Voulodimos et al., 2018). First, the camera in a CNC machine is mounted and calibrated, next images of the manufactured parts are captured using the camera. Then, advanced image processing techniques, such as spatial filtering and Gaussian smoothing, are applied to enhance the quality and interpretability of the images (Feng et al., 2019). Next, shape contour features are extracted from the enhanced images to extract shape deviation features (Voulodimos et al., 2018).

ISSN: 2531-2189
RENIECYT-CONAHCYT: 1702902

Meraz-Méndez, Manuel, Muñoz-López, Luis Enrique, Reynoso-Jardón, Elva Lilia and Corral- Ramírez, Guadalupe. [2024]. Camera calibration procedure for extracting form deviation features in machined parts through computer vision algorithms. Journal of Mechanical Engineering. 8[21]-1-: e30821111.
DOI: https://doi.org/10.35429/JME.2024.8.21.3.11

Shape deviation features allow for precise analysis of part geometry and identification of any deviations from the intended shape. This is particularly important in CNC machining, where even minor deviations can significantly impact the performance and functionality of a machined part. Computer vision technology, combined with machine learning techniques, has emerged as a valuable tool in manufacturing.

Camera mounting and calibration of the image acquisition system

The spatial calibration of the acquisition system is a procedure to determine the intrinsic and extrinsic parameters of the camera, such as the camera focal length, rotation matrix I, and translation matrix (t) for the image acquisition process. The calibration procedure determines the intrinsic parameters ku, kv, u0, and v0 which are substituted into the intrinsic matrix expressed in Equation 6. These parameters define the 3D position of the camera on the CNC machine for image capture.

$$C_k = \begin{bmatrix} k_v & 0 & v_0 \\ 0 & k_u & v_0 \\ 0 & 0 & 1 \end{bmatrix} \quad [6]$$

where *ku* is the horizontal focal length of the lens in millimeters (X-axis), *kv* is the vertical focal length of the lens in millimeters (Y-axis), and [*u0, v0*] are the coordinates of the image center in pixels.

To carry out the calibration, a calibration pattern was created, which consists of squares distributed uniformly at a predefined distance. The chessboard pattern was chosen as the calibration pattern printed on adhesive paper attached to a rectangular piece measuring 100x127 mm to prevent folding and warping. The pattern format consists of an even number (4) of squares along the Y-axis and an odd number (5) of squares along the X-axis.

The size of the squares is 23 mm. The representation of the calibration pattern is shown in Figure 3.

Box 3

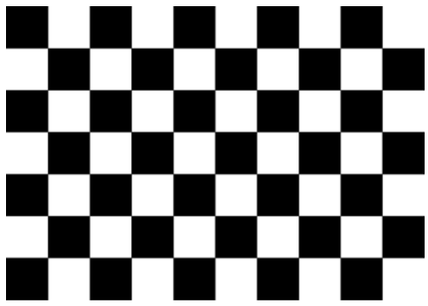

Figure 3
Calibration Pattern

Steps for calibration:

1. Preparation and mounting of the calibration pattern: The calibration pattern is placed on the machine press aligned parallel to the X and Y axes of the machine table.

2. Camera mounting: the camera is mounted on top of the CNC machine perpendicular to the table and parallel to the calibration pattern to eliminate distortion. The camera view should be clear and unobstructed as shown in Figure 4.

Box 4

Figure 4
Camera calibration procedure

3. Calibration Procedure: Following the recommendation of Mejia and Varona (2014), 3 calibration tests are conducted by capturing 12 images (totaling 36 images) of the calibration pattern, performing translations along the X and Y axes (See Appendix B) with respect to the CNC machine zero coordinates. The "Camera Calibrator" application of Matlab is used for calibration (refer to Figure 5).

ISSN: 2531-2189
RENIECYT-CONAHCYT: 1702902

Meraz-Méndez, Manuel, Muñoz-López, Luis Enrique, Reynoso-Jardón, Elva Lilia and Corral- Ramírez, Guadalupe. [2024]. Camera calibration procedure for extracting form deviation features in machined parts through computer vision algorithms. Journal of Mechanical Engineering. 8[21]-1-: e30821111.
DOI: https://doi.org/10.35429/JME.2024.8.21.3.11

4. Determination of Calibration Parameters: The algorithm proposed by Zhang (2000) is employed to determine the intrinsic and extrinsic camera parameters for each test (See Appendix section).

5. Calibration Evaluation: The calibration precision is evaluated using metrics such as reprojection error. Calibration parameters are adjusted if necessary, and the camera is recalibrated if the precision is unsatisfactory.

6. Application of Calibration: The intrinsic and extrinsic camera parameters are applied in the image capture process of the piece on the CNC machine table. Based on the calibration tests presented at the Appendix section, the camera position coordinates relative to the machine zero are determined as X −215.261, Y 34.405, Z 300.0, which generate minimal distortion. This will allow obtaining corrected and metrically precise images of the piece for analysis and processing.

7. Testing and Adjustment: Additional tests are carried out with the calibrated camera to ensure that it is capturing images with the required precision, and further adjustments are made if necessary.

Box 5

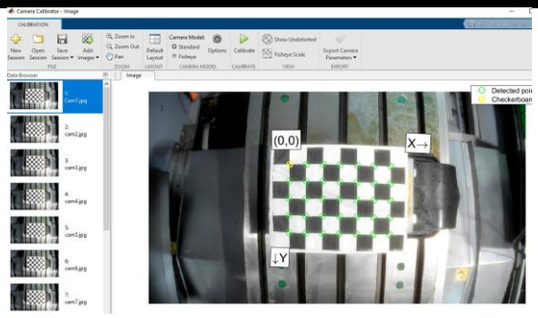

Figure 5
App Camera Calibrator

Source: Matlab 2021

Three tests were conducted for the final camera calibration, capturing 12 images for each test in various positions with consideration of translation and rotation. The results of the captured images are depicted in figures 6, 7 and 8 for each test.

Camera calibration tests:

Box 6

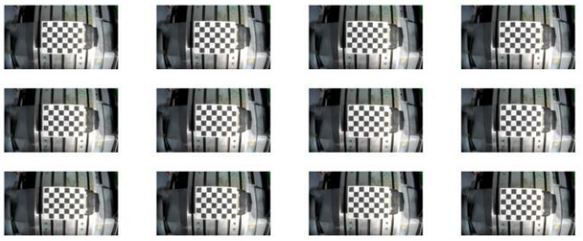

Figure 6
Images to calibration Test 1

Source: Matlab 2021

Box 7

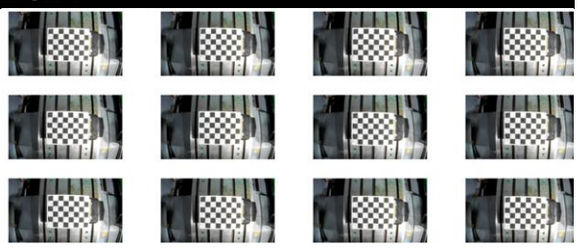

Figure 7
Images to calibration Test 2

Box 8

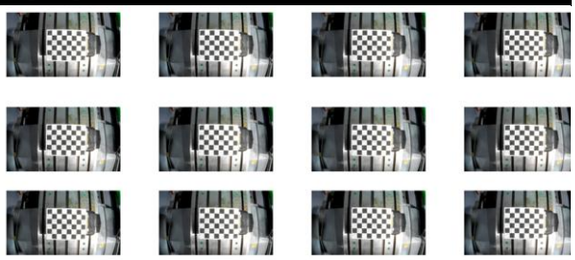

Figure 8
Images to calibration Test 3

The results for each test are shown in Table 1, which displays the camera's position relative to the machine coordinate system (MCS) zero for each test.

ISSN: 2531-2189
RENIECYT-CONAHCYT: 1702902

Meraz-Méndez, Manuel, Muñoz-López, Luis Enrique, Reynoso-Jardón, Elva Lilia and Corral- Ramírez, Guadalupe. [2024]. Camera calibration procedure for extracting form deviation features in machined parts through computer vision algorithms. Journal of Mechanical Engineering. 8[21]-1-: e30821111.
DOI: https://doi.org/10.35429/JME.2024.8.21.3.11

Box 9

Table 1

Calibration Coordinates results for Haas VF1 VMC Machine

Test	Calibration 1	Calibration 2	Calibration 3
1	-215.261 31.705	-218.161 20.505	-215.261 36.605
2	300.00	275.00	266.00
3	-215.261 38.205	-218.161 25.405	-215.261 37.705
4	300.00	275.00	266.00
5	-215.261 39.005	-218.161 27.105	-215.261 39.305
6	300.00	275.00	266.00
7	-215.261 36.305	-218.161 30.205	-215.261 34.205
8	300.00	275.00	266.00
9	-215.261 35.505	-218.161 33.405	-215.261 33.34 266.00
10	300.00	275.00	-215.261 32.205
11	-215.261 34.405	-218.161 36.605	266.00
12	300.00	275.00	-210.00 36.605 266.00
	-214.161 37.705	-215.26 36.605 275.00	-212.00 36.605 266.00
	300.00	-218.161 36.605	-214.76 36.605 266.00
	-213.461 37.705	275.00	-208.261 36.605
	300.00	-222.061 36.605	266.00
	-212.461 37.705	275.00	-206.961 36.605
	300.00	-224.061 36.605	266.00
	-216.361 37.705	275.00	-204.961 36.605
	300.00	-227.861 36.605	266.00
	-217.361 37.705	275.00	
	300.00	-213.161 36.605	
	-218.361 37.705	275.00	
	300.00		

Source [Own]

Calibration Results

The final camera calibration parameters were based on calibration test 3, as it resulted in the lowest reprojection errors with an average value of 0.28 pixels, which falls within the acceptable range of less than 1 pixel as defined by Zhang (2000). The intrinsic and extrinsic parameters from this test are shown in Figure 9.

Box 10

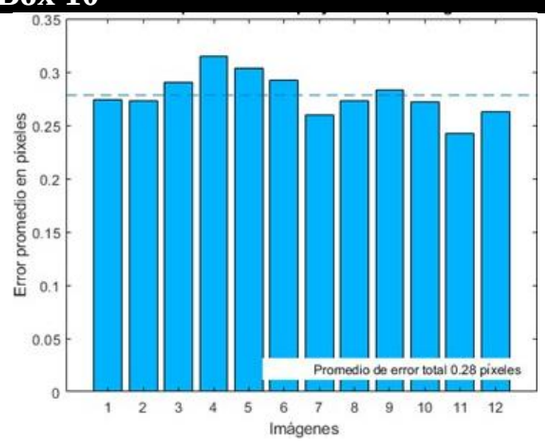

Figure 9

Average Projection Error

Image Acquisition

Image acquisition of the machining parts is carried out using a system consisting of a computer, acquisition card, and the HIKVISION IP camera mounted on the column of the CNC machine. The camera is positioned perpendicular to the table and parallel to the workpiece, as shown in Figure 10.

Box 11

Figure 10

Part mounting in CNC machine

The acquisition system is designed to transmit images to the computer via Ethernet communication with a fixed IP address to a configured folder, which is directed to the algorithm to acquire the images and perform processing.

The images captured by the camera are generated in RGBβ(x,y) color format with three channels, as illustrated in Figure 11. These images correspond to curved, straight, and sloped geometries respectively.

Box 12

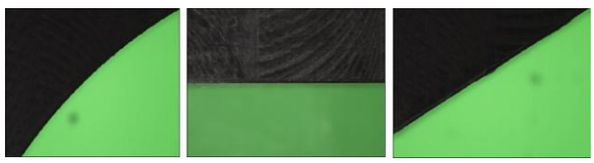

Figure 11

Image Capture: curve, straight line, and curve geometries

Image Preprocessing

Image preprocessing plays a fundamental role by acting as the first line of enhancement and refinement of the captured images. In the first stage, spatial filters such as smoothing and Gaussian filters are applied to improve the quality and interpretability of the captured images before extracting contour shape features.

ISSN: 2531-2189
RENIECYT-CONAHCYT: 1702902

Meraz-Méndez, Manuel, Muñoz-López, Luis Enrique, Reynoso-Jardón, Elva Lilia and Corral- Ramírez, Guadalupe. [2024]. Camera calibration procedure for extracting form deviation features in machined parts through computer vision algorithms. Journal of Mechanical Engineering. 8[21]-1-: e30821111.
DOI: https://doi.org/10.35429/JME.2024.8.21.3.11

As the second stage of image processing, the algorithm executes the transformation of the original image RGBβ(x,y) to a representation in grayscale Grβ(x,y) format through the application of the rgb2gray(Id,γ) conversion algorithm. This conversion process aims to reduce the dimensionality of the image from three channels to a single channel to handle less information and achieve faster computational speed. Subsequently, the transformation of the image into a binary format Bβ(x,y) is carried out using the imbinarize(Id,γ) algorithm, to segment objects of interest from the background, as shown in Figure 12 of the transformation process.

Box 13

Figure 12

Image Transformation Process: RGB to Gray and Binary

The transformation process aims to express the visual information contained in the image in a way that is interpretable and manipulable by the computational system. Additionally, the process is carried out to simplify information, detect edges, recognize patterns, and improve computational performance to facilitate subsequent operations in the realm of digital image processing. The binary representation is specifically chosen for its ability to simplify and optimize the manipulation of visual data, enabling a more efficient and precise analysis in the later stages of the image processing treatment process.

Feature Extraction

The subsequent stage is precisely dedicated to the extraction of fundamental features present in the processed images. In this process, the algorithm transforms the binary image Bβ(x,y) into a 2D representation called a "signature" SGβ(x,y). This transformation is achieved through the application of the cv2.findContours(Id,γ) algorithm, specifically designed for edge and corner detection, identifying points of change and corners in the shapes present in the images, as visualized in Figure 13.

Box 14

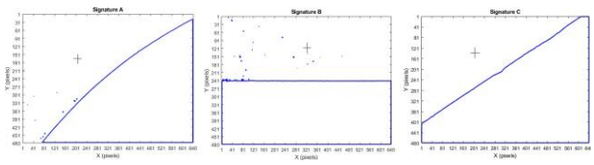

Figure 13

Edge Extraction in Images: SGβ(x,y).

This approach efficiently highlights and characterizes regions of interest in the images, which is essential for detailed analysis and subsequent decision-making in the context of image processing.

To obtain dimensional contour variation information about the geometry of the parts, the algorithm applies the Gaussian filter (cv2.GaussianBlur) with a threshold σ = 2 and the bilateral filter (cv2.bilateralFilter) with a kernel size k = 3 to eliminate noise to obtain an image representation free of imperfections, as illustrated in Figure 14. This noise removal process is essential to ensure a clean and sharp image, providing a solid foundation for subsequent stages of analysis and data processing within the context of the algorithm.

Box 15

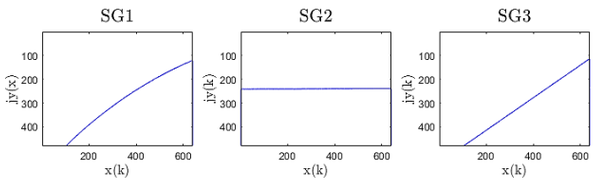

Figure 14

Noise Reduction in Images: SGβ(x,y).

Results

Image Acquisition Results

Below are the results of the captured images of the parts corresponding to curved, straight, and sloped geometries shown in Figures 15,16 and 17. During the acquisition process, 135 images were captured, considering the resolution and quality of the camera used. The camera resolution of 1600x1200 pixels facilitated capturing contour variation features of the parts to be machined.

ISSN: 2531-2189
RENIECYT-CONAHCYT: 1702902

Meraz-Méndez, Manuel, Muñoz-López, Luis Enrique, Reynoso-Jardón, Elva Lilia and Corral- Ramírez, Guadalupe. [2024]. Camera calibration procedure for extracting form deviation features in machined parts through computer vision algorithms. Journal of Mechanical Engineering. 8[21]-1-: e30821111.
DOI: https://doi.org/10.35429/JME.2024.8.21.3.11

Box 16

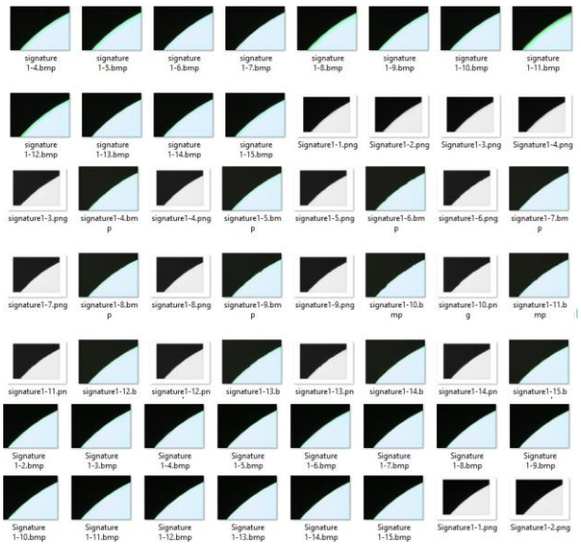

Figure 15
Captured images of curve geometry

Box 17

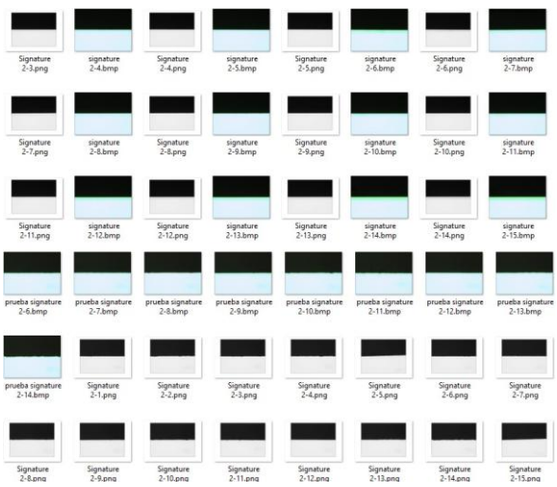

Figure 16
Captured images of line geometry

Box 18

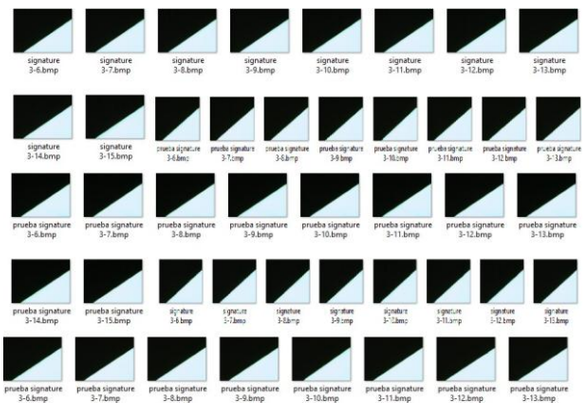

Figure 17
Captured images of slope geometry

Results of Contour Variation Feature Extraction

As a result, a total of 135 shape variation features were extracted from each geometry, corresponding to 45 presented below in Figures 18,19 and 20:

Box 19

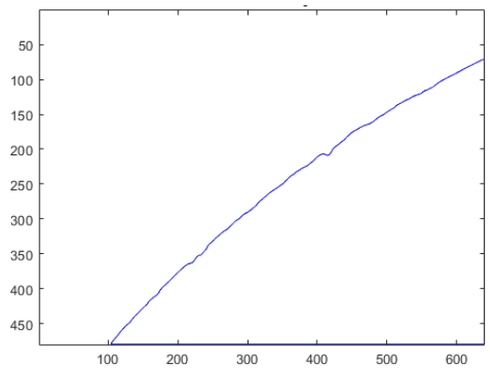

Figure 18
Curves with smooth and sinuous contours (units: pixels)

Box 20

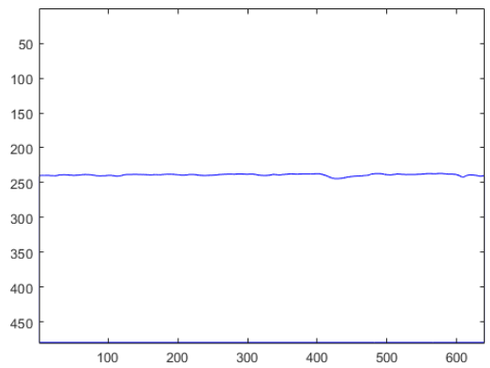

Figure 19
Identification of key features, parts with line geometry (units: pixels)

Box 21

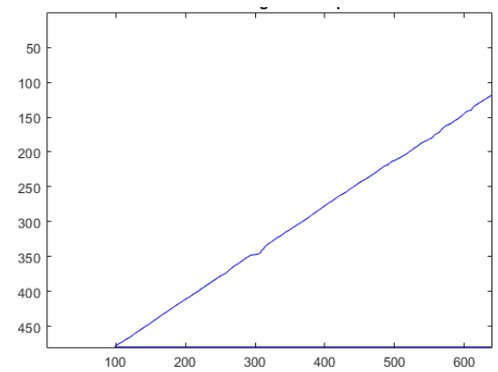

Figure 20
Identification of key features, parts with sloped geometry (units: pixels)

ISSN: 2531-2189
RENIECYT-CONAHCYT: 1702902

Meraz-Méndez, Manuel, Muñoz-López, Luis Enrique, Reynoso-Jardón, Elva Lilia and Corral- Ramírez, Guadalupe. [2024]. Camera calibration procedure for extracting form deviation features in machined parts through computer vision algorithms. Journal of Mechanical Engineering. 8[21]-1-: e30821111.
DOI: https://doi.org/10.35429/JME.2024.8.21.3.11

Discussions

1. Diversity of Shapes and Sizes: The diversity of shapes and sizes encountered when dealing with parts of curved geometry was notable. By analyzing Figures 18,19 and 20 corresponding to delrin material, characteristics such as smooth and sinuous contours, pronounced curves, and diversity in shapes and sizes were observed in these parts, demonstrating the inherent complexity of curved, line, and slope geometry. Each of these shapes presented its own peculiarities and visual characteristics, requiring a meticulous approach to effectively identify and correlate key features. The ability of the algorithm to adapt to the complexity of the shapes necessitated a higher degree of sophistication in image processing.

2. Distinctive Features: Throughout the process of feature extraction from parts with curved, line, and slope geometry, the identification and isolation of a series of highly distinctive characteristics were conducted. Figures 18, 19, and 20 also offer an enlightening view of these unique features of Delrin found in curved parts. Among them, inflection points, maximum curvatures, concavity points, and other critical geometric attributes can be observed, which play a fundamental role in the detailed description of the shape and structure of a representative sample of curved geometry. Each of these distinctive characteristics presents its complexity, and their identification and analysis require a meticulous and sophisticated approach.

3. Scale Variation: During the feature extraction process on the set of parts with curved, line, and slope geometry, considerable scale variation was observed. When examining the delrin samples shown in Figure 19, it is apparent that some parts exhibited reduced dimensions and variation in their contour, while others stood out for their substantial size. This diversity in the scale of the parts was notable and posed an additional challenge in the feature extraction process. Adapting the feature extraction algorithms to this variability became an essential component for achieving precise and coherent results. Smaller-scale parts required a meticulous approach to identify fine details, whereas larger parts demanded a more robust processing capability to handle more complex structures. The ability of feature extraction algorithms to address this wide range of sizes is a testament to their versatility and efficiency. Adaptation to different scales is not only relevant in the context of curved geometry but is also a valuable characteristic for their applicability in various computer vision applications, where scale variability is a constant factor.

4. Adaptability to Lighting Variations: The adaptability of feature extraction algorithms to variations in lighting conditions proved fundamental in the image capture process, as exemplified in Figure 20. Despite changes in intensity and type of lighting, the algorithms maintained a strong capacity for adaptation. Even in situations with diffuse lighting or the presence of shadows, the identification of features in curved parts remained robust and effective. This capability is essential in manufacturing and processing environments, where lighting conditions can vary due to various circumstances, highlighting the efficacy of the algorithms in practical applications.

Box 22

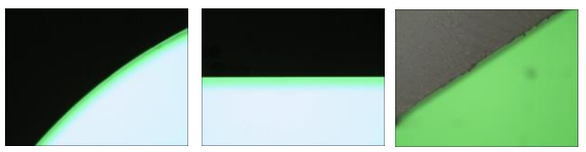

Figure 21
Parts with different lighting

Conclusions

The results obtained through the application of computer vision technology in manufacturing have been highly promising (Feng et al., 2019). They have shown significant improvements in terms of accuracy, efficiency, and quality (Wuest et al., 2016). Moreover, the ability of machine learning algorithms to detect complex patterns and make accurate predictions has further enhanced the effectiveness of computer vision technology in manufacturing processes (Nichols et al., 2018).

ISSN: 2531-2189
RENIECYT-CONAHCYT: 1702902

Meraz-Méndez, Manuel, Muñoz-López, Luis Enrique, Reynoso-Jardón, Elva Lilia and Corral- Ramírez, Guadalupe. [2024]. Camera calibration procedure for extracting form deviation features in machined parts through computer vision algorithms. Journal of Mechanical Engineering. 8[21]-1-: e30821111.
DOI: https://doi.org/10.35429/JME.2024.8.21.3.11

These advancements have led to reduced errors, increased productivity, and improved overall product performance (Wuest et al., 2016). Computer vision technology has revolutionized the manufacturing industry by enabling precise analysis of part geometry and identifying shape deviations (Ando et al., 2016). This technology has proved to be invaluable in CNC machining, where even minor deviations can have a significant impact on the performance and functionality of machined parts (Feng et al., 2019). Furthermore, the combination of computer vision technology and machine learning algorithms opens new possibilities for optimizing manufacturing processes (Qi et al., 2020) and improving overall product performance (Wuest et al., 2016). In summary, the contour variation feature extraction from parts with different geometries proved essential for improving precision and efficiency in CNC machining operations. The ability to identify and manage variability, position, inclination, and lighting was crucial for the success of the process. These results underscore the importance of feature extraction in manufacturing parts with diverse geometries and its positive impact on determining the World Coordinate System (WCS).

Conflict of interest

The authors declare no conflicts of interest.

Author's contribution

Manuel Meraz Méndez: Contributed to the project idea, research method, algorithms design, camera calibration design procedure, and technique.

Luis Enrique Muñoz López: Contributed to the analysis, and machining of workpieces

Elva Lilia Reynoso Jardon: Contributed to the research method and article writing.

Guadalupe Corral Ramirez: Contributed to the research method and article writing.

Founding

The authors acknowledge the support received from various areas at the Technological University of Chihuahua and the PRODEP program.

Aknowlegmenths

The authors express their gratitude for the support received in various areas from the Technological University of Chihuahua (Department of Industrial Maintenance Engineering) and Ing. Raul Villareal for scientific collaboration and the ease of use of equipment and laboratories

References

Burger, W., & Burge, M. J. (2022). Digital image processing: An algorithmic introduction. Springer Nature.

Wang, L., & Yang, Q. (2009, November 1). Research and development of product model based on CNC technology. https://doi.org/10.1109/caidcd.2009.5374931

Wang, H., Cai, Z., Lin, L., & Sun, X. (2009, November 1). Research on CAD/CAM/CNC system for thin-walled part made of light metal based on spherical coordinate. https://doi.org/10.1109/caidcd.2009.5375039

Feng, X., Jiang, Y., Yang, X., Du, M., & Li, X. (2019, November 1). Computer vision algorithms and hardware implementations: A survey. Elsevier BV, 69, 309-320. https://doi.org/10.1016/j.vlsi.2019.07.005

Ngiam, J., Khosla, A., Kim, M., Nam, J., Lee, H., & Ng, A Y. (2011, June 28). Multimodal Deep Learning. Pp. 689-696.

Sun, J., Wang, P., Qin, Z., & Qiao, H. (2014, June). Overview of camera calibration for computer vision. In Proceeding of the 11th World Congress on Intelligent Control and Automation (pp. 86-92). IEEE.

Yang, X. (2020, December 1). An Overview of the Attention Mechanisms in Computer Vision. IOP Publishing, 1693(1), 012173-012173. https://doi.org/10.1088/1742-6596/1693/1/012173

Voulodimos, A., Doulamis, A., Doulamis, A., & Protopapadakis, E. (2018, January 1). Deep Learning for Computer Vision: A Brief Review. Hindawi Publishing Corporation, 2018, 1-13. https://doi.org/10.1155/2018/7068349

ISSN: 2531-2189
RENIECYT-CONAHCYT: 1702902

Meraz-Méndez, Manuel, Muñoz-López, Luis Enrique, Reynoso-Jardón, Elva Lilia and Corral- Ramírez, Guadalupe. [2024]. Camera calibration procedure for extracting form deviation features in machined parts through computer vision algorithms. Journal of Mechanical Engineering. 8[21]-1-: e30821111.
DOI: https://doi.org/10.35429/JME.2024.8.21.3.11

Wuest, T., Weimer, D R., Irgens, C., & Thoben, K. (2016, January 1). Machine learning in manufacturing: advantages, challenges, and applications. Taylor & Francis, 4(1), 23-45. https://doi.org/10.1080/21693277.2016.1192517

Nichols, J A., Chan, H W H., & Baker, M A B. (2018, September 4). Machine learning: applications of artificial intelligence to imaging and diagnosis. Springer International Publishing, 11(1), 111-118. https://doi.org/10.1007/s12551-018-0449-9

Ando, H., Niitsu, Y., Hirasawa, M., Teduka, H., & Yajima, M. (2016, July 1). Improvements of Classification Accuracy of Film Defects by Using GPU-accelerated Image Processing and Machine Learning Frameworks. https://doi.org/10.1109/nicoint.2016.15

Qi, S., Yang, J., & Zhong, Z. (2020, September 18). A Review on Industrial Surface Defect Detection Based on Deep Learning Technology. https://doi.org/10.1145/3426826.3426832

ISSN: 2531-2189
RENIECYT-CONAHCYT: 1702902

Meraz-Méndez, Manuel, Muñoz-López, Luis Enrique, Reynoso-Jardón, Elva Lilia and Corral- Ramírez, Guadalupe. [2024]. Camera calibration procedure for extracting form deviation features in machined parts through computer vision algorithms. Journal of Mechanical Engineering. 8[21]-1-: e30821111.
DOI: https://doi.org/10.35429/JME.2024.8.21.3.11

Journal of Mechanical Engineering 8[21]1-16: e40821116
Article

Experimental proposal of a 'HALO'-type security device in a FORMULA SAE 2024 type vehicle

Propuesta experimental de dispositivo de seguridad tipo ‘HALO’ en un vehículo de tipo FORMULA SAE 2024

Noguez-Jimenez, Víctor Manuel[a], Cordero-Guridi, José de Jesús[b], Peréz-Carrillo, Daniel[c] and García-Tépox, José Domingo[d]

[a] Universidad Popular Autónoma del Estado de Puebla • 0009-0009-6354-4789
[b] Universidad Popular Autónoma del Estado de Puebla • 0000-0001-5201-1906
[c] Universidad Popular Autónoma del Estado de Puebla • 0009-0000-3902-9546
[d] Universidad Popular Autónoma del Estado de Puebla • 0000-0001-7030-7735

CONAHCYT classification:

Area: Engineering
Field: Engineering
Discipline: Mechanical engineering
Subdiscipline: Vehicle safety

https://doi.org/10.35429/JME.2024.8.21.1.16
Article History:
Received: January 12, 2024
Accepted: December 31, 2024

* ✉ [josejesus.cordero@upaep.mx]

Abstract

This study conducts a numerical and experimental analysis of the use of a "Halo" device, inspired by Formula 1, within the Formula SAE competition. Several alternatives were developed to meet the regulatory requirements of Formula SAE, and the selected proposal was modeled in CATIA V5 using both surface and solid modeling techniques. The model underwent a structural analysis similar to the "Quasi-static Test 1" used for the Formula 1 "Halo," utilizing ANSYS Workbench 2023 R2 for finite element analysis (FEA). Additionally, physical tests were carried out to validate and compare the virtual results, with the aim of assessing the relevance and benefits of this safety device.

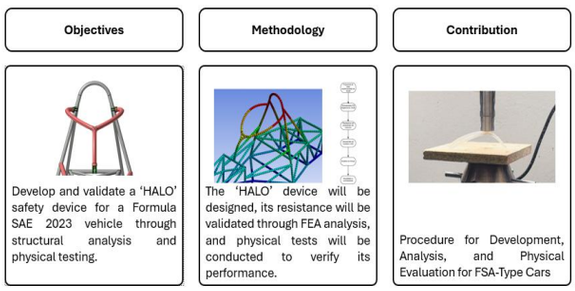

Formula SAE, ANSYS, CATIA, FEA, SAFETY DEVICE, HALO

Resumen

Este estudio analiza numérica y experimentalmente el uso de un dispositivo tipo "Halo", inspirado en Fórmula 1, dentro del contexto de la competencia Fórmula SAE. Se desarrollaron diversas alternativas para cumplir con los requisitos regulatorios de la Fórmula SAE, y la propuesta seleccionada fue modelada en CATIA V5 utilizando técnicas de modelado de superficies y sólidos. El modelo fue sometido a un análisis estructural similar al "Quasi-static Test 1" del "Halo" de Fórmula 1, empleando el software de análisis por elementos finitos (FEA) ANSYS Workbench 2023 R2. Además, se realizaron pruebas físicas para validar y comparar los resultados virtuales, con el objetivo de evaluar la relevancia y beneficios de este dispositivo de seguridad..

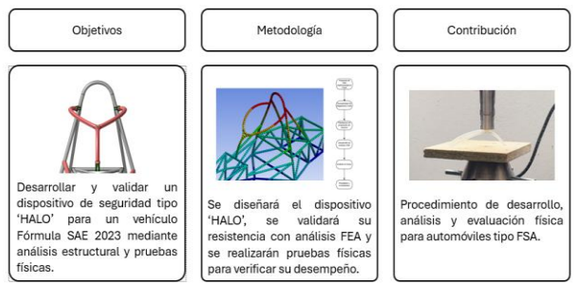

Formula SAE, ANSYS, CATIA, FEA, SEGURIDAD, HALO

Citation: Noguez-Jimenez, Víctor Manuel, Cordero-Guridi, José de Jesús, Peréz-Carrillo, Daniel and García-Tépox, José Domingo. [2024]. Experimental proposal of a 'HALO'-type security device in a FORMULA SAE 2024 type vehicle. Journal of Mechanical Engineering. 8[21]-1-16: e40821116.

Journal of Mechanical Engineering 8[21]1-16: e40821116
Article

Introduction

The Formula SAE competition, organised by the Society of Automotive Engineers (SAE), represents a unique challenge for engineering students to design, build and race vehicles that demonstrate and apply knowledge in a practical and safe environment. This event encompasses tests such as acceleration, skidpad, autocross, endurance and efficiency, and not only encourages innovation and creativity, but also emphasises safety as a fundamental aspect of automotive design. Within the framework of the competition, a rigorous set of rules and regulations governs the requirements for team participation. These regulations, designed to ensure both the functionality and safety of the vehicles during the various tests, emphasise the importance of the vehicle structure as a key element for the integrity of the car and the protection of the driver. [5] In this context, a proposal arose to use a Halo-type device, similar to that used on Formula 1 cars, as an additional safety measure for Formula SAE vehicles. To validate this proposal, a Quasi-static 1 test was carried out on an A36 steel structure. Complemented with the finite element analysis (FEA) performed in ANSYS Workbench 2023 software and a visualisation analysis with dummy in CATIA V5 software to validate the visual section requested by the student competition regulations. [1, 5]

Statistics from organisations such as the World Health Organization (WHO) and the Insurance Institute for Highway Safety (IIHS) highlight the importance of improving vehicle safety, reporting in their 2021 fatality statistics that there were 10,229 fatalities due to frontal crashes or rollovers. At racing events, where the risk of accidents is inherent, it is vital to prioritise the safety of participants. [3]

To assess the safety of the Halo device in terms of head injury protection, the Head Injury Criterion (HIC) is used. The HIC is a measure used in biomechanics to determine the probability of an impact causing a serious head injury. This metric is calculated using the acceleration recorded during an impact and provides an estimate of the risk of injury as a function of the duration and magnitude of the acceleration. In this project, simulations were performed to calculate the HIC and evaluate how the "Halo" device influences the reduction of injury risk in the event of a crash [6].

Finite Element Analysis (FEA) focuses on understanding how the Halo device affects the vehicle structure and ultimately the protection of the driver. This study uses numerical methods to break a complex object into small elements in order to model its behaviour, evaluating each element individually to gain a detailed view of the system's response under various conditions.

Project approach

The main objective of the project is to improve driver safety in Formula SAE competition through the implementation of a safety device known as the "Halo", endorsed by the Fédération Internationale de l'Automobile (FIA). The "Halo" is a titanium arch designed to surround the cockpit of the car, providing an additional physical barrier to protect the driver's head. [9, 7].

Box 1

Figure 1
Demonstration image of the Halo device used in F1

Source: FIA STANDARD 8869-2018

The implementation of this device is based on fundamental reasons centred on rider safety, addressing two critical aspects:

1. rider head protection: the Halo was specifically designed to protect the rider's head, acting as a physical barrier that reduces the risk of injury caused by large objects, such as parts of other vehicles. [9]

2. Rollover Risk: The Halo is also designed to prevent injury to the rider's head by providing a solid structure that prevents direct contact of the vehicle with the rider's helmet in the event of a rollover. [9]

ISSN: 2531-2189
RENIECYT-CONAHCYT: 1702902

Noguez-Jimenez, Víctor Manuel, Cordero-Guridi, José de Jesús, Peréz-Carrillo, Daniel and García-Tépox, José Domingo. [2024]. Experimental proposal of a 'HALO'-type security device in a FORMULA SAE 2024 type vehicle. Journal of Mechanical Engineering. 8[21]-1-16: e40821116.
DOI: https://doi.org/10.35429/JME.2024.8.21.1.16

Planning

Develop a driver protection system (Halo) for the Formula SAE vehicle, complying with competition safety standards.

Box 2

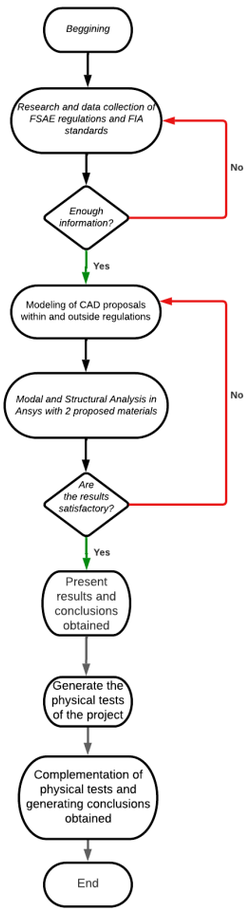

Figure 2
Method used in the development of the project.

Source: Own elaboration

Part I: Planning and Design

- Investigation of security requirements.
- Defining objectives and design criteria.
- Creating the design plan and assigning roles.

Part II: Development and Prototyping

- Creation of CAD models of the prototype.
- Strength testing and preliminary adjustments.

Part III: Implementation and Validation

- Procurement of materials.
- Integration of the Halo into the vehicle.
- Final functional, safety and endurance testing.
- Validation of compliance with standards.

Constraints, Risks and Assumptions

With the above approach it is expected that our research will be limited by various situations, such as: the material on which it is planned to print in the final stage of the project, failures in the study machines, poor execution of the tests made to the prototype. It is also taken into account that we have an important restriction where we are restricted to use only the materials that the school has, which in this case is Onyx or Resin V5 [B].

Benchmarking

In the study of Head Injury Analysis of Vehicle Occupant in Frontal Crash Simulation: Case Study of ITB's Formula SAE Race Car, a study was carried out to analyse the effect of speed on the impact of a Formula SAE type vehicle, where it was found that for speeds of less than 40 km/h the attenuator requested by the regulations may be sufficient to avoid generating a major trauma, based on the HIC scale, as values of less than 700 safe values are produced. However, once the speed exceeds 43 km/h these values are higher as the G forces experienced are greater than 140 G ‘s, at this point the probability of a skull fracture increases to 5% [6].

Box 3

Table 1
Table of accidents by type of accident and type of vehicle

Passenger deaths per vehicle in all accidents by point of impact and type of vehicle in 2021								
Initial point of impact	Car		Pickup		SUV		All	
	Number	%	Number	%	Number	%	Number	%
Frontal	8742	59	2891	60	3892	59	15742	59
Side	3662	25	843	17	1258	19	5824	22
Rear	853	6	181	4	369	6	1423	8
Other (rollover)	1487	10	940	19	1117	17	2596	14
Total	14744	100	4855	100	6636	100	26555	100

Source: NHTSA and the IIHS

ISSN: 2531-2189
RENIECYT-CONAHCYT: 1702902

Noguez-Jimenez, Víctor Manuel, Cordero-Guridi, José de Jesús, Peréz-Carrillo, Daniel and García-Tépox, José Domingo. [2024]. Experimental proposal of a 'HALO'-type security device in a FORMULA SAE 2024 type vehicle. Journal of Mechanical Engineering. 8[21]-1-16: e40821116.
DOI: https://doi.org/10.35429/JME.2024.8.21.1.16

The project proposes the implementation of a "Halo" type safety device for Formula SAE competition vehicles, inspired by the model used in Formula 1, with the aim of improving driver protection in situations of head-on collisions and rollovers, which according to Fatality Facts 2021 - Passenger vehicle occupants statistics, account for almost 10,300 fatalities. It focuses on adapting this professional technology to a school environment, taking into account the specific constraints and requirements of competition. [3]

Box 4

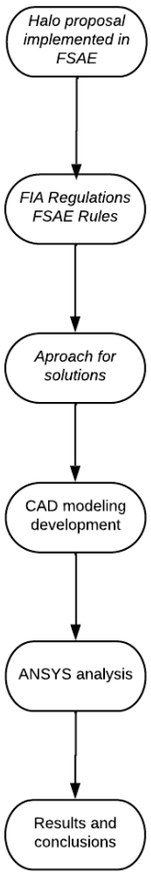

Figure 3
Method used for the development of the project

Source: *Own elaboration*

The method followed for the development of the project is noted. As such, the scope of the project was considered experimental, recognising that the proposed modifications may affect compliance with certain sections of the Formula SAE regulations, particularly sections F.1.13 and F.5.6.3, which refer to vehicle geometry.

Reference is made to FIA STANDARD 8869-2018, which sets out the design requirements for Additional Frontal Protection (AFP) systems on open cockpit vehicles, ensuring that the Halo device is designed and fitted in accordance with the criteria defined in that standard. In addition, the project must comply with the specific Formula SAE regulations, including aspects such as cockpit dimensions (section T1), the position of the main hoop and front hoop of the chassis (F.5.6), and the protection of the steering system (F.5.14). Structural integrity, dictated by the triangulation of elements (F.3.2.1), is essential to meet these stringent standards. [5]

To assess the strength of the Halo device, a Quasi Static Test 1 similar to that used in Formula 1 is performed. It is important to take up the scope of this project as the Halo device used in an F1 car is a professional grade device, in this case being a school project we consider a maximum deformation tolerance higher than that of the tests of a real Halo device, which is 45 mm where we double the value over the aforementioned, given that the value given by FIA justifying that this is subjected to an average speed of a Formula 1 car, which is 264 km/h in the fastest circuits and 167 km/h in the slowest ones, otherwise in a Formula SAE the speeds are much lower, generally limited to 80 km/h, thus resulting in a maximum allowed deformation of 90 mm. [1, 8, 10].

Box 5

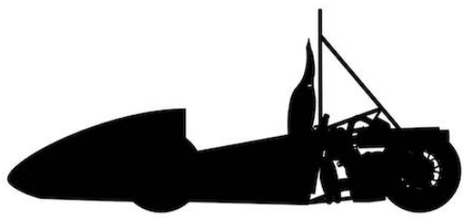

Figure 4
Representative image of a Formula SAE type vehicle.

Source: Own elaboration

The use of A36 steel is proposed for the structure of the "Halo", evaluating its performance under the specific conditions of the competition. The design process can be divided into 2 main stages, starting with the research and data collection of the FSAE regulations and the FIA (Halo) standard, where the following design constraints are highlighted. [5]

ISSN: 2531-2189
RENIECYT-CONAHCYT: 1702902

Noguez-Jimenez, Víctor Manuel, Cordero-Guridi, José de Jesús, Peréz-Carrillo, Daniel and García-Tépox, José Domingo. [2024]. Experimental proposal of a 'HALO'-type security device in a FORMULA SAE 2024 type vehicle. Journal of Mechanical Engineering. 8[21]-1-16: e40821116.
DOI: https://doi.org/10.35429/JME.2024.8.21.1.16

Box 6

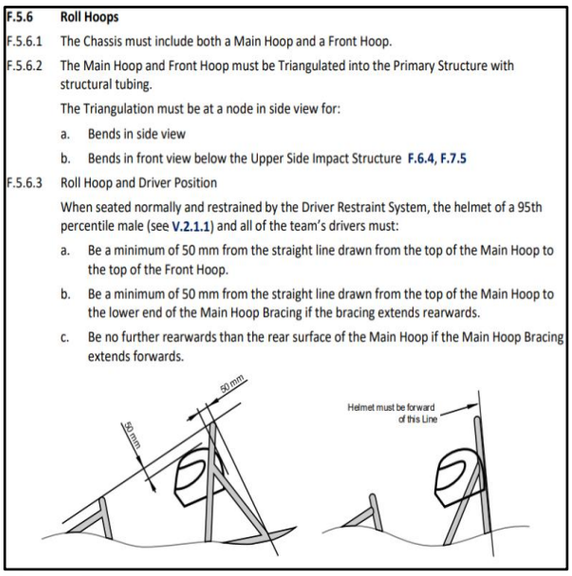

Figure 5
Restriction F.5.6

Source: FSAE Regulation 2023

Box 7

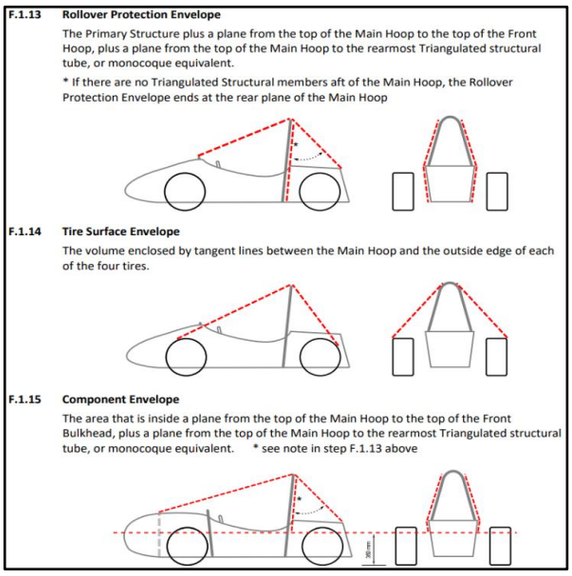

Figure 6
Constraint F.1.13

Source: *FSAE Regulation 2023*

Box 8

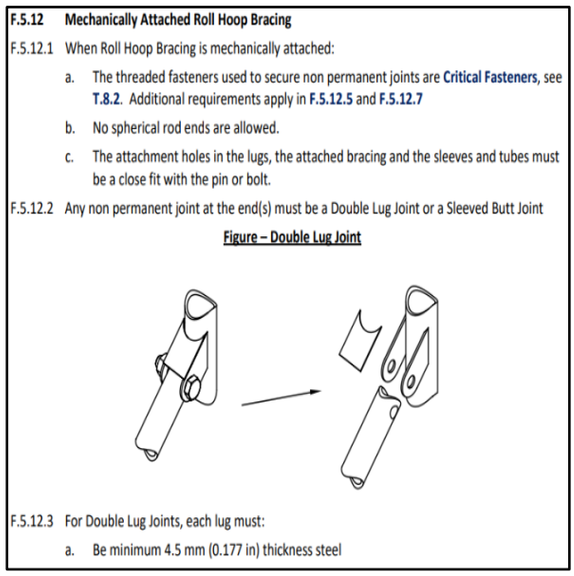

Figure 1
Restraint of restraint F.5.12

Source: *FSAE Regulation 2023*

An optimisation to the CAD model of the Halo safety device was considered, with the aim of reducing the amount of material used while maintaining or increasing its performance.

This optimisation was achieved by modifying the design for weight reduction in non-critical areas, resulting in a more efficient design.

A new clamping geometry was proposed that retains the lug design, but reducing the amount of material. In addition, a smaller diameter solid profile is suggested for the tubular instead of hollow.

Despite being solid, its dimensions were reduced while maintaining structural rigidity. This optimisation strategy reflects an innovative and progressive approach to safety in FSAE competition. [5]

ISSN: 2531-2189
RENIECYT-CONAHCYT: 1702902

Noguez-Jimenez, Víctor Manuel, Cordero-Guridi, José de Jesús, Peréz-Carrillo, Daniel and García-Tépox, José Domingo. [2024]. Experimental proposal of a 'HALO'-type security device in a FORMULA SAE 2024 type vehicle. Journal of Mechanical Engineering. 8[21]-1-16: e40821116.
DOI: https://doi.org/10.35429/JME.2024.8.21.1.16

Box 9

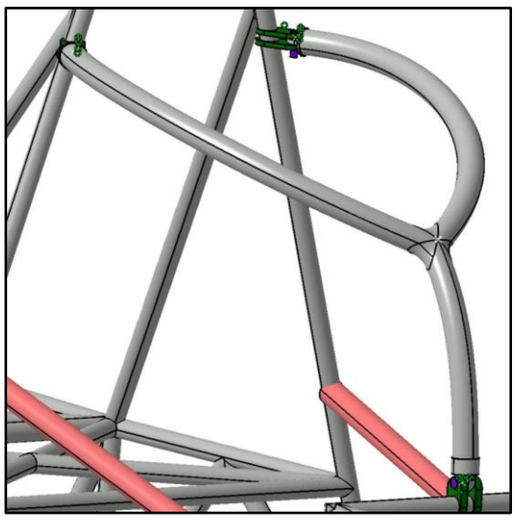

Figure 8
HALO FSAE 2024 proposal

Source: Own elaboration

So the assembly consists of a double-ear fastening system, with a minimum requested thickness of 4.5 mm [5]. But a thickness of 8.0 mm is chosen to ensure greater robustness and structural strength. These fasteners are joined by a 10.0 x 70.0 mm hex bolt and nut, ensuring a secure and stable connection between the Halo device and the vehicle frame, as shown below:

Box 10

Figure 9
Technical characterisation of a Formula 1 joint assembly

Source: FIA STANDARD 8869-2018

Box 11

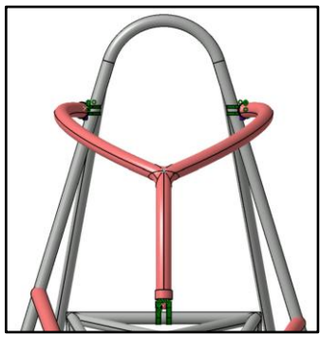

Figure 10
Proposed linkage of the CAD model for FSAE 2024

Source: Own elaboration

Box 12

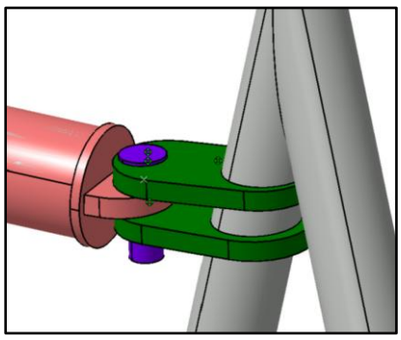

Figure 11
Proposed linking of the CAD model in FSAE 2024

Source: Own elaboration

For the validation of the design of the Halo device for the Formula SAE vehicle, it is essential to apply the principles of Failure Mode and Effect Analysis (FMEA) in a rigorous and structured manner. This ensures a thorough assessment of every critical component of the Halo, from the main structure to the mounting brackets and attachment connections, identifying potential failure modes and developing effective strategies to mitigate risks. Considering the points on how to do the FEA and apply them towards the design. [A]

Planning and Preparation:

Clear objectives were set and a multidisciplinary team was assembled.

The scope of the FMEA was defined and roles and responsibilities were assigned.

ISSN: 2531-2189
RENIECYT-CONAHCYT: 1702902

Noguez-Jimenez, Víctor Manuel, Cordero-Guridi, José de Jesús, Peréz-Carrillo, Daniel and García-Tépox, José Domingo. [2024]. Experimental proposal of a 'HALO'-type security device in a FORMULA SAE 2024 type vehicle. Journal of Mechanical Engineering. 8[21]-1-16: e40821116.
DOI: https://doi.org/10.35429/JME.2024.8.21.1.16

Structure Analysis:

Critical components of the Halo were identified and thoroughly analysed, including the main structure, mounting brackets, attachment connections, cross members and surface finish. The function of each component was assessed and potential failure modes were identified, considering their severity and occurrence.

Risk Analysis:

Current failure prevention and detection controls were assessed for each component.

Severity, occurrence and detection scores were assigned to calculate the level of risk associated with each failure mode.

Optimisation:

Prevention and detection actions were proposed and prioritised to mitigate the identified risks.

An implementation plan was established for each proposed action and progress is monitored.

Implemented actions were periodically reviewed to ensure their continued effectiveness.

Visual tools, such as flow charts and risk matrices, are used to represent the results of the FMEA analysis in a clear and concise manner. Tables are used to summarise the identified failure modes, along with their severity, occurrence and detectability, facilitating the identification of critical areas requiring attention during optimisation. Failure Mode and Effect Analysis (FMEA) was an essential tool in our process to improve the HALO design. Through this analysis, potential failure risks in each component were identified and addressed, allowing the safety and reliability of the Halo to be strengthened. This tool directly contributes to improving the safety and quality of the Halo design for the Formula SAE vehicle [A].

Initially, only the CAD model of the Formula SAE vehicle frame lines was available. To which the silhouette of a Halo device was added, trying to stick to the original design of the device. Proposals were generated for further evaluation, shown below:

Box 13

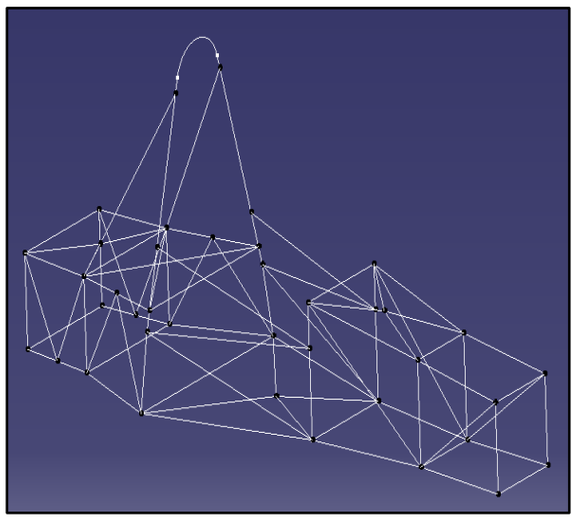

Figure 12
Demonstration image of the CAD model of the FSAE 2023 lines

Source: Own elaboration

Several proposals were made, modelled and evaluated for comparison, and the proposals generated are shown below.

Box 14

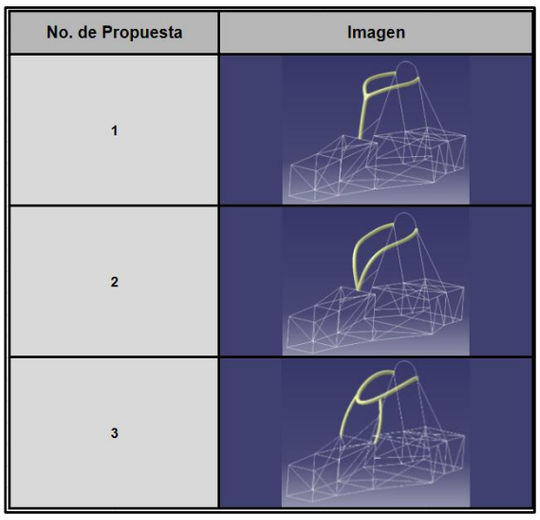

Figure 13
Proposals generated

Source: Own elaboration

ISSN: 2531-2189
RENIECYT-CONAHCYT: 1702902

Noguez-Jimenez, Víctor Manuel, Cordero-Guridi, José de Jesús, Peréz-Carrillo, Daniel and García-Tépox, José Domingo. [2024]. Experimental proposal of a 'HALO'-type security device in a FORMULA SAE 2024 type vehicle. Journal of Mechanical Engineering. 8[21]-1-16: e40821116.
DOI: https://doi.org/10.35429/JME.2024.8.21.1.16

After the design stage, analyses were carried out in CATIA V5 and ANSYS software to demonstrate the functionality of the proposal. Starting with the CATIA software where the visibility tests were carried out with the dummy in order to validate the point of view, being also a requirement requested and limiting the design by the FSAE regulation in section V.2.2 which specifies as a requirement to have a visibility to the sides of 100° [5].

Box 15

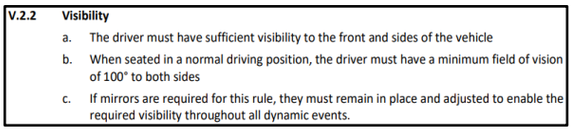

V.2.2 Visibility

a. The driver must have sufficient visibility to the front and sides of the vehicle

b. When seated in a normal driving position, the driver must have a minimum field of vision of 100° to both sides

c. If mirrors are required for this rule, they must remain in place and adjusted to enable the required visibility throughout all dynamic events.

Figure 14
Constraint V.2.2

Source: FSAE Regulation 2023

Using a percentile dictated by the same regulation in section F.5.6.5 [5], the visibility test was carried out on the 6 proposals to finally select the one with the highest visibility, using the following position:

Box 16

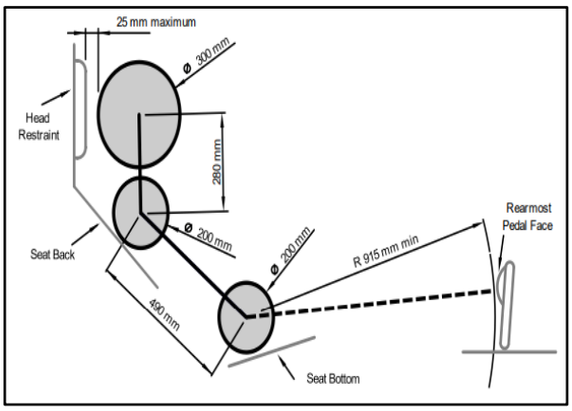

Figure 15
Pilot position determined

Source: FSAE Regulations 2023

With the Point of View (POV) tool, the following results are obtained from the proposals:

Box 17

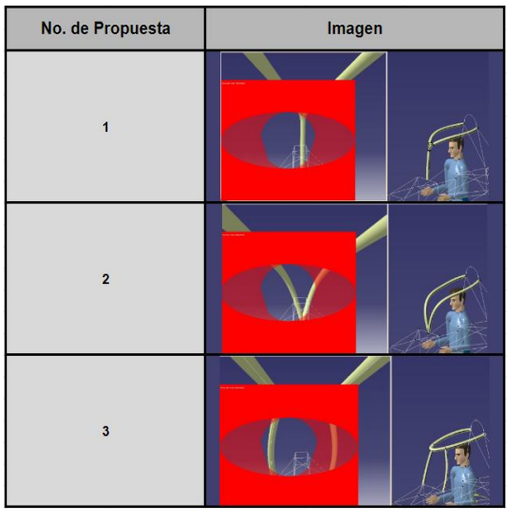

Figure 16
Comparison of the results obtained in CATIA V5 POV

Source: Own elaboration

Where it was observed that proposal number 1 was the best as it obstructed visibility the least, thus meeting the 100° visibility requirement without complications. Therefore, the design stage was resumed based on the proposed geometry number 1.

Box 18

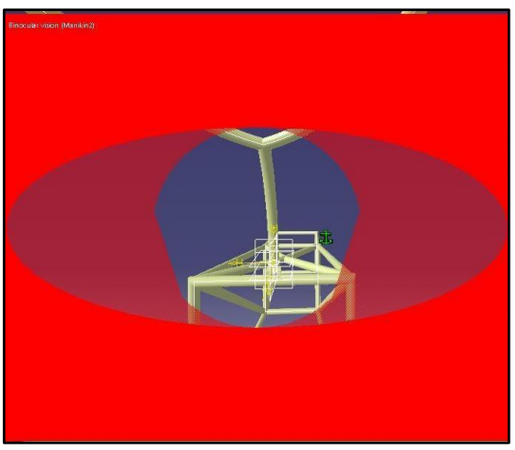

Figure 17
Results of the right-eye view on the modified CAD proposal

Source: Own elaboration

ISSN: 2531-2189
RENIECYT-CONAHCYT: 1702902

Noguez-Jimenez, Víctor Manuel, Cordero-Guridi, José de Jesús, Peréz-Carrillo, Daniel and García-Tépox, José Domingo. [2024]. Experimental proposal of a 'HALO'-type security device in a FORMULA SAE 2024 type vehicle. Journal of Mechanical Engineering. 8[21]-1-16: e40821116.
DOI: https://doi.org/10.35429/JME.2024.8.21.1.16

Box 19

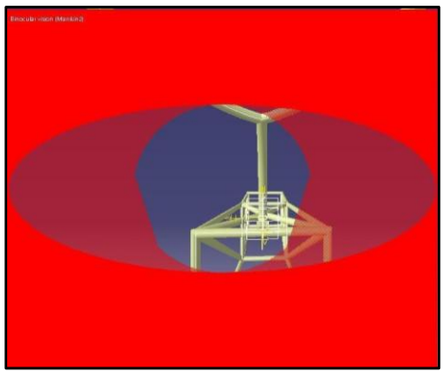

Figure 18
Results of the left-eye view of the modified CAD proposal

Source: Own elaboration

Therefore, a model was generated from the following sketches:

Box 20

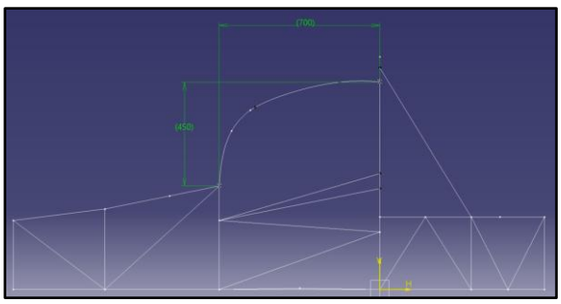

Figure 19
Lateral dimensional image

Source: Own elaboration

Box 21

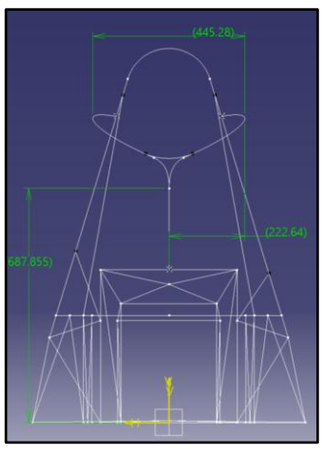

Figure 20
Front dimensional image

Source: Own elaboration

Box 22

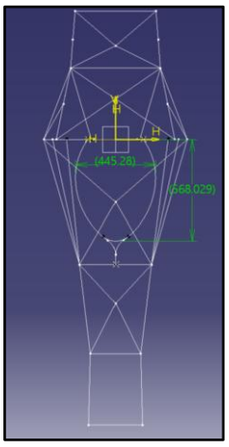

Figure 21
Front dimensional image

Source: Own elaboration

The second software used was ANSYS Workbench 2023 R2 for the analysis and validation of the chosen proposal. The analysis proposed was a modal analysis and a structural analysis following the mechanics and magnitudes of the Quasi Static Test 1 to the original frame as a starting point for comparison and to the modelled proposal. These analyses consist of a modal analysis and a structural analysis. These analyses were carried out under the conditions mentioned below. For the structural analysis, we used the Quasi Static Test 1 [1] conditions and A36 Steel or Structural Steel as the material chosen for the fabrication of the Halo.

Analysis Approach

As mentioned, tests were performed on the HALO device to validate its stiffness and strength, the tests consist of a modal analysis and a structural analysis following the evaluation method used in the real F1 HALO device. Called Quasi Static Test 1 and Quasi Static Test 2, it consists of the application of force at a point in such a way that a controlled deformation is generated on the device. In the case of modal analysis, this consists of the analysis of those frequencies that could enter into ‘resonance’ with the frame.

Meshing characteristics

The characteristics of the mesh used for the analyses carried out are as follows.

ISSN: 2531-2189
RENIECYT-CONAHCYT: 1702902

Noguez-Jimenez, Víctor Manuel, Cordero-Guridi, José de Jesús, Peréz-Carrillo, Daniel and García-Tépox, José Domingo. [2024]. Experimental proposal of a 'HALO'-type security device in a FORMULA SAE 2024 type vehicle. Journal of Mechanical Engineering. 8[21]-1-16: e40821116.
DOI: https://doi.org/10.35429/JME.2024.8.21.1.16

Box 23

Table 2
Table of location of supports and loads on structural analysis

Study	Modal	Structural
Element size	7	7
Element type	1D	1D
Number of mesh elements	1466	1466

Source: Own elaboration

The material used was A36 steel, better known as structural steel, which was selected due to its properties, accessibility and validity according to the FSAE competition regulations. These properties are shown below:

Box 24

Table 3
Material properties table Steel A36

Property	Value	Unit
Density	7.85e-0	kg/mm³
Young's modulus	2e+05	MPa
Poisson's Ratio	0.3	-
Shear modulus	76923	MPa
Compressive yield strength	250	MPa

Source: Own elaboration

Modal analysis

The first analysis performed is the modal analysis, carried out to determine and locate the natural frequencies and vibration modes to avoid in order to keep the frame away from resonances and/or structural failures. This ensures that the frame does not have natural frequencies that coincide with engine or ground excitations, improving durability and performance. The conditions of the analysis are shown below:

Box 25

Table 4
Table of location of supports and loads on structural analysis

Type of load/holding	Location
Fixed Support - Front	Front suspension
Fixed Bracket - Rear	Suspension rear

Source: Own elaboration

Box 26

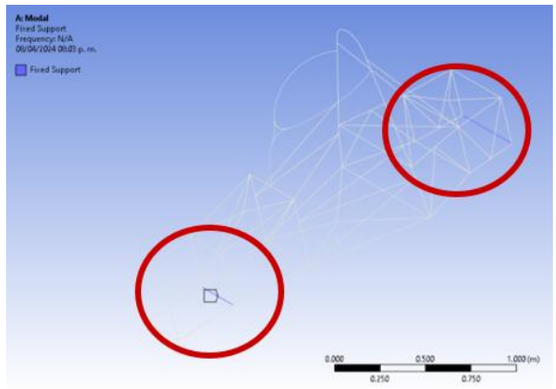

Figure 22
Image showing the location of the supports

Source: Own elaboration

Box 27

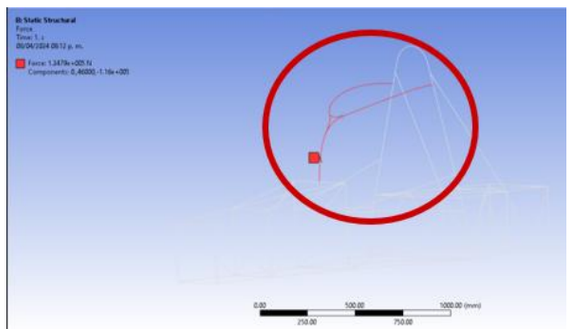

Figure 23
Image showing the load used for structural analysis

Source: Own elaboration

As mentioned above, the modal analysis was carried out to avoid that the frequencies induced to the frame coincide with the frequencies produced by the vibration of the engine, mentioned below:

Box 27

Table 5
Table of results of the modal analysis on the original FSAE model

Force Induced	Value	Units
Engine Revolutions	**13000**	rpm

Source: Own elaboration

Modal analysis studies were carried out before and after the modifications in order to obtain a comparison between the two. The following results were obtained:

ISSN: 2531-2189
RENIECYT-CONAHCYT: 1702902

Noguez-Jimenez, Víctor Manuel, Cordero-Guridi, José de Jesús, Peréz-Carrillo, Daniel and García-Tépox, José Domingo. [2024]. Experimental proposal of a 'HALO'-type security device in a FORMULA SAE 2024 type vehicle. Journal of Mechanical Engineering. 8[21]-1-16: e40821116.
DOI: https://doi.org/10.35429/JME.2024.8.21.1.16

Box 28

Table 6
Table of results of modal analysis on the FSAE model

No. of Frequency	Value (Hz)
1	47.768
2	72.249
3	74.955
4	88.846
5	104.26
6	116.94

Source: Own elaboration

Box 29

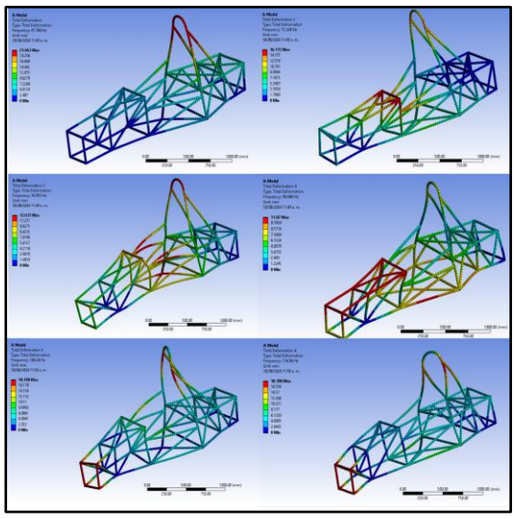

Figure 24
Deformation results obtained from modal analysis (A36 STEEL) prior to Halo modification

Source: Own elaboration

Once the modifications to the frame had been made, the analysis was carried out again, obtaining the following results:

Box 30

Table 7
Table of results of modal analysis on the FSAE model

No. of Frequency	Value (Hz)
1	43.636
2	71.349
3	79.554
4	80.394
5	101.58
6	109.87

Source: Own elaboration

Box 31

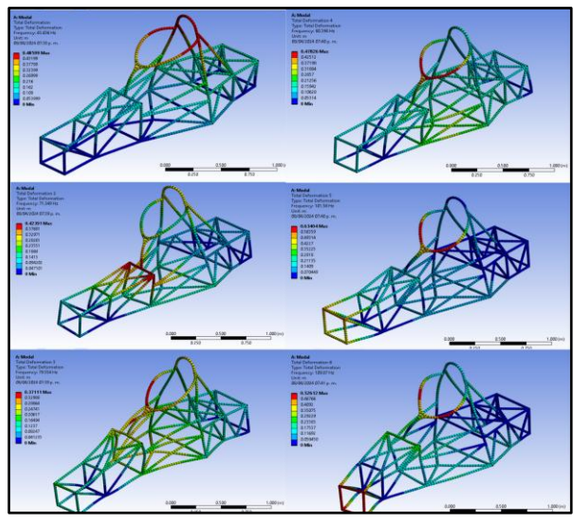

Figure 25
Deformation results from modal analysis

Source: Own elaboration

The values of frequencies that could cause the proposed structure to resonate (216 Hz frequency of the electric motor) can be found. As can be seen, the results vary little.

Structural Analysis

The next analysis performed was the structural analysis, carried out to determine the total deformation according to the determined forces. In this case, as mentioned, the analysis is based on the Quasi Static Test 1 [1] performed on the Halo devices for F1. Thus ensuring that the Halo complies with the maximum allowable deformation of 90 mm. The conditions of the analysis are shown below:

Box 32

Table 8
Table of location of supports and loads on structural analysis

Type of load/holding	Value	Location
Constant force on Y-axis	-46 kN	HALO Impact Zone
Constant force on Z-axis	-116 kN	Halo Impact Zone

Source: Own elaboration

From this analysis, the total deformation and the directional deformation were sought, and the following results were obtained:

ISSN: 2531-2189
RENIECYT-CONAHCYT: 1702902

Noguez-Jimenez, Víctor Manuel, Cordero-Guridi, José de Jesús, Peréz-Carrillo, Daniel and García-Tépox, José Domingo. [2024]. Experimental proposal of a 'HALO'-type security device in a FORMULA SAE 2024 type vehicle. Journal of Mechanical Engineering. 8[21]-1-16: e40821116.
DOI: https://doi.org/10.35429/JME.2024.8.21.1.16

Box 33

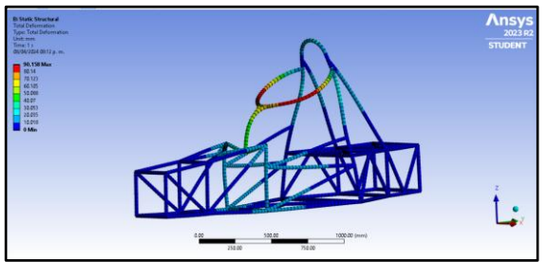

Figure 26
Total deformation of structural analysis on the FSAE model

Source: Own elaboration

Box 34

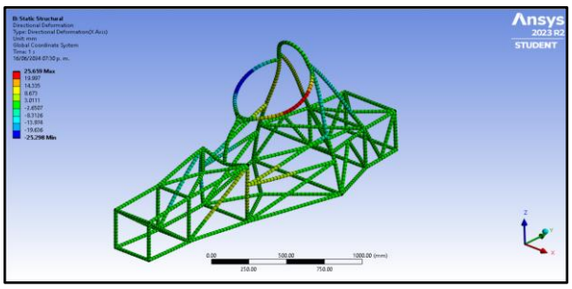

Figure 27
Directional deformation of the structural analysis on the FSAE model

Source: Own elaboration

Box 35

Table 9
Results obtained from the Structural Analysis

Structural static analysis	
Type	Final Model
	Value
Total deformation	90.158 mm
Directional deformation	25.659 mm

Source: Own elaboration

From this analysis, the total deformation was found to be 90.158 mm at its maximum point, which shows that the impact on the main hoop generates a deformation that exceeds by 0.158 mm the tolerance values initially proposed under these test conditions.

Physical Tests

For the validation and corroboration of the results a physical model was generated by 3D printing, this device was scaled at a ratio of 1:8 because this scale was the one that best fit the printing bed of the 3D printer.

The material Onyx [B] was chosen due to its mechanical properties and the current availability of the material.

These mechanical properties and under the environmental conditions shown below:

Box 36

Table 10
Properties of Onyx

Condition	Value	Unit
Young's modulus	2400	MPa
Elongation at break	25	%
Flexural strength	81	MPa
Flexural modulus	2900	MPa

Source: Own elaboration

Box 37

Table 11
3D printing conditions

Condition / Material	Valor / Number	Model/Unit
3D printer	Marforged	Mark Two
Temperature	24	°C
Curing time	45	min

Source: Own elaboration

Box 38

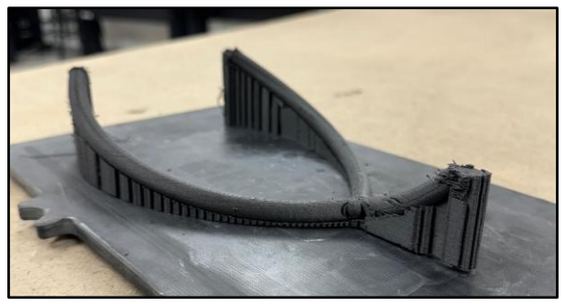

Figure 28
3D printing at Onyx

Source: Own elaboration

However, some problems arose in the printing, details such as marks and a weakened node invalidated the print, so another option had to be implemented.

ISSN: 2531-2189
RENIECYT-CONAHCYT: 1702902

Noguez-Jimenez, Víctor Manuel, Cordero-Guridi, José de Jesús, Peréz-Carrillo, Daniel and García-Tépox, José Domingo. [2024]. Experimental proposal of a 'HALO'-type security device in a FORMULA SAE 2024 type vehicle. Journal of Mechanical Engineering. 8[21]-1-16: e40821116.
DOI: https://doi.org/10.35429/JME.2024.8.21.1.16

Box 39

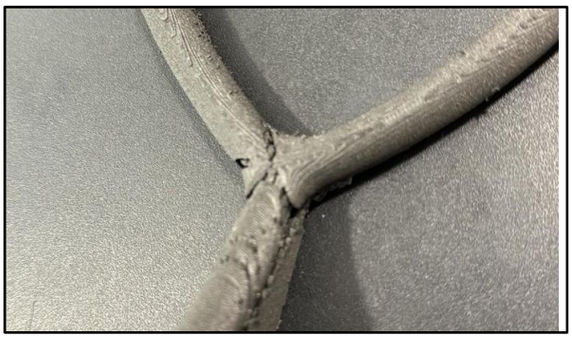

Figure 29
3D printing at Onyx

Source: Own elaboration

Due to the printing failures and the lack of more Onyx material, it was decided to print with clear V5 resin [B], with its mechanical properties shown below.:

Box 40

Table 12
Properties of V5 resin

Condition	Value	Unit
Young's modulus	2750	MPa
Elongation at break	10	%
Flexural strength	92	MPa
Flexural modulus	2450	MPa

Source: Own elaboration

The following results were obtained from this print. For this print, the HALO was rescaled to a ratio of 1:9 to fit the printer bed.

Box 41

Figure 30
Printing of HALO in Resin V5
Source: Own elaboration

The print was subjected to a cleaning process in a vat of ethyl alcohol for 40 minutes and a curing process of 45 minutes at 70 °C. Subsequently, physical tests were carried out using a universal stress machine. This equipment allowed to progressively apply force on the Halo as a function of time.

Box 42

Figure 31
3D printing at Onyx
Source: Own elaboration

Once positioned, the upper plunger of the machine was positioned at a height almost touching the Halo protection device to obtain accurate measurements and to avoid non-contact data between the plunger and the Halo. The machine was programmed to lower by 10 mm every minute, thus measuring the force at which the Halo deformed and/or failed.

Box 43

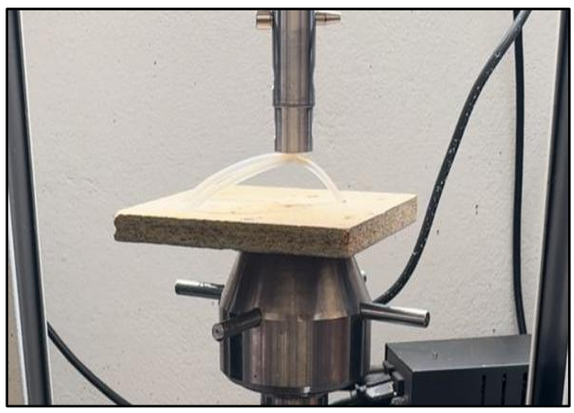

Figure 32
3D printing at Onyx

Source: Own elaboration

The tests showed that the failure effect occurred at 137.05 N of force applied on the V5 resin Halo, with a deformation of up to 20.81 mm extension

ISSN: 2531-2189
RENIECYT-CONAHCYT: 1702902

Noguez-Jimenez, Víctor Manuel, Cordero-Guridi, José de Jesús, Peréz-Carrillo, Daniel and García-Tépox, José Domingo. [2024]. Experimental proposal of a 'HALO'-type security device in a FORMULA SAE 2024 type vehicle. Journal of Mechanical Engineering. 8[21]-1-16: e40821116.
DOI: https://doi.org/10.35429/JME.2024.8.21.1.16

Box 44

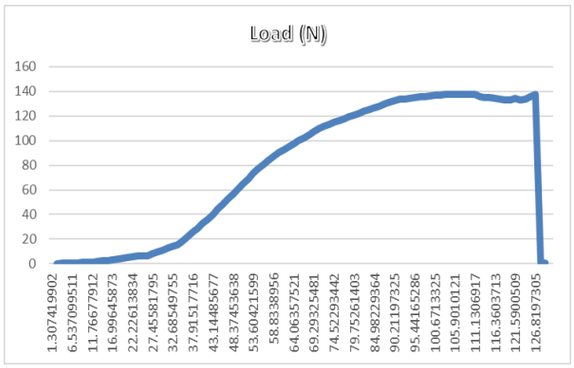

Figure 33
Behaviour of force applied on the HALO

Source: Own elaboration

Box 45

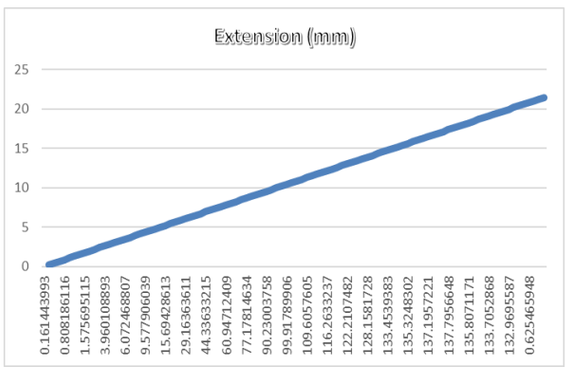

Figure 34
Elongation behaviour against applied force

Source: Own elaboration

These results demonstrate that, under the test conditions described, the HALO printed on V5 resin presents a deformation capacity and specific resistance that is crucial for its evaluation in future applications.

Analysis Results

The modal analysis is performed to validate the structural stiffness of the frame and to visualise the interaction between the frequencies of the medium and the frame, the structural analysis is performed to validate the structural toughness against a possible impact, and as a requirement/complement the visual comparison in order to fulfil the design requirement, adding value towards the inclusion of the device. As mentioned in the modal analysis, it is maintained over the frequency range that would cause the frame to resonate, demonstrating that the stiffness of the structure is preserved.

In the case of the point of view analysis it is observed that the field of view is only obstructed at the centre and was therefore not considered relevant compared to the structural and safety benefits observed. As expected due to the characteristics of the material, the steel is a tough and resistant option to the test, however it fails the tests under the conditions of Quasi Static Test 1 exceeding the tolerance defined by a difference of less than 0.158 mm of deformation, this is a point that is considered for future improvements and starting point for redesign of the geometry or even the choice of material, in this case being of experimental subject is considered as valid because in this geometry and with this material is discarded for professional use.

Conclusions

After the research and analysis carried out in the project, it was concluded that the inclusion of a Halo type device in a Formula SAE type vehicle represents a benefit as it maintains the rigidity and resistance without compromising the aesthetics of the vehicle, at the same time as it increases pilot safety in the event of any eventuality in a competition or test. It is concluded that if it is desired to open the competition to a wheel-to-wheel type, the Halo device would be of great use as part of the safety and damage prevention elements. The results of the physical tests allowed a comparison to be made with the initial graph showing the behaviour of the steel, it is assumed that the proposed Halo structure could withstand a possible impact under 124, 787.82 Newton at 338.37°. It is important to note that these assumptions are based on the study and knowledge of the behaviour of each material. However, in order to obtain more accurate and realistic results, it is recommended that a prototype be made using the proposed material. Digital analysis suggests that the A36 Steel Halo construction is effective in providing protection against critical deformations, ensuring the safety and integrity of the driver in collision situations.

Conflict of interest

The authors declare that they have no conflicts of interest. They have no known competing financial interests or personal relationships that could have influenced the article reported in this paper.

ISSN: 2531-2189
RENIECYT-CONAHCYT: 1702902

Noguez-Jimenez, Víctor Manuel, Cordero-Guridi, José de Jesús, Peréz-Carrillo, Daniel and García-Tépox, José Domingo. [2024]. Experimental proposal of a 'HALO'-type security device in a FORMULA SAE 2024 type vehicle. Journal of Mechanical Engineering. 8[21]-1-16: e40821116.
DOI: https://doi.org/10.35429/JME.2024.8.21.1.16

Authors' contribution

The contribution of each researcher in each of the points developed in this research was defined based on:

Noguez-Jimenez, Victor-Manuel: He contributed to the construction of the CAD models and their analysis, ensuring compliance with the theoretical analyses and their numerical validation. As well as the generation of the physical experiments on the 3D model.

Perez-Carrillo, Daniel: Contributed to the elaboration and evaluation of the CAD models, the analysis of the models presented, as well as the evaluation and execution of the 3D printing of the models.

Cordero-Guridi, José de Jesús: Contributed to the development of the research method as a guide and validation of the project.

García-Tépox, José Domingo: Contributed to the diversification of ideas on the generation of the physical tests and the generation of the 3D printed physical model.

Acknowledgements

The authors of this work would like to thank José de Jesús Cordero Guridi, José Domingo García-Tépox, the colleagues of the Formula SAE UPAEP team and the Universidad Popular Autónoma del Estado de Puebla for the use of the facilities and the support provided.

Funding

This work was fully funded by the Universidad Popular Autónoma del Estado de Puebla A.C.

Abbreviations

CAD - Computer-Aided Design

FEA - Failure Modes and Effects Analysis

FMEA - Failure Modes and Effects Analysis

FEA - Finite Element Analysis

HIC - Head Injury Criterion

FIA - Federation Internationale de l'Automobile

FSAE - Formula SAE

POV - Point of View

Annexes

[A] Design Failure Mode and Effect Failure Analysis (PMFE) - Halo Design for Formula SAE

[B] Clear Resin V5 Datasheet

References

Background

[2] World Health Organization (2018). Global status report on road safety 2018. World Health Organization.

[6] Head Injury Analysis of Vehicle Occupant in Frontal Crash Simulation: Case Study of ITB's Formula SAE Race Car. J.Eng. Technal. Sci., Vol.49, No. 4, 2017, 534-545

[8] Redbull (2023, May). F1's fastest circuits: Where speed pushes the limits.

Basics

[1] FIA. (2018). FIA STANDARD 8869-2018: SINGLE-SEATER ADDITIONAL FRONTAL PROTECTION - HALO. Fédération Internationale de l'Automobile.

[3] Insurance Institute for Highway Safety (2023, May). Trends: Passenger vehicle occupants. Insurance Institute for Highway Safety.

[4] National Highway Traffic Safety Administration(2022). Characteristics of Fatal Rollover Crashes. United States Department of Transportation.

[5] Society of Automotive Engineers (2023). Formula SAE 2023 Rules. Society of Automotive Engineers.

[7] How to make an F1 halo (2018, 13 March). Federation Internationale de l'Automobile.

[9] Monroe, C. A Critical Review of the 'Halo' Device in Formula One.

ISSN: 2531-2189
RENIECYT-CONAHCYT: 1702902

Noguez-Jimenez, Víctor Manuel, Cordero-Guridi, José de Jesús, Peréz-Carrillo, Daniel and García-Tépox, José Domingo. [2024]. Experimental proposal of a 'HALO'-type security device in a FORMULA SAE 2024 type vehicle. Journal of Mechanical Engineering. 8[21]-1-16: e40821116.
DOI: https://doi.org/10.35429/JME.2024.8.21.1.16

[10] Arteaga, O., Mena, S., Caiza, V., & Vilaña, J. (2015). Design, simulation, optimization and construction of a bodywork of a formula SAE type vehicle. Latacunga, Ecuador: Escuela Politécnica del Ejército (p. 3).

ISSN: 2531-2189
RENIECYT-CONAHCYT: 1702902

Noguez-Jimenez, Víctor Manuel, Cordero-Guridi, José de Jesús, Peréz-Carrillo, Daniel and García-Tépox, José Domingo. [2024]. Experimental proposal of a 'HALO'-type security device in a FORMULA SAE 2024 type vehicle. Journal of Mechanical Engineering. 8[21]-1-16: e40821116.
DOI: https://doi.org/10.35429/JME.2024.8.21.1.16

Journal of Mechanical Engineering 8[21]1-9: e50821109
Article

Design and implementation of an embedded data logger for MAP sensors in automotive systems

Diseño e implementación de un registrador embebido para sensores MAP en sistemas automotrices

Durán-Fonseca, Miguel Ángel*[a], Charre-Ibarra, Saida[b], Murgan-Ibañez, Jorge[c] and Gudiño-Lau, Jorge[d]

[a] Universidad de Colima • 9495-2024 • 0000-0002-0780-6192
[b] Universidad de Colima • 6851-2018 • 0000-0002-3823-5388
[c] Universidad de Colima • 0009-0009-0998-8995
[d] Universidad de Colima • Q-6844-2018 • 0000-0002-0585-908X • 122644

CONAHCYT classification:

Area: Engineering
Field: Engineering
Discipline: Mechanical Engineering
Subdiscipline: Automotive industries

https://doi.org/10.35429/JME.2024.8.21.5.9
Article History:
Received: January 30, 2024
Accepted: December 31, 2024

* ✉ [mduran@ucol.mx]

Abstract

This paper presents the design and construction of an embedded system for recording and analyzing data from a Manifold Absolute Pressure (MAP) sensor. The system integrates a PIC18F4620 microcontroller, a microSD storage module, a DS3231 real-time clock, and a Bluetooth communication module. This data logger enables real-time evaluation of the performance of an ecological valve installed in a gasoline engine. Tests under different operating conditions were conducted, assessing its impact on engine efficiency and fuel consumption.

Objetive	Methodology	Contribution
To design and implement an embedded system to record and analyze data generated by a MAP sensor. 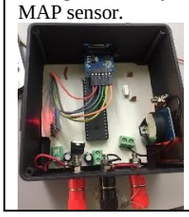	1. System Design 2. Prototype Implementation 3. Experimental Testing 4. Data Analysis and Validation 	1. Design of a functional embedded logger 2. Real-time evaluation 3. Mobile application 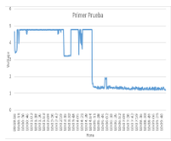

Manifold, Ecological, Evaluation

Resumen

Este artículo presenta el diseño y la construcción de un sistema embebido para el registro y análisis de datos provenientes de un sensor de presión absoluta del múltiple de admisión (MAP). El sistema integra un microcontrolador PIC18F4620, un módulo de almacenamiento en microSD, un reloj en tiempo real DS3231 y un módulo de comunicación Bluetooth. Este registrador permite la evaluación en tiempo real del desempeño de una válvula ecológica instalada en un motor a gasolina. Se incluyeron pruebas en distintas condiciones de operación, evaluando su impacto en la eficiencia del motor y el consumo de combustible.

Objetivo	Metodología	Contribución
Diseñar e implementar un sistema embebido para registrar y analizar los datos generados por un sensor MAP. 	1. Diseño del Sistema 2. Implementación del Prototipo 3. Pruebas Experimentales 4. Análisis de Datos y Validación 	1. Diseño de un registrador embebido funcional 2. Evaluación en tiempo real 3. Aplicación móvil 

Múltiple de admisión, Ecológica, Evaluación

Citation: Durán-Fonseca, Miguel Ángel, Charre-Ibarra, Saida, Murgan-Ibañez, Jorge and Gudiño-Lau, Jorge. [2024]. Design and implementation of an embedded data logger for MAP sensors in automotive systems. Journal of Mechanical Engineering. 8[21]-1-9: e50821109.

Introduction

Internal combustion engines play an essential role in global transport and industry. However, their efficiency and sustainability are constantly challenged by environmental factors, such as variations in atmospheric pressure due to altitude. These variations affect the air-fuel mixture, negatively impacting engine performance, increasing fuel consumption and contributing to environmental pollution (Heywood, 2018), (Stone, 2012), (Zhao, Lai, Harrington, 1999).

Internal combustion engines face numerous challenges in maintaining their efficiency and sustainability, especially at high altitudes. Technologies such as the eco-valve offer effective solutions by dynamically adjusting the proportion of air in the air-fuel mixture, optimising engine performance and reducing pollutant emissions.

Against this background, technologies that optimise engine performance, such as eco-valves and associated monitoring systems, are of great relevance to mitigate these effects and promote more sustainable practices.

The Manifold Absolute Pressure (MAP) sensor is a device designed to measure the volume of air entering the engine. Its signal is interpreted in terms of flow rate, expressed in grams per second. An increase in air flow to the engine translates into an increase in revolutions per minute (RPM). The MAP sensor plays a critical role in the accurate calculation of fuel injection timing.

When the MAP sensor malfunctions, black smoke, an indication of high fuel consumption, is common. These faults are often reflected in the codes P0101, P0102 and P0103 when the system is scanned (Booster, 2014). The MAP sensor has three wires: one to receive the supply voltage, connected via a fuse located in the engine fuse box; another that connects to earth ground (chassis); and a third that transmits the detected air flow data directly to the computer.

An eco-valve acts as a height compensator and is installed in the intake manifold to maintain the proper proportions of air and petrol entering the engine.

This adjustment is made according to altitude above sea level, allowing the optimum amount of air to be metered for efficient mixing with the petrol. As a result, the overall performance of new or used engines in any type of automobile is improved (Marclais, 2014).

The air intake regulated by the eco-valve depends on both how quickly the throttle is depressed and changes in atmospheric pressure associated with altitude. During hard acceleration, such as when starting or overtaking another vehicle, excess fuel is generated in the mixture; in these situations, the eco-valve acts immediately to allow additional air intake to balance the air/fuel ratios. Conversely, when the accelerator is released or when the mixture is already adequate, the valve suspends the entry of additional air into the engine (Marclais, 2014).

This work addresses the design and implementation of an embedded data logging system specifically designed for MAP sensors. This system not only allows real-time monitoring of the performance of devices such as eco-valves, but also provides a cost-effective and efficient platform for the collection of critical data on engine behaviour under different operating conditions.

The added value of the developed system lies in its integration of compact, inexpensive and easy-to-implement technologies, such as a PIC18F4620 microcontroller, a microSD storage module, a DS3231 real-time clock and a Bluetooth module. Unlike other techniques that often require expensive and more complex equipment (Bosch, 2022), this system offers an affordable and versatile solution that not only monitors but also stores the data in a readable format and allows for subsequent analysis in an efficient way. In addition, Bluetooth connectivity enables real-time monitoring via mobile devices, significantly improving the user experience and responsiveness to changing engine conditions.

The proposed design is notable for the following features:

- Portability and versatility: The system can be implemented in various vehicle models and adapted to other applications.

ISSN: 2531-2189
RENIECYT-CONAHCYT: 1702902

Durán-Fonseca, Miguel Ángel, Charre-Ibarra, Saida, Murgan-Ibañez, Jorge and Gudiño-Lau, Jorge. [2024]. Design and implementation of an embedded data logger for MAP sensors in automotive systems. Journal of Mechanical Engineering. 8[21]-1-9: e50821109.
DOI: https://doi.org/10.35429/JME.2024.8.21.5.9

- Hardware and software integration: Its modular design includes electronic components and a mobile application developed in App Inventor for real-time data visualisation and storage.

- Accuracy and reliability: The use of a real-time clock ensures the traceability of recorded data, while the microSD module facilitates its storage in an organised and secure manner.

- Economic efficiency: The components used are affordable, which significantly reduces the overall cost of the system without compromising its functionality.

The problem to be solved centres on the need to monitor and analyse the performance of eco-valves installed in gasoline engines, especially under critical operating conditions, such as high altitudes and steep slopes. These conditions generate a variation in the air-fuel ratio, which compromises engine performance and increases fuel consumption (Santamaria, 2010). The central hypothesis argues that the developed data logger will accurately and reliably demonstrate the operational and environmental benefits of eco-valves, providing a valuable tool for their evaluation, validation and mass adoption.

The proposed embedded system not only addresses a relevant technical and environmental problem, but also introduces an innovative and affordable solution, broadening the field of applications in the automotive industry and strengthening efforts towards sustainability.

The following sections detail the structure and operation of the MAP sensor recorder, addressing each of its key components and their integration into the system. A description of the developed mobile application is included, which allows the visualisation and storage of the collected data in real time. Likewise, the design and configuration of the electronic circuit used to carry out the experimental tests is presented, highlighting its implementation and validation. Finally, the results obtained during the tests are analysed, emphasising the impact of the recorder in the evaluation of the performance of the eco-valve under various operating conditions.

MAP sensor recorder

The intake manifold absolute pressure (MAP) sensor is essential for measuring the air pressure in the engine, providing fundamental data for calculating the air-fuel mixture and optimising engine performance (Bravo Morocho, 2022). The implementation of data loggers, such as those described by (Sanchez Perez and Galindo Valencia, 2024), highlights the importance of recording key parameters such as temperature and pressure in real time to optimise engine operation.

The developed system consists of an embedded data logger designed to collect and analyse the information generated by a MAP sensor. This system allows to evaluate the performance of devices such as eco-valves in internal combustion engines under different operating conditions.

The system design included the integration of hardware and software, allowing the development of an electronic circuit and the programming of the PIC18F4620 microcontroller. This approach is consistent with that described by (Betancourt Rodriguez, 2024), who emphasises the importance of integrated solutions that combine both elements to meet specific automation requirements.

The MAP recorder consists of the following elements:

- PIC18F4620 microcontroller: Responsible for processing the signals coming from the MAP sensor.

- microSD module: Allows the data to be stored in a readable format (CSV), facilitating subsequent analysis.

- DS3231 Real Time Clock: Provides accurate time stamps for each data record.

- Bluetooth Module HC-06: Facilitates real-time display via a mobile application.

- MAP Sensor: Detects the pressure in the intake manifold, emitting signals proportional to the air flow.

ISSN: 2531-2189
RENIECYT-CONAHCYT: 1702902

Durán-Fonseca, Miguel Ángel, Charre-Ibarra, Saida, Murgan-Ibañez, Jorge and Gudiño-Lau, Jorge. [2024]. Design and implementation of an embedded data logger for MAP sensors in automotive systems. Journal of Mechanical Engineering. 8[21]-1-9: e50821109.
DOI: https://doi.org/10.35429/JME.2024.8.21.5.9

This device allows real-time monitoring of engine operating conditions, with a particular focus on the evaluation of the eco-valve. A microcontroller-based system aims to provide an accessible and efficient tool for recording signals, processing and storing them together with time stamps. This facilitates the evaluation of engine performance and the optimisation of engine operation under various conditions.

Mobile application

The mobile application developed for this project allows the visualisation and management of the data collected by the MAP sensor logger in real time. Using wireless connectivity technologies, such as Bluetooth, an efficient and reliable transmission is ensured. This aligns with the principles described by (Rubio-Quintanilla, 2024) on the use of communication standards in embedded systems to ensure interoperability and reliability. The design should provide an intuitive and accessible interface for users (Chennakesava, 2009).

The application was created using App Inventor, a platform that allows the development of Android applications using visual block programming. This tool simplifies the design of interfaces and the integration of specific functionalities, such as Bluetooth connection and data storage. Figure 1 shows the user interface of the developed application.

Box 1

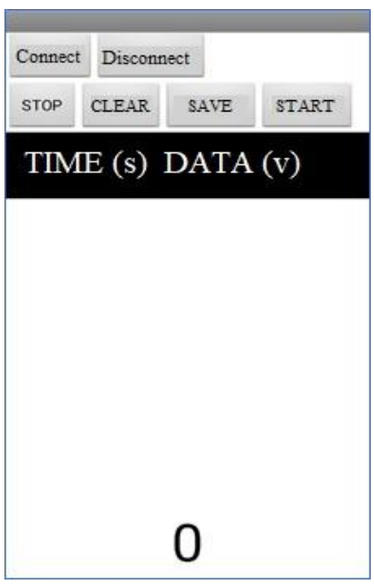

Figure 1
Mobile application

The interface was designed to be user-friendly and functional. It includes clearly identified buttons to perform specific actions, such as:

- Connect: Allows you to select the Bluetooth module and establish communication.
- Start: Activates the reception and display of data in real time.
- Stop: Ends data transmission.
- Save: Generates a CSV file with the stored readings.
- Restart: Clears the logs and restarts the interface.

The application includes the following functionalities:

- Bluetooth connection: Scanning of paired devices. Selection and connection to the MAP logger.
- Real Time Monitoring: Continuous display of MAP sensor readings. Data representation in a simple and clear interface.
- Data Storage: Generation of files in CSV format with the recorded readings. Possibility to name and save files for later analysis.
- Operations Management: Buttons to start, stop and restart data transmission. Options to delete logs stored in the application.

The application was tested on Android devices with different versions of the operating system, ensuring its compatibility and functionality. During the tests, the connection to the MAP logger proved to be stable, with smooth and uninterrupted data transmission.

The addition of the mobile app significantly enhances the user experience, allowing the user to monitor and analyse engine performance immediately and conveniently. In addition, the ability to store data facilitates detailed log analysis, contributing to predictive maintenance and fuel consumption optimisation.

ISSN: 2531-2189
RENIECYT-CONAHCYT: 1702902

Durán-Fonseca, Miguel Ángel, Charre-Ibarra, Saida, Murgan-Ibañez, Jorge and Gudiño-Lau, Jorge. [2024]. Design and implementation of an embedded data logger for MAP sensors in automotive systems. Journal of Mechanical Engineering. 8[21]-1-9: e50821109.
DOI: https://doi.org/10.35429/JME.2024.8.21.5.9

Electronic circuit

This section presents the design of the electronic circuit of the MAP recorder, which must efficiently integrate the necessary components for data collection, processing and storage (Wolf, 2022). The circuit includes the following key elements: PIC18F4620 microcontroller, MAP sensor, DS3231 RTC module, microSD module, HC-06 Bluetooth module and power supply. The system design includes a plastic housing manufactured based on the technical specifications of the MAP sensor and the installation requirements in the car. This design, made in SolidWorks, aims to protect the electronic components, ensure accessibility to the functional elements of the recorder and facilitate its integration in various vehicular environments. Figure 2 presents the finished housing, showing a compact and functional design that houses all the components of the data logger. Power is supplied to the system via clearly labelled slots. There is one slot labelled 'SD', specifically designed for the safe insertion and removal of the microSD memory, where the data collected by the embedded system is stored. Another slot is for the connection of the MAP sensor signal. This input allows the logger to capture the data from the sensor and process it for storage in the microSD memory. The strategic arrangement of these slots ensures fast and efficient installation of the system in the engine compartment.

Box 2

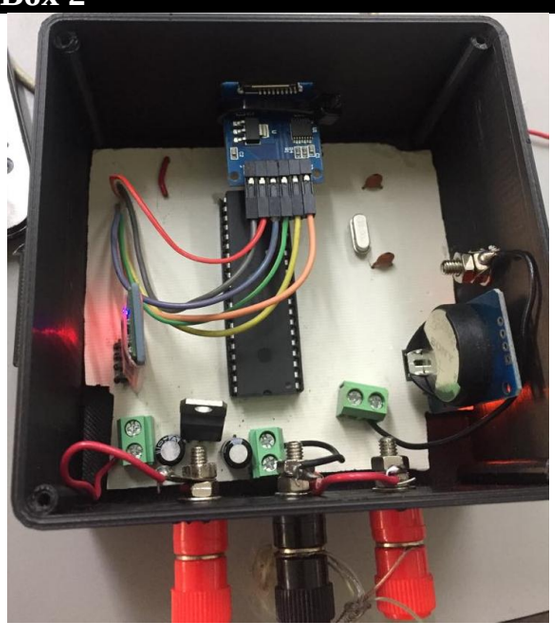

Figure 2
Circuit mounted in the housing

This housing not only protects the internal hardware from adverse conditions, such as dust or moisture, but also contributes to the durability and transportability of the device. This compact and secure design ensures the protection of the electronic components and facilitates their integration into the automotive environment.

Tests and results

The mechanical installation of the recorder was carried out on a 1985 Volkswagen Golf. The process consisted of making a bifurcation in the vehicle's intake manifold, where a hose was connected to extend the air signal to the cabin. Inside the cabin, the eco-valve was installed, to which another hose was connected, leading the flow to the MAP sensor. This design allows data to be monitored and recorded directly from the engine compartment. Figure 3 shows the bifurcation made in the intake manifold to connect the eco-valve to the engine.

Box 3

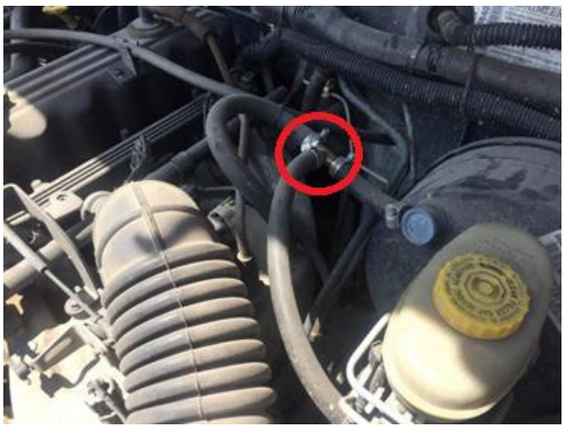

Figure 3
Bifurcation for connection inside the engine compartment of the vehicle

Inside the vehicle cabin, the eco-valve was connected via the hose coming from the intake manifold. This hose runs through the driver's compartment and connects to the MAP sensor input, allowing the data required to evaluate the system's performance to be recorded.

The datalogger is wired via a USB adapter connected to the vehicle's 12V socket, which provides power to the system. The MAP sensor has three cables: two power cables and one signal cable.

ISSN: 2531-2189
RENIECYT-CONAHCYT: 1702902

Durán-Fonseca, Miguel Ángel, Charre-Ibarra, Saida, Murgan-Ibañez, Jorge and Gudiño-Lau, Jorge. [2024]. Design and implementation of an embedded data logger for MAP sensors in automotive systems. Journal of Mechanical Engineering. 8[21]-1-9: e50821109.
DOI: https://doi.org/10.35429/JME.2024.8.21.5.9

Figure 4 shows the path taken during the testing of the eco-valve. This path was specifically designed to evaluate the performance of the system under varying conditions, including significant changes in altitude. During the tests, key data such as distance travelled, travel time, altitude, average speed and maximum speed were recorded.

Box 4

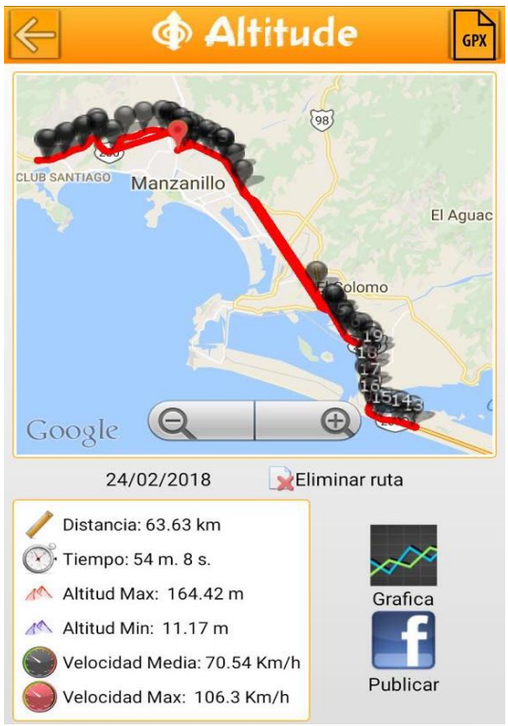

Figure 4
Path

Among all the variables analysed, altitude was identified as the most relevant (Ferguson, Kirkpatrick, 2016), as the main objective of the eco-valve is to compensate for the decrease in available oxygen at high altitudes. By adjusting the proportion of air entering the engine, the valve improves combustion efficiency, thus optimising engine performance. To evaluate this behaviour, a route was selected that included different altitude levels, ensuring challenging conditions for the engine. This allowed us to observe how the valve is activated to balance the air-fuel mixture in response to oxygen depletion at higher altitudes. In the graph shown in figure 5, the variations in altitude along the route can be clearly seen, providing a visual representation of the environment in which the system operated.

Box 5

Figure 5
Altitudes during the journey

The design of these tests not only verified the functionality of the system, but also highlighted its ability to record and analyse data in real time. This ensures that the MAP logger is a reliable tool for assessing the impact of devices such as the eco-valve in real operating environments.

During testing, the system collected critical data on engine behaviour and eco-valve activation under different operating conditions. This supports the need for reliable systems to monitor processes in real time, as highlighted by (Asmad Vereau and Falero Siancas, 2024) in industrial monitoring and control applications.

Figure 6 shows the results obtained when the eco-valve is connected and operational. The graph shows how the recorded voltage varies over time, indicating the activations of the valve. When the voltage reaches 5V, it is evident that the engine requires additional oxygen supply, which activates the valve to compensate for the lack of oxygen in the air-fuel mixture. Thus, the graph reflects the number of times the valve was actuated during the trip.

ISSN: 2531-2189
RENIECYT-CONAHCYT: 1702902

Durán-Fonseca, Miguel Ángel, Charre-Ibarra, Saida, Murgan-Ibañez, Jorge and Gudiño-Lau, Jorge. [2024]. Design and implementation of an embedded data logger for MAP sensors in automotive systems. Journal of Mechanical Engineering. 8[21]-1-9: e50821109.
DOI: https://doi.org/10.35429/JME.2024.8.21.5.9

Box 6

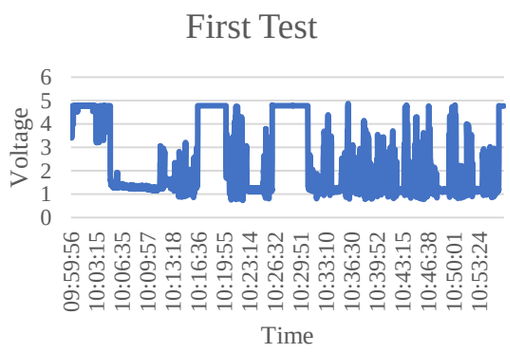

Figure 6
Results when the valve is active

Figure 7 highlights the data obtained during the first 10 minutes of the first test. During this period, frequent activations of the valve are observed, particularly in situations such as passing another vehicle, which requires a sharp acceleration, or when ascending steep slopes, where oxygen levels decrease due to the altitude. In these cases, the valve helps to maintain engine efficiency by delivering more oxygen rather than increasing fuel consumption.

Box 7

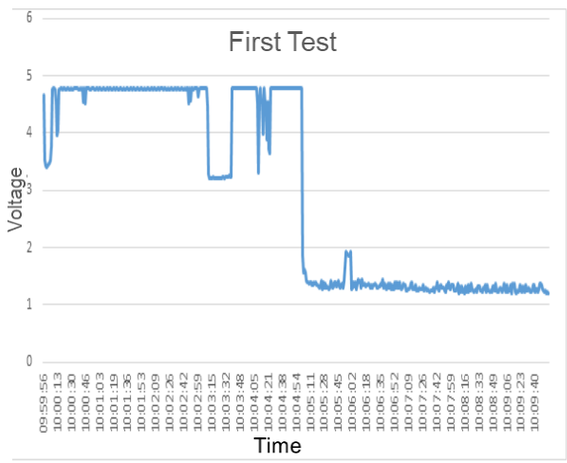

Figure 7
Results when the valve is active (extract)

On the other hand, Figure 8 shows the results obtained when the eco-valve is not connected. Under these conditions, the graph indicates that the valve is not activated, which negatively affects the efficiency of the engine. The lack of compensation for oxygen depletion in similar situations reduces combustion efficiency, which can lead to higher fuel consumption and lower performance.

Box 8

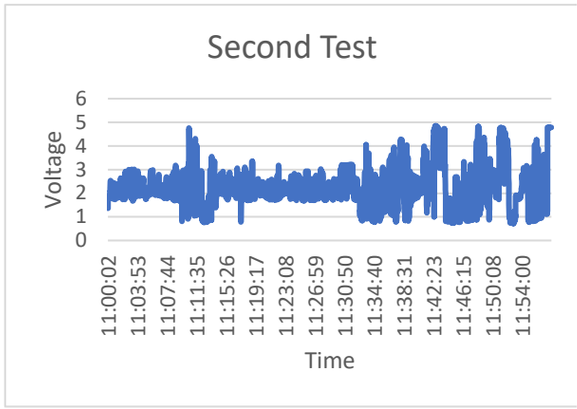

Figure 8
Results when the valve is not active

Figure 9 presents the data obtained during the first 10 minutes of the second test, where the same path was repeated as in the first test, but without the valve connection. When comparing both results, it is evident that the engine did not receive the benefit of oxygen compensation, which reinforces the importance of the valve in improving engine performance under these conditions.

Box 9

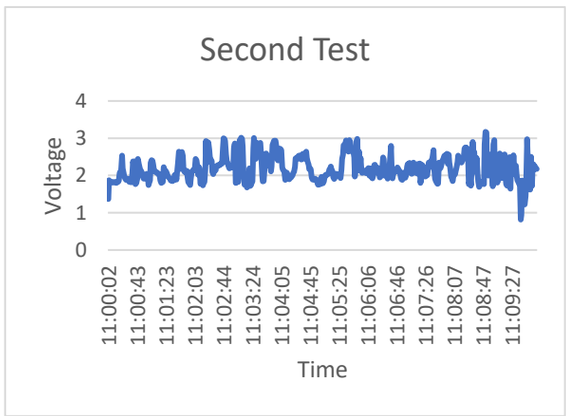

Figure 9
Results when the valve is not active (excerpt)

Finally, Figure 10 shows the results of a third test performed to evaluate the operation of the prototype over a longer period of time. This analysis confirmed the stability and reliability of the system in long-term data collection, as well as the effectiveness of the valve in responding to the needs of the engine in different scenarios.

ISSN: 2531-2189
RENIECYT-CONAHCYT: 1702902

Durán-Fonseca, Miguel Ángel, Charre-Ibarra, Saida, Murgan-Ibañez, Jorge and Gudiño-Lau, Jorge. [2024]. Design and implementation of an embedded data logger for MAP sensors in automotive systems. Journal of Mechanical Engineering. 8[21]-1-9: e50821109.
DOI: https://doi.org/10.35429/JME.2024.8.21.5.9

Box 10

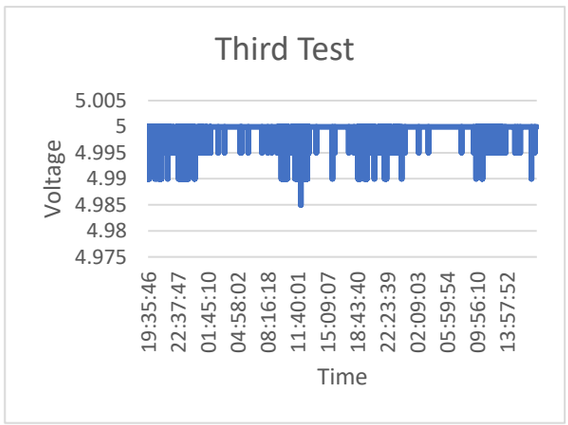

Figure 10
Test results over a longer period of time

This series of tests clearly demonstrates the ability of the embedded system to accurately monitor and record the performance of the eco-valve, providing key information to assess its impact on engine efficiency.

Conclusions

The eco-valve has proven to be highly efficient in cars operating at altitudes above 1,000 metres above sea level. Its implementation not only optimises engine performance by maintaining more efficient combustion, but also contributes to prolonging engine life. In addition, the valve generates significant fuel savings by dynamically adjusting the proportion of air in the air-fuel mixture, thus reducing energy waste and pollutant emissions.

In the present work, a detailed sampling and continuous recording of the behaviour of this fuel-saving device was carried out. The results show that the eco-valve is mainly activated in critical operating situations, such as steep gradients and abrupt acceleration changes. In these scenarios, the valve regulates the additional oxygen supply needed to optimise combustion, thus improving overall engine efficiency. In addition, the data collected provides valuable information about the driving patterns of each user, which can be useful for studies related to driving habits and their impact on fuel consumption.

The development and analysis of the data loggers used in this study highlight the importance of having accurate tools to monitor and evaluate the behaviour of technological devices. The information generated not only supports research tasks, but also allows validation of the effectiveness of technologies such as the eco-valve under different operating conditions.

The designed device has a high degree of versatility, as it can be adapted to various applications where signal recording is required. Its only limitation is that the recorded signals must be within the range of 0 to 5V, which makes it suitable for a wide variety of sensors in automotive and other systems. This aspect underlines its potential to be used in future projects focusing on engine optimisation and monitoring of similar devices.

Disclosures

Conflict of interest

The authors declare that they have no conflicts of interest. They have no known competing financial interests or personal relationships that might have appeared to influence the article reported in this paper.

Authors' contribution

The contribution of each researcher in each of the points developed in this research, are:

Durán-Fonseca, Miguel-Ángel: He contributed with the revision of the prototype design, experimental tests, analysis of results and the integration of the final document.

Charre-Ibarra, Saida: Contributed with the central idea of the project, design of the prototype and coordinated the work of the members.

Murgan-Ibañez, Jorge: Built the prototype, developed the mobile application and participated in the experimental tests.

Gudiño-Lau, Jorge: Contributed with the programming of the microcontroller and data analysis.

ISSN: 2531-2189
RENIECYT-CONAHCYT: 1702902

Durán-Fonseca, Miguel Ángel, Charre-Ibarra, Saida, Murgan-Ibañez, Jorge and Gudiño-Lau, Jorge. [2024]. Design and implementation of an embedded data logger for MAP sensors in automotive systems. Journal of Mechanical Engineering. 8[21]-1-9: e50821109.
DOI: https://doi.org/10.35429/JME.2024.8.21.5.9

Availability of data and materials

For more information on project data and materials contact scharre@ucol.mx

Funding

The project was developed with own resources.

Acknowledgements

The authors would like to thank the Faculty of Electromechanical Engineering of the University of Colima for the facilities to carry out this research project.

Abbreviations

CSV	Comma-Separated Values (valores separados por comas)
MAP	Manifold Absolute Pressure (Manifold Absolute Pressure)
RPM	Revolutions Per Minute
SD	Secure Digital
USB	Universal Serial Bus

References

Background

Ferguson, C. R., Kirkpatrick, A. T. (2016). Internal Combustion Engines: Applied Thermosciences, 3ed. Wiley.

Heywood, J. B. (2018). Internal combustion engine fundamentals, 2nd Edition. McGraw-Hill Education

Santamaría, P. J. (2010). Evaluación de válvula ecológica Marclais. Medellín: Grupo GIMEL.

Stone, R. (2012). Introduction to Internal Combustion Engines 4th Edition. *Palgrave Macmillan*.

Zhao, F., Lai, M. C., & Harrington, D. L. (1999). Automotive spark-ignited direct-injection gasoline engines. *Progress in Energy and Combustion Science*, *25*(5), 437–562.

Basics

Booster, a. (2014). Curso de sensores MAP. NEXICO: Encendido electronico.

Bosch, R. (2022). Automotive Handbook (11th ed.). Wiley.

Chennakesava, R. (2009). Principles of Industrial Instrumentation and Control Systems. Cengage Learning Asia.

Wolf, M. (2022). Computers as Components: Principles of Embedded Computing System Design, *Fifth Edition*. Elsevier.

Support

Asmad Vereau, J. J., & Falero Siancas, J. C. (2024). Implementación de sistema de control y monitoreo para almacenamiento en frío de palta hass en empresa agroindustrial de La Libertad.

Sanchez Perez, D. A., & Galindo Valencia, J. E. (2024). Desarrollo de un data logger para lectura de temperatura y presión, con materiales de alta resistencia, con lector de datos de manera local y remota, acoplado a un motor CAT C280-12 TIER 4.

Differences

Bravo Morocho, V. D. B. M., Montufar Paz, P. A., Condo Ulloa, C. A., & Manzano Valencia, M. V. (2022). Evaluación del consumo y emisiones de un vehículo implementado una válvula MARCLAIS a 2754 msnm. AlfaPublicaciones, 4(2.2), 89–105.

Rico Romero, M. (2024). Instalación de generación fotovoltaica de 740, 3 kWp conectada a red, situada en Cam. de la Cruz a Nieva, 13600 de Ciudad Real (Doctoral dissertation, Universitat Politècnica de València).

Rubio-Quintanilla Vicedo, A. (2024). Implementación de un transceiver basado en el estándar de comunicaciones aeronaúticas ARINC-717 (Doctoral dissertation, Universitat Politècnica de València).

Discussions

Betancourt Rodriguez, C. C. (2024). Diseño de un sistema de automatización que permita la apertura de puertas de acceso para el ingreso de aeronaves en el hangar de la empresa CIAC LTDA.

Marclais. (2014). ¿Qué es la válvula ecológica?

ISSN: 2531-2189
RENIECYT-CONAHCYT: 1702902

Durán-Fonseca, Miguel Ángel, Charre-Ibarra, Saida, Murgan-Ibañez, Jorge and Gudiño-Lau, Jorge. [2024]. Design and implementation of an embedded data logger for MAP sensors in automotive systems. Journal of Mechanical Engineering. 8[21]-1-9: e50821109.
DOI: https://doi.org/10.35429/JME.2024.8.21.5.9

[Title in TNRoman and Bold No. 14 in English and Spanish]

Surname, Name 1st Author*[a], Surname, Name 1st Co-author[b], Surname, Name 2nd Co-author[c] and Surname, Name 3rd Co-author[d] [No.12 TNRoman]

[a] Affiliation institution, Researcher ID, ORC ID, SNI-CONAHCYT ID or CVU PNPC [No.10 TNRoman]
[b] Affiliation institution, Researcher ID, ORC ID, SNI-CONAHCYT ID or CVU PNPC [No.10 TNRoman]
[c] Affiliation institution, Researcher ID, ORC ID, SNI-CONAHCYT ID or CVU PNPC [No.10 TNRoman]
[d] Affiliation institution, Researcher ID, ORC ID, SNI-CONAHCYT ID or CVU PNPC [No.10 TNRoman]

All ROR-Clarivate-ORCID and CONAHCYT profiles must be hyperlinked to your website.

Prot- University of South Australia • 7038-2013• 0000-0001-6442-4409 • 416112

CONAHCYT classification:
https://marvid.org/research_areas.php [No.10 TNRoman]
Area:
Field:
Discipline:
Subdiscipline:

DOI: https://doi.org/
Article History:
Received: [Use Only ECORFAN]
Accepted: [Use Only ECORFAN]
Contact e-mail address:
* ✉ [example@example.org]

Check for updates

Abstract [In English]

Must contain up to 150 words

Graphical abstract [In English]

Authors must provide an original image that clearly represents the article described in the article. Graphical abstracts should be submitted as a separate file. Please note that, as well as each article must be unique. File type: the file types are MS Office files.No additional text, outline or synopsis should be included. Any text or captions must be part of the image file. Do not use unnecessary white space or a "graphic abstract" header within the image file.

Keywords [In English]
Indicate 3 keywords in TNRoman and Bold No. 10

Abstract [In Spanish]

Must contain up to 150 words

Graphical abstract [In Spanish]

Authors must provide an original image that clearly represents the article described in the article. Graphical abstracts should be submitted as a separate file. Please note that, as well as each article must be unique. File type: the file types are MS Office files.No additional text, outline or synopsis should be included. Any text or captions must be part of the image file. Do not use unnecessary white space or a "graphic abstract" header within the image file.

Keywords [In Spanish]
Indicate 3 keywords in TNRoman and Bold No. 10

Citation: Surname, Name 1st Author, Surname, Name 1st Co-author, Surname, Name 2nd Co-author and Surname, Name 3rd Co-author. Article Title. Journal of Mechanical Engineering. Year. V-N: Pages [TN Roman No.10].

Introduction

Text in TNRoman No.12, single space.

General explanation of the subject and explain why it is important.

What is your added value with respect to other techniques?

Clearly focus each of its features.

Clearly explain the problem to be solved and the central hypothesis.

Explanation of sections Article.

Development of headings and subheadings of the article with subsequent numbers

[Title No.12 in TNRoman, single spaced and bold]

Products in development No.12 TNRoman, single spaced.

Including figures and tables-Editable

In the article content any table and figure should be editable formats that can change size, type and number of letter, for the purposes of edition, these must be high quality, not pixelated and should be noticeable even reducing image scale.

[Indicating the title at the bottom with No.10 and Times New Roman Bold]

Box

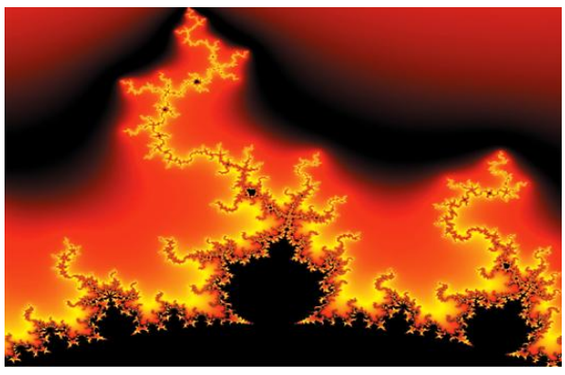

Figure 1

Title [Should not be images-everything must be editable]

Source [in italic]

Box

Table 1

Title [Should not be images-everything must be editable]

Source [in italic]

The maximum number of Boxes is 10 items

For the use of equations, noted as follows:

$$Y_{ij} = \alpha + \sum_{h=1}^{r} \beta_h X_{hij} + u_j + e_{ij} \quad [1]$$

Must be editable and number aligned on the right side.

Methodology

Develop give the meaning of the variables in linear writing and important is the comparison of the used criteria.

Results

The results shall be by section of the article.

Conclusions

Clearly explain the results and possibilities of improvement.

Annexes

Tables and adequate sources.

The international standard is 7 pages minimum and 14 pages maximum.

Declarations

Conflict of interest

The authors declare no interest conflict. They have no known competing financial interests or personal relationships that could have appeared to influence the article reported in this article.

ISSN: 2531-2189
RENIECYT-CONAHCYT: 1702902

Author contribution

Specify the contribution of each researcher in each of the points developed in this research.

Prot-
Benoit-Pauleter, *Gerard*: Contributed to the project idea, research method and technique.

Availability of data and materials

Indicate the availability of the data obtained in this research.

Funding

Indicate if the research received some financing.

Acknowledgements

Indicate if they were financed by any institution, University or company.

Abbreviations

List abbreviations in alphabetical order.

Prot-

ANN	Artificial Neural Network

References

Use APA system. Should not be numbered, nor with bullets, however if necessary numbering will be because reference or mention is made somewhere in the Article.

Use the Roman alphabet, all references you have used should be in Roman alphabet, even if you have cited an article, book in any of the official languages of the United Nations [English, French, German, Chinese, Russian, Portuguese, Italian, Spanish, Arabic], you should write the reference in Roman alphabet and not in any of the official languages.

Citations are classified the following categories:

Antecedents. The citation is due to previously published research and orients the citing document within a particular scholarly area.

Basics. The citation is intended to report data sets, methods, concepts and ideas on which the authors of the citing document base their work.

Supports. The citing article reports similar results. It may also refer to similarities in methodology or, in some cases, to the reproduction of results.

Differences. The citing document reports by means of a citation that it has obtained different results to those obtained in the cited document. This may also refer to differences in methodology or differences in sample sizes that affect the results.

Discussions. The citing article cites another study because it is providing a more detailed discussion of the subject matter.

The URL of the resource is activated in the DOI or in the title of the resource.

Prot-

Mandelbrot, B. B. [2020]. Negative dimensions and Hölders, multifractals and their Hölder spectra, and the role of lateral preasymptotics in science. Journal of Fourier Analysis and Applications Special. 409-432.

Intellectual Property Requirements for editing:

- Authentic Signature in Color of Originality Format Author and Coauthors.
- Authentic Signature in Color of the Acceptance Format of Author and Coauthors.
- Authentic Signature in blue color of the Conflict of Interest Format of Author and Co-authors.

ISSN: 2531-2189
RENIECYT-CONAHCYT: 1702902

Reservation to Editorial Policy

Journal of Mechanical Engineering reserves the right to make editorial changes required to adapt the Articles to the Editorial Policy of the Research Journal. Once the Article is accepted in its final version, the Research Journal will send the author the proofs for review. ECORFAN® will only accept the correction of errata and errors or omissions arising from the editing process of the Research Journal, reserving in full the copyrights and content dissemination. No deletions, substitutions or additions that alter the formation of the Article will be accepted.

Code of Ethics - Good Practices and Declaration of Solution to Editorial Conflicts

Declaration of Originality and unpublished character of the Article, of Authors, on the obtaining of data and interpretation of results, Acknowledgments, Conflict of interests, Assignment of rights and Distribution

The ECORFAN-Mexico, S.C Management claims to Authors of Articles that its content must be original, unpublished and of Scientific, Technological and Innovation content to be submitted for evaluation.

The Authors signing the Article must be the same that have contributed to its conception, realization and development, as well as obtaining the data, interpreting the results, drafting and reviewing it. The Corresponding Author of the proposed Article will request the form that follows.

Article title:

– The sending of an Article to Journal of Mechanical Engineering emanates the commitment of the author not to submit it simultaneously to the consideration of other series publications for it must complement the Format of Originality for its Article, unless it is rejected by the Arbitration Committee, it may be withdrawn.

– None of the data presented in this article has been plagiarized or invented. The original data are clearly distinguished from those already published. And it is known of the test in PLAGSCAN if a level of plagiarism is detected Positive will not proceed to arbitrate.

– References are cited on which the information contained in the Article is based, as well as theories and data from other previously published Articles.

– The authors sign the Format of Authorization for their Article to be disseminated by means that ECORFAN-Mexico, S.C. In its Holding Spain considers pertinent for disclosure and diffusion of its Article its Rights of Work.

– Consent has been obtained from those who have contributed unpublished data obtained through verbal or written communication, and such communication and Authorship are adequately identified.

– The Author and Co-Authors who sign this work have participated in its planning, design and execution, as well as in the interpretation of the results. They also critically reviewed the paper, approved its final version and agreed with its publication.

– No signature responsible for the work has been omitted and the criteria of Scientific Authorization are satisfied.

– The results of this Article have been interpreted objectively. Any results contrary to the point of view of those who sign are exposed and discussed in the Article.

Copyright and Access

The publication of this Article supposes the transfer of the copyright to ECORFAN-Mexico, SC in its Holding Spain for its Journal of Mechanical Engineering, which reserves the right to distribute on the Web the published version of the Article and the making available of the Article in This format supposes for its Authors the fulfilment of what is established in the Law of Science and Technology of the United Mexican States, regarding the obligation to allow access to the results of Scientific Research.

Article Title:

Name and Surnames of the Contact Author and the Coauthors	Signature
1.	
2.	
3.	
4.	

Principles of Ethics and Declaration of Solution to Editorial Conflicts

Editor Responsibilities

The Publisher undertakes to guarantee the confidentiality of the evaluation process, it may not disclose to the Arbitrators the identity of the Authors, nor may it reveal the identity of the Arbitrators at any time.

The Editor assumes the responsibility to properly inform the Author of the stage of the editorial process in which the text is sent, as well as the resolutions of Double-Blind Review.

The Editor should evaluate manuscripts and their intellectual content without distinction of race, gender, sexual orientation, religious beliefs, ethnicity, nationality, or the political philosophy of the Authors.

The Editor and his editing team of ECORFAN® Holdings will not disclose any information about Articles submitted to anyone other than the corresponding Author.

The Editor should make fair and impartial decisions and ensure a fair Double-Blind Review.

Responsibilities of the Editorial Board

The description of the peer review processes is made known by the Editorial Board in order that the Authors know what the evaluation criteria are and will always be willing to justify any controversy in the evaluation process. In case of Plagiarism Detection to the Article the Committee notifies the Authors for Violation to the Right of Scientific, Technological and Innovation Authorization.

Responsibilities of the Arbitration Committee

The Arbitrators undertake to notify about any unethical conduct by the Authors and to indicate all the information that may be reason to reject the publication of the Articles. In addition, they must undertake to keep confidential information related to the Articles they evaluate.

Any manuscript received for your arbitration must be treated as confidential, should not be displayed or discussed with other experts, except with the permission of the Editor.

The Arbitrators must be conducted objectively, any personal criticism of the Author is inappropriate.

The Arbitrators must express their points of view with clarity and with valid arguments that contribute to the Scientific, Technological and Innovation of the Author.

The Arbitrators should not evaluate manuscripts in which they have conflicts of interest and have been notified to the Editor before submitting the Article for Double-Blind Review.

Responsibilities of the Authors

Authors must guarantee that their articles are the product of their original work and that the data has been obtained ethically.

Authors must ensure that they have not been previously published or that they are not considered in another serial publication.

Authors must strictly follow the rules for the publication of Defined Articles by the Editorial Board.

The authors have requested that the text in all its forms be an unethical editorial behavior and is unacceptable, consequently, any manuscript that incurs in plagiarism is eliminated and not considered for publication.

Authors should cite publications that have been influential in the nature of the Article submitted to arbitration.

Information services

Indexation - Bases and Repositories

LATINDEX (Scientific Journals of Latin America, Spain and Portugal)
EBSCO (Research Database - EBSCO Industries)
RESEARCH GATE (Germany)
GOOGLE SCHOLAR (Citation Indexes-Google)
MENDELEY (Bibliographic References Manager)
REDIB (Ibero-American Network of Innovation and Scientific Knowledge- CSIC)
HISPANA (Bibliographic Information and Guidance-Spain)

Publishing Services

Citation and Index Identification H
Management of Originality Format and Authorization
Testing Article with PLAGSCAN
Article Evaluation
Certificate of Double-Blind Review
Article Edition
Web layout
Indexing and Repository
ArticleTranslation
Article Publication
Certificate of Article
Service Billing

Editorial Policy and Management

38 Matacerquillas, CP-28411. Moralzarzal –Madrid-España. Phones: +52 1 55 6159 2296, +52 1 55 1260 0355, +52 1 55 6034 9181; Email: contact@ecorfan.org www.ecorfan.org

Journal of Mechanical Engineering

2531-2189
ISSN 2531-2189
www.ecorfan.org